Aeolian geomorphology of northeast Graham Island, Haida Gwaii (Queen Charlotte Islands), British Columbia

by

Kim Irene Pearce

B.Sc., University of Victoria, 2002

A Thesis Submitted in Partial Fulfillment of the
Requirements for the Degree of

MASTER OF SCIENCE

in the Department of Geography

Supervisor: Dr. Ian J. Walker

Abstract

This study investigates the modern aeolian morphodynamics of East Beach, Haida Gwaii, British Columbia. Qualitative assessments show this coast is host to diverse aeolian landforms maintained by strong, year-round winds and an abundant supply of sediment, despite a moist marine climate. Quantitative assessments from three models of sediment drift potential and dune mobility show high annual aeolian activity with a seasonal shift from the fall and winter months to the summer. The morphodynamics of a foredune-trough blowout complex are examined during a two-year period through topographic surveys, cross-shore profiles and a network of surface change pins. Results show the foredune plain accreted by 55 m^3 m-width^{-1} a^{-1}, the shoreline retreated up to 37 m while the foredune remained relatively unchanged. This study provides a detailed geomorphic assessment of a highly sensitive, yet understudied, Canadian coastal dune system.

Supervisor: Dr. Ian J. Walker, (Department of Geography)

Table of Contents

List of Tables

List of Figures

Page

List of Equations

Page

Acknowledgements

I gratefully acknowledge my supervisor, Dr. Ian J. Walker, for this opportunity and for his support and friendship through all stages of learning during this journey. Thanks also go to the members of my supervisory committee, Drs. Dan Smith and Vaughn Barrie, as well as my external examiner, Dr. Stephen Wolfe, for their invaluable input during the final stages of this thesis.

To all the basement dwellers, both current (DA, JA, TC, WZ) and those who have managed to escape (JA, SJ, KT), thank you for your assistance and support but mostly for your friendship along this epic journey. Thanks also go to all those who managed (or attempted) to kidnap me in my hours of frustration, allowing me to refocus my kaleidoscopic view and to remember that this thesis, though important, will not define my life or how I choose to live it.

Mom and Dad, thank you for your unwavering love and support through all of my life choices. Nick and Deborah, thank you for your technical, editorial but most importantly emotional support. To Simon, my life companion, for standing by me through all the ups and downs, and for loving, encouraging and caring for me always. Without you all, this thesis would not have been completed.

I would also like to acknowledge Drs. Stephen Wolfe (Geological Survey of Canada-Ottawa) and Dave Huntley (Simon Fraser University Physics) for providing the optical dates used for this geomorphic assessment of East Beach, HG. Gratitude is also extended to the Council of the Haida Nation and to the Naikoon Provincial Park rangers for access to the site and logistical support. Thanks to the Geological Society of America (GSA), the Canadian Northern

Scientific Training Program (NSTP) and the Derrick Sewell Graduate Scholarship for funding my research. Funding for this research was also provided by the Natural Sciences and Engineering Research Council and the Canadian Foundation for Innovation granted to Dr. Walker.

1.0 Introduction and Research Objectives

1.1 Introduction

Haida Gwaii (HG), also known as the Queen Charlotte Islands (QCI), located 80 km off the northwest coast of British Columbia (Figure 1.1), is host to one of Canada's most dynamic sedimentary coastlines. The Naikoon Peninsula has diverse coastal morphology, from low gradient, dissipative beaches backed by prograding aeolian dune ridges on North Beach, to intermediate beaches with multiple shore-attached bars backed by a complex dune system of foredunes, blowouts and migrating parabolic dunes on East Beach (Figure 1.2).

This landscape exists in a high-energy environment with frequent high winds (> 18 m s^{-1}), a macro-tidal range (HHWMT exceeding 7 m) and an energetic wave climate with frequent storm surge. Under these conditions, the east coast experiences a high rate of retreat of 1 to 3 m a^{-1} (Barrie 2002), while the north coast has a moderate progradation rate of 0.3 to 0.6 m a^{-1} (Harper 1980). Given the tidal range, wind and wave regime, ongoing sea-level rise of 1.6 mm a^{-1} and erodibility of this coastline, the Geological Survey of Canada has recognized it as one of Canada's most sensitive to the impacts of climate change and sea-level rise (Shaw et al. 1998). Despite this recognition, the coastal morphodynamics of northeast Graham Island are understudied.

1.1.1 Research purpose and objectives

Most aeolian geomorphic research in Canada is focused on the coastal dunes of the Great Lakes (e.g., Davidson-Arnott and Law 1990; Byrne 1997) and

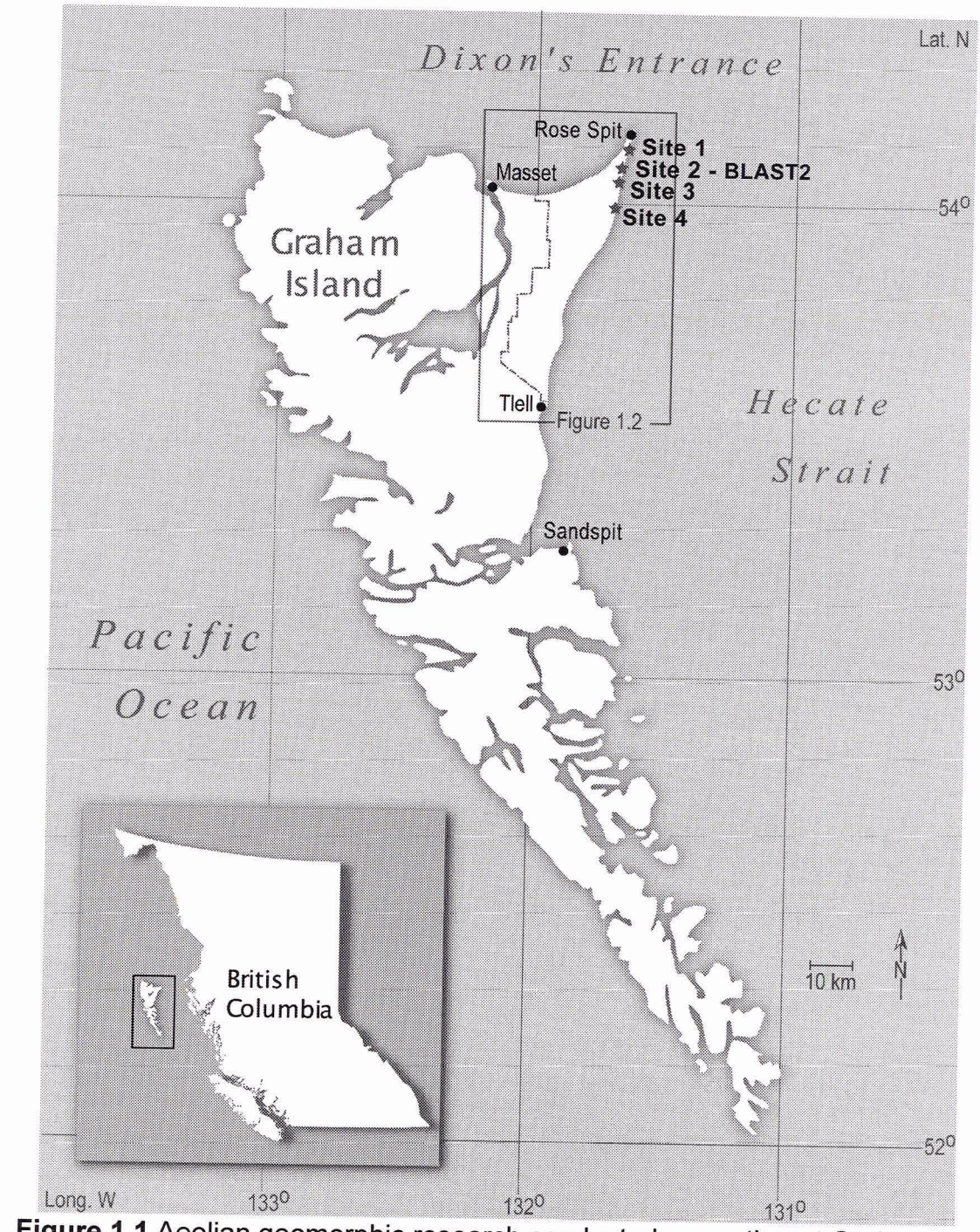

Figure 1.1 Aeolian geomorphic research conducted on northeast Graham Island, Haida Gwaii, at four distinct sites is combined with an assessment of aeolian activity using meteorological data from three stations: Environment Canada stations at Rose Spit and Sandspit as well as BLAST2, a specialized station established by the UVic Geography Boundary Layer and Sediment Transport (BLAST) lab in June 2002.

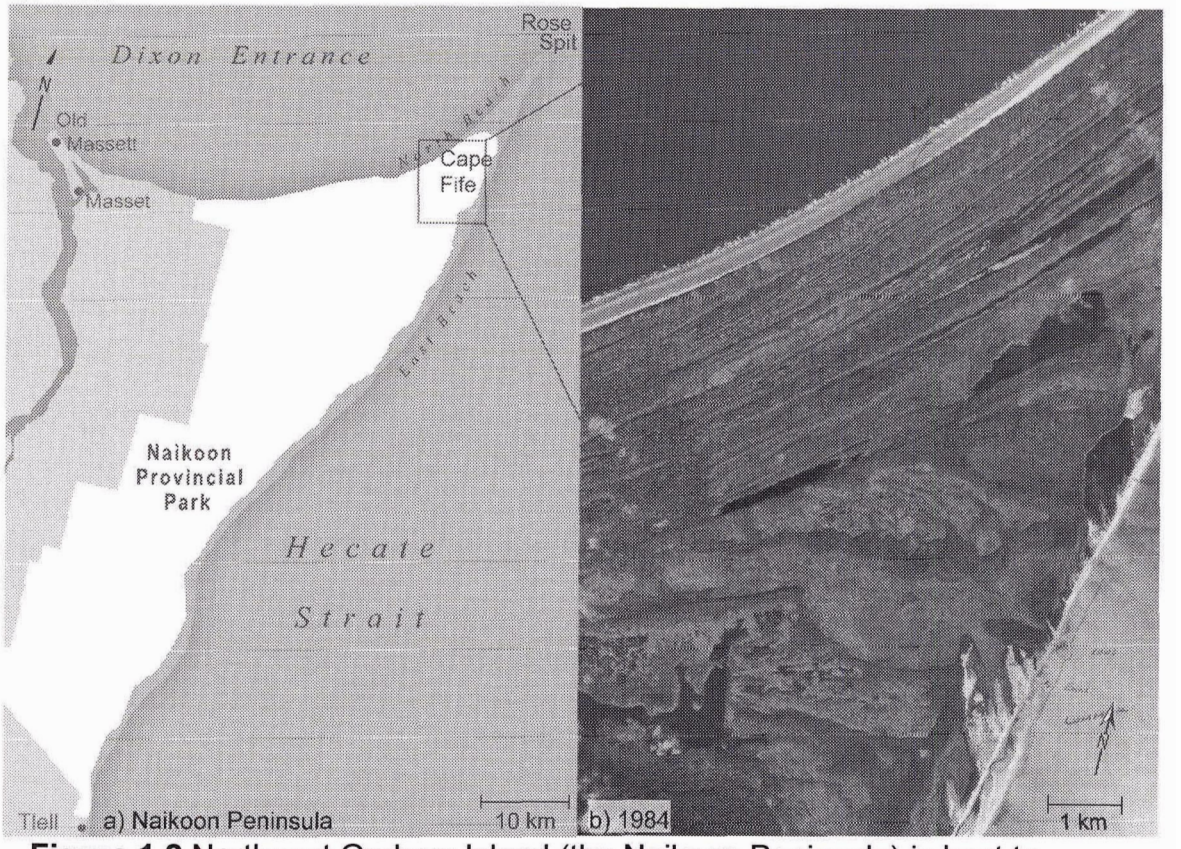

Figure 1.2 Northeast Graham Island (the Naikoon Peninsula) is host to prograding beach ridges on North Beach and active foredunes and parabolic dunes on East Beach. b) Provincial airphoto BC40109_116 1984.

the Maritimes (e.g., Byrne and McCann 1993; Davidson-Arnott et al. 2003; Walker et al. 2003; Hesp et al. 2004) plus the semi-arid dunes of the Great Plains (e.g. Wolfe et al. 1995; Muhs and Wolfe 1999; Wolfe and Lemmen 1999; Wolfe et al. 2000). There are very few studies focused on the dynamics of dunes on the Canadian West Coast, or on dune systems in humid, high-energy macrotidal environments. This study contributes to Canadian geomorphology by assessing the contemporary aeolian geomorphology of East Beach, HG. To accomplish this, the following objectives were identified:

1. To document and describe aeolian geomorphology on East Beach,

2. To assess regional aeolian activity and relate to seasonal dune morphodynamics, and
3. To measure and examine the morphodynamics of a foredune-trough blowout complex on East Beach.

1.1.2 Thesis outline

This thesis is structured as follows. Chapter 2 sets the context for this research by reviewing key scholarship on aeolian sediment transport and coastal dune evolution and morphology. Chapter 3 presents the methods used to obtain each of the objectives above. Chapter 4 describes the aeolian geomorphology of East Beach, including a discussion of the biogeographical setting of these dunes. Chapter 5 assesses regional aeolian activity by applying and critiquing three models of sediment drift potential and dune mobility. Chapter 6 focuses on the morphological response of a foredune-trough blowout complex over a two-year period (June 2002-June 2004). A summary and general conclusions from the thesis form the seventh chapter.

2.0 Research Context

2.1 Aeolian sediment transport

Aeolian sediment transport is the movement of sediment by the force of wind and occurs when the forces of lift and shear stress (τ) exerted by the wind exceed the resisting forces of weight and interparticle cohesion acting on grains at the surface. Lift results from the decrease in fluid static pressure at the top of the grain, and shear stress is exerted by the wind blowing over the surface (Sarre 1987). The resisting forces of weight and cohesion are related to grain characteristics (i.e., size and sorting) and the presence of agents that bond grains together (e.g., moisture, precipitated salts, algae) (Nickling and Davidson-Arnott 1990).

When air flows over an aerodynamically smooth surface, boundary layer theory states the lower 10 to 20% of the boundary layer, where the surface continues to affect the flow, can be described by a log-linear increase in velocity with elevation (Oke 1978). The Law of the Wall, described by the Prandtl-von Karman equation, describes this portion of the profile, or the constant stress regions of the boundary layer, as follows:

$$\frac{u_z}{u_*} = \frac{1}{k} \ln \frac{z}{z_o} \qquad (1)$$

where u_z is the wind speed (m s^{-1}) measured at height z (m), u_* is wind shear velocity (m s^{-1}) at the bed, z_0 is the aerodynamic roughness length (m) and k is the unitless von Kármán constant (~0.41) (Schlichting 1955). In sedimentary environments, τ is primarily responsible for sediment transport, but this value can

not be measured directly. A relation of shear velocity (u_*) and air density (ρ) is used to estimate shear stress:

$$\tau = \rho u_*^2 \quad (2)$$

To estimate u_*, the slope of a time-averaged wind speed profile plotted from anemometers set at logarithmic spacing can be used.

The initiation of sediment transport occurs when a threshold shear velocity (u_{*t}) is reached (Hsu 1971; Nickling 1988). This velocity can be converted to wind speed measured at a different elevation (e.g., 10 m) using Equation 1 and a roughness length for the surface. Commonly accepted wind speed thresholds for aeolian sedimentary systems, measured at 10 m (u_{*t10}), range from 5 to 8 m s^{-1} (Bagnold 1941; Fryberger 1979; Pye 1985; Arens 1996b; McKenna Neuman et al. 2000; Davidson-Arnott et al. 2003; Tsoar and Arens 2003).

Once particles begin to move, they are transported in one of four main modes: surface creep, suspension, saltation and modified saltation, where the trajectories of saltating grains are modified by turbulent eddies. These modes of transport exist in a continuum dependent on particle size, sediment availability and wind speed (Sarre 1987). From wind tunnel tests, grains travelling in saltation generally range from 100 to 1,000 μm in diameter (McKenna Neuman 1993) and account for at least 75% of the total sediment in transport (Bagnold 1941). Finer grains (< 100 μm) may be kept aloft by turbulent eddies over longer distances in suspension, whereas larger grains (> 1,000 μm) are generally transported as surface creep by rolling and bouncing along the surface (Nickling and Davidson-Arnott 1990).

Bagnold (1941) was the first investigator to develop a mathematical relation to quantify aeolian sediment flux based on field observations and wind tunnel tests. He found that mass sediment flux (q), in both saltation and creep, is proportional to the cube of the shear velocity, as shown in the following expression:

$$q = u_*^3 * \rho/g * C\left(d/D\right)^{1/2} \quad (3)$$

where g is acceleration due to gravity (9.8 m s^{-2}), C is a unitless empirical constant related to grain size distribution ranging from 1.5 for nearly uniform sand to 3.5 for a pebbly surface, d is the mean grain size and D is a standard grain size (250 μm). This model expresses sediment flux as a function of wind shear and characteristics of the grains to be transported. In Bagnold's (1941) original equation, there is no threshold term, and therefore, sediment transport is predicted at shear velocities lower than that required for sediment entrainment. This serves to inflate sediment flux estimates (Belly 1964).

Kawamura (1951) was the first to propose a model that includes a threshold shear velocity term in a predictive equation of sediment transport as follows:

$$q = C(u_* - u_{*_t})(u_* + u_{*_t})^2 \rho / g \quad (4)$$

where u_{*_t} is the shear threshold velocity. Unlike Bagnold's (1941) equation, this model does not include parameters that characterize grain size.

Similar in form to Bagnold's (1941) model, Lettau and Lettau (1978) provide a sediment transport equation that incorporates a threshold shear velocity (u_{*_t}) and includes parameters to describe grain characteristics:

$$q = C\sqrt{\frac{d}{D}}\frac{\rho}{g}u_*^2(u_* - u_{*_t}) \quad (5)$$

where C has a value of 4.2. These three equations yield sediment flux values (q) in dimensions of M L^{-1} T^{-1} or mass of sediment transported per unit width of surface per unit time (e.g., kg m^{-1} s^{-1}). The dimensions of flux do not include a height term, therefore the height of measurement is assumed to be infinite (Nickling and McKenna Neuman 1999).

Since Bagnold's (1941) pioneering work, a multitude of sediment transport equations, derived both empirically and theoretically, have been developed to predict rates of sediment transport as reviewed by Sarre (1987), Anderson and Willetts (1991) and Sherman et al. (1998). One major limitation for most models when applied in natural environments is that they assume a 'transport-limited' condition (i.e., the major control on flux rates is the frequency, magnitude and directional variability of the wind) (Bird 2003). However, most natural sedimentary surfaces tend to be limited by the availability of the surface to supply grains to the wind (e.g., grain characteristics, moisture, bonding agents, vegetation) (Sherman and Hotta 1990; Kocurek and Lancaster 1999). Thus, when models of sediment flux are applied without consideration of these conditions, sediment flux estimates can deviate by orders of magnitude from the actual measured rates (Anderson and Willetts 1991; Arens 1996b; Jackson and McCloskey 1997; Sherman et al. 1998; van der Wal 1998).

2.1.1 Controls of aeolian sediment transport

In general, natural surfaces have a higher threshold shear velocity and a lower sediment availability as textural and surficial conditions hold the grain to the bed (e.g., grain characteristics, surface moisture, precipitated salts) (Nickling and Davidson-Arnott 1990). Grain characteristics that control the threshold of entrainment are grain size, shape, sorting and density (Sarre 1987). The size of a grain will directly influence its weight; thus, increasing the sediment particle size will increase the threshold of entrainment (Folk 1966; Willetts 1979; Willetts 1983). This does not hold, though, for silt- and clay-sized particles, as their platy shape increases their surface area and potential cohesion, as well as the additional electrostatic charges, resulting in an increase in the threshold of entrainment (Sarre 1987). Grain sorting will alter the availability of sediments to entrainment, as fine sediments are more easily removed by wind, leaving behind larger grains that could potentially shelter a layer of fines underneath (Willetts 1979; Willetts 1983; Kocurek and Lancaster 1999). Grain density also influences the entrainment of sediment, as increased density increases the weight of grains, thereby increasing the transport threshold.

The second major control, moisture on sandy surfaces, limits the availability of sediments for aeolian transport by increasing the interparticle cohesion, thereby increasing the threshold for sediment transport (McKenna Neuman and Scott 1998; Wiggs et al. 2004). Wind tunnel experiments conducted by McKenna Neuman and Nickling (1989) found that even strong winds can not entrain sediments with surface moisture contents greater than 1% by weight. A

more recent field study by Wiggs et al. (2004) determined that the critical moisture content for sediment transport on a beach ranged from 4 to 6%, much higher than found in earlier studies.

The sources of moisture on sandy surfaces are variable but include precipitation, mist, dew, ground water emergence and, in coastal areas, tidal swash, storm wave run-up and sea spray. As most sands are highly porous, water can generally permeate quickly away from the surface to lower layers (Tsoar 2002). Thus, the frequency and quantity of moisture received over a certain time will alter the capacity of the surface to yield transportable sediments. For instance, when large quantities of rain fall over a short period, a sedimentary surface will have a high moisture content for a short period of time, but the upper transportable sediments will dry relatively quickly once the rainfall stops (Jackson and Nordstrom 1998). During light to moderate rainfall over longer periods, the surface sediments remain saturated longer, preventing or limiting entrainment (van Dijk et al. 1996; Jackson and Nordstrom 1998).

Recent field and wind tunnel experiments of aeolian sediment transport under varying surface moisture conditions indicate that due to rain splash effects and differential drying, sediment transport may occur even when models estimate no transport due to high surface moisture content (van Dijk et al. 1996). Although u_{*t} for the moist surface has not been reached, the force of raindrops on the surface can eject grains into the air where they can then be transported in the airflow (Erpul et al. 2004). Differential drying of the surface sediments occurs as high winds blow over a moist surface, thereby enhancing evaporation of the

surface layer (Wiggs et al. 2004). For these reasons, actual rates of sediment flux during precipitation are controlled not only by the magnitude, duration and frequency of the precipitation event, but also by the wind strength and duration (Wiggs et al. 2004). The effects of surface moisture content on sediment transport rates are usually modelled as an impact on the threshold shear velocity as proposed by Belly (1964), which uses the percent moisture content per weight.

When ground water emerges on a sedimentary surface, aeolian sediment transport is inhibited, as the moisture at the surface prevents entrainment (Kocurek et al. 2001). Unlike precipitation that falls for a short period of time and then infiltrates, ground water emergence maintains moisture at or near the surface over much longer periods.

The availability of sediment for transport is also limited by the presence of bonding agents. These include precipitated salts as well as chemical or organic bonding agents that increase the interparticle cohesion of grains, thereby increasing the threshold of entrainment (van den Anker et al. 1985; McKenna Neuman and Maxwell 1999). Precipitated salts develop when saline surface water evaporates, crystallizing the salts and cementing particles together (Pye and Tsoar 1990). Cementing is also caused by the presence of clay skins, fungal hyphae, algae and lichens (van den Anker et al. 1985; McKenna Neuman and Maxwell 1999).

Surface roughness elements (e.g., vegetation, driftwood, flotsam) influence sediment transport by lowering the transport ability of the wind by

disrupting airflow and by covering the surface, limiting the ability of sediments to be entrained. Surface roughness elements alter the lower portion of the wind speed profile by imposing enhanced drag on the flow versus flow over a flat surface (Arens et al. 1995; Nickling and McKenna Neuman 1999). Surface roughness elements further reduce the shear stress available to entrain sediment by displacing the surface at which the shear stress acts upward and by extracting a large portion of the shear stress on a non-erodible surface (Nickling and Davidson-Arnott 1990; Wolfe and Nickling 1993; Wiggs et al. 1996a).

Vegetation on a sedimentary surface may also act as a surface cover, reducing the exposure of sediments to entrainment by airflow, as well as creating an obstacle for saltating grains, causing entrained sediments to be deposited (Wasson and Nanninga 1986; Blumberg and Greeley 1993; Wolfe and Nickling 1993). When airflow encounters vegetation, wind speed is significantly reduced by up to 1,000 times (Arens 1996a). If the wind speed is reduced below the threshold of entrainment, sediment will be deposited. At higher wind speeds, when enhanced erosion of the surface might be expected, vegetation can reduce actual entrainment as grasses may be blown flat over the surface, providing a dense cover over a larger surface (Wiggs et al. 1995; Lancaster and Baas 1998).

Recently, driftwood has been recognized as a major roughness element on the backshore in coastal environments (Komar 1976; Hesp 2002; Walker and Barrie 2004). Driftwood is a hard, relatively large roughness element that interrupts airflow, reduces wind speed and results in the deposition of entrained sediments. Driftwood may also induce localized jetting and erosion, but in higher

densities, it appears to act as an accretion anchor, producing a sediment sink on the backshore (Walker and Barrie 2004). Sediment-laden driftwood jams may provide a buffer for a coastline against wave attack by releasing stored sediments, or by preventing or slowing major scarping of the foredune toe, depending on the severity and frequency of wave attack.

Topography influences aeolian sediment transport and the pattern of deposition through localized flow perturbations. As airflow approaches a hill or dune, wind speed, and thereby shear stress, is reduced at the base (McKenna Neuman et al. 1997; Walker and Nickling 2002). This results from a stagnation effect where positive pressure builds up on the lower windward slope of the hill. As air flows over the hill, it is accelerated up the windward slope due to flow streamline compression, which results in a rapid increase in wind speed and surface shear stress (Taylor and Lee 1984; Rasmussen 1989; Wolfe and Nickling 1993; Wiggs et al. 1996b; Bullard et al. 2000; Walker and Nickling 2002).

Perturbations induced on airflow by topography pose difficulties for estimating sediment transport over dunes. Estimates of u_*, τ and, hence, q are ideally derived from the lower portion of the wind speed profile within the constant stress region (Walker and Nickling 2002). However, this constant stress region has been estimated at only a few centimetres thick over small to moderate sized dunes (McKenna Neuman et al. 1997), prohibiting the measurement of wind speed and the development of a profile for this region. In light of this, a proxy measure of near surface stress is derived by assuming horizontal stress remains constant within a wider region and developing a wind speed profile from

measurements within this region. Using this profile technique, there may be non log-linear segments to the profile resulting in an over- or underestimation of surface stress and thereby q.

2.1.2 Aeolian sediment transport in coastal environments

In continental settings, aeolian sediment transport is generally limited by the availability of sediment grains to be transported, controlled by the parameters described above. In environments where there is no external supply of sediment, the supply is directly proportional to the sediment availability. For example, during droughts when vegetation cover is reduced, sediment availability, and thereby supply, is increased. However, in fluvial, lacustrine and coastal settings, an external source of sediment increases supply, and the sediment budget is no longer solely dependent on vegetation cover and moisture.

In coastal environments, an additional sediment supply may be present through nearshore dynamics, littoral transport and aeolian transport from the beach into the dune system. Tidal stage combined with varying fetch lengths influence the rate and efficiency of aeolian sediment transport from the beach by limiting boundary layer development and sediment available for transport (Bauer and Davidson-Arnott 2002). The width of the beach influences the efficiency of sediment transport not only via increased availability of sediment, but also by providing greater distance for boundary layer and sediment transport development. For the sediment transport process to become fully developed, a critical fetch distance is required (Nickling and Davidson-Arnott 1990; Dong et al.

2003). From empirical studies, Davidson-Arnott and Law (1990) determined that the critical fetch length on a beach for winds exceeding 50 km hr^{-1} (~13.9 m s^{-1}) is 40 m.

In areas subject to tides, sediment availability is also dependent on water level fluctuations as the beach and nearshore are rhythmically exposed and covered by water. On a beach, fetch distance changes continuously with tide stage and incident angle of the wind (Sherman 1990; Bauer and Davidson-Arnott 2002). Winds blowing directly onshore will have markedly less distance over which to entrain sediments than those blowing oblique (e.g., 35-60 degrees) to the foredune crest (Sherman and Bauer 1993). In coastal environments, an increase in wind speed will not directly relate to increased sediment flux, as would be predicted from many sediment flux models. This results from decreased beach fetch due to increased storm surge height and wave run-up during high magnitude on-shore winds (Davidson-Arnott and Law 1990).

2.2 Coastal dune geomorphology

Coastal dunes form above the high water mark on coastlines where there is an ample supply of sand-sized sediments and competent onshore winds to transport them. Because coastal dunes develop at the interface of three environmental systems (i.e., marine, atmospheric and terrestrial), they are dynamic, responsive and complex landforms (Carter 1988). Coastal dunes play an important role in the evolution and stability of sedimentary coasts, as they can buffer and protect against wave attack and storm surge by storing and recycling

sediments to the beach when depleted by heavy storms (Hesp 2000). They also shelter inland waters, wetlands and developed landscapes and provide habitat for wildlife and recreational areas for human activities (Klee 1999). The following is a brief discussion of the evolution and morphology of the four predominant coastal dune types: foredunes, blowouts, parabolic dunes and transgressive dunefields.

2.2.1 Foredunes

Foredunes are depositional shore-parallel dune ridges that form on the backshore (Hesp 1999). Their morphology is diverse but is generally classified into two main categories: incipient and established foredunes (Hesp 2002). Incipient, also known as embryo or newly forming, foredunes develop by the accretion of aeolian sands in discrete zones of vegetation or high tide debris on the backshore. Their morphology depends principally on the density and height of vegetation or roughness, the wind regime and the rate of sand transport to the backshore (Hesp 2002). Incipient foredunes are exposed frequently to marine influences (i.e., waves and storm surge), and as such, they are ephemeral landforms.

Established foredunes are generally older landforms, often developing from incipient foredunes that are maintained over several seasons or years. They are distinguished from incipient foredunes by the establishment and growth of intermediate plant species and the increased morphologic complexity (Hesp 2004). Established foredune morphology reflects the rate of sediment supply, the

distribution and type of plant species (a function of local climate and biogeography), the pattern of aeolian sand transport and the frequency and magnitude of wind and waves, as well as the degree of human interference and the stability of the coastline (e.g., retreating stable or prograding) (Hesp 1999).

There are several foredune morphologic classifications (Hesp 1982, 1988; Carter 1988; Arens 1994), but the most recent by Hesp (1999) combines aspects of its predecessors to provide a comprehensive model of foredune morphology and evolution (Figure 2.1). The five main morpho-ecological stages (1 to 5) depict decreasing vegetation cover progressing with increased aeolian activity and erosion. Hesp (1999) associates foredune stages 1 to 3 with generally prograding coasts, while stages 3 to 5 are more likely associated with erosional coasts. Hesp's (1999) model can be used to assess foredune evolution at varying temporal scales from annual and event-based changes (e.g., wave scarp) to medium- or long-term coastal dune evolution.

Hesp's (1999) model illustrates morphological stages of an established foredune in which the foredune may remain for most of its existence, or the evolutionary stages through which it may progress given changes in vegetation cover, varying conditions of erosion or wave scarp events. Hesp (2002) states that under favorable conditions for dune formation and stabilization, a foredune may progress in reverse, for example, from a Stage 4 to a Stage 3, although complete reversal from a Stage 5 to a Stage 1 is unlikely. A wave erosion event, as in Box D, of either wave scarp or overwash, will rapidly shift a foredune into a

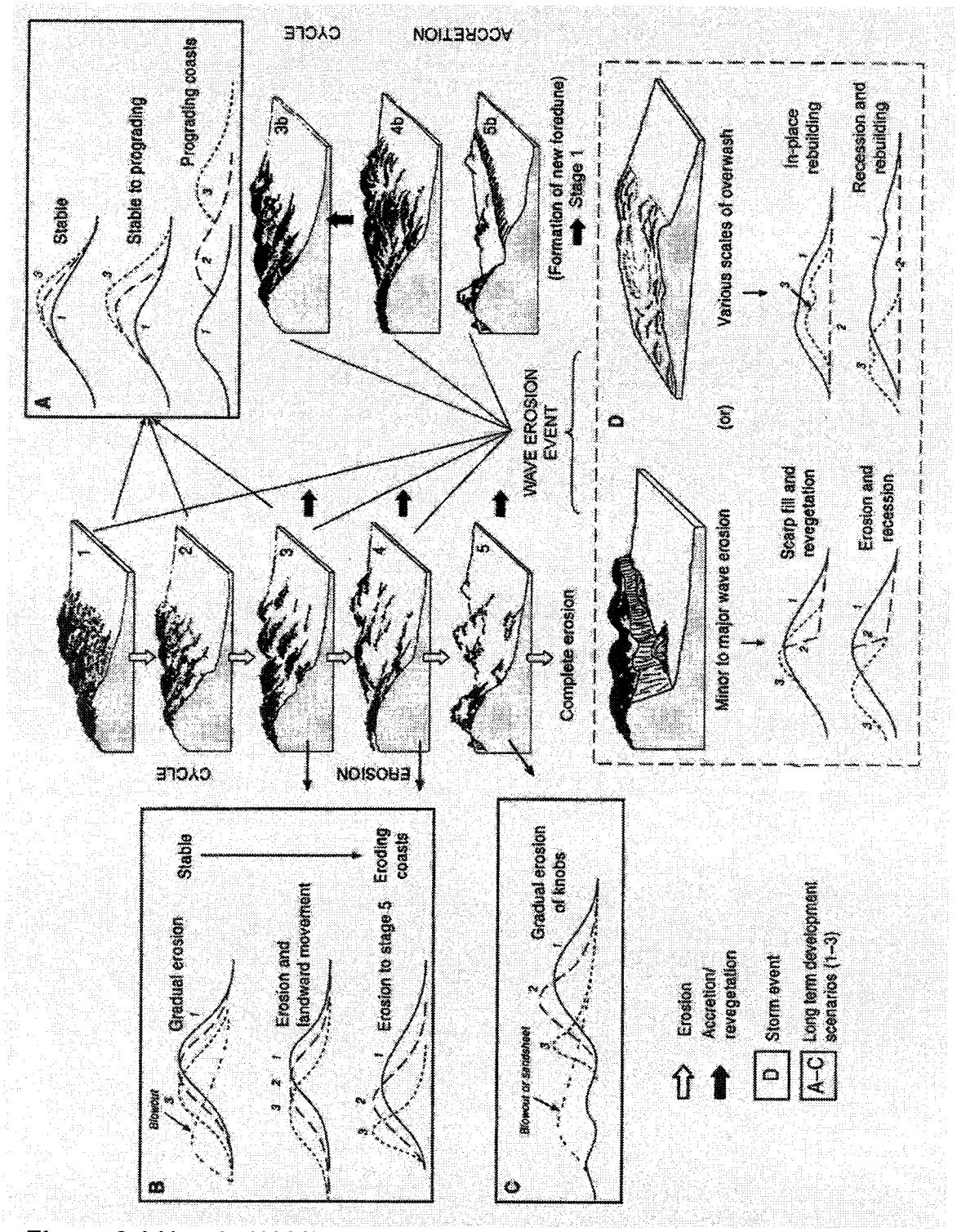

Figure 2.1 Hesp's (1999) model of established foredune morphology evolution (Hesp 1999: p. 158, reprinted with permission of the author).

new stage. As the foredune recovers, it will likely pass through several stages of foredune evolution.

2.2.1.1 Airflow over coastal foredunes

Airflow over foredunes has received much recent attention within coastal aeolian geomorphic research (e.g., Rasmussen 1989; Sarre 1989; Arens 1994; 1996a; Arens et al. 1995; Davidson-Arnott 1996; Olivier and Garland 2003; Walker et al. 2003; Hesp et al. 2004). This research shows that as airflow approaches a dune, wind speed is reduced due to positive pressure buildup or flow stagnation. Where present, surface roughness elements such as vegetation, driftwood and debris further reduce wind speeds, increasing the potential for deposition at the foredune toe (Arens 1996a). Above the vegetation canopy, airflow is topographically accelerated up the windward (stoss) slope of a foredune, typically increasing surface shear stress and sand transport (Arens et al. 1995; Hesp et al. 2004). Due to flow expansion and separation at the foredune crest, wind speed is reduced, resulting in crest and lee slope deposition.

Winds that approach from oblique incident angles tend to maintain higher speeds over a foredune than those blowing dune-normal, as the foredune causes less stagnation as it appears less steep to the flow (i.e., effectively has a lower aspect ratio to the flow) (Hesp et al. 2004; Parsons et al. 2004). Oblique winds are also topographically steered toward dune-normal (i.e., toward an incipient angle of 90° to the foredune crest) as the dune-normal flow vector increases up

the stoss slope (Arens et al. 1995; Hesp et al. 2004; Walker et al. in press). Arens (1996a) found that a combination of dune-normal and oblique onshore winds promotes foredune development and maintenance, as oblique winds transport the majority of sediment from the beach to the toe of the dune, while dune-normal winds promote the transport of sediment up the stoss slope. Recent studies by Walker et al. (in press) also found that even during offshore wind events, airflow may be steered alongshore on the beach and then deflected toward the foredune, promoting dune maintenance.

2.2.2 Blowouts

Blowouts are erosional dune features that form on established dunes and are initiated by an alteration in the airflow causing localized flow acceleration and amplified erosion rates. Blowouts are characterized by an unvegetated to sparsely vegetated hollow or erosional basin and a landward depositional lobe (Hesp 1996) (Figure 2.2). Although there are a wide variety of blowout morphologies, most can be classified into two main types: saucer or trough (Cooper 1958). Saucer blowouts are semi-circular or saucer shaped with shallower deflation basins, whereas trough blowouts tend to be more elongated, with a deeper deflation hollow or throat and steeper lateral walls (Hesp 1999) (Figure 2.2).

Blowouts maybe initiated in a variety of ways, including wave and water erosion, topographic acceleration of airflow, changes in vegetation cover, and

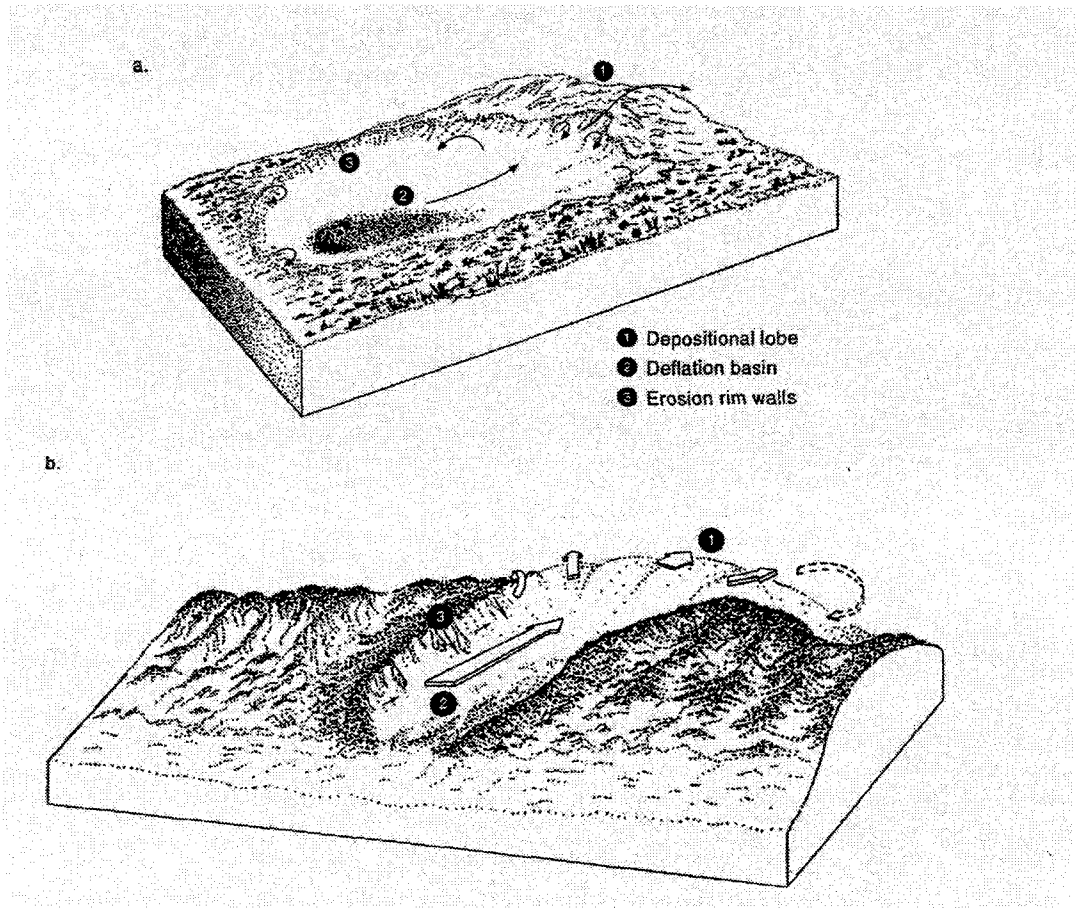

Figure 2.2 Morphology and generalized flow conditions for saucer (a) and trough (b) blowouts (Hesp 1999: p. 161, reprinted with permission of the author).

human disturbances (Hesp and Hyde 1996). The actual size, shape, location and subsequent evolution of blowouts are dependent on several factors including: i) the height and width of the sediment deposit in which the blowout is developing, ii) the size of the initial constriction, iii) the type of vegetation and its distribution, iv) the frequency, magnitude and direction of the wind, and v) the degree of exposure of the blowout to those winds (Hesp 1999). Each of these operates at varying temporal and spatial scales, providing diverse blowout morphologies.

Blowouts are self-amplifying geomorphic features (Hesp and Hyde 1996). Once initiated, significant topographic acceleration up the axis of the blowout

increases erosion in the deflation basin and lateral walls (Hesp 2002). Sediments are eroded from the basin and deposited downwind, creating a depositional lobe and depositional plain. Steep topography from the basin up the windward slope of the depositional lobe causes airflow expansion and deceleration, resulting in deposition of entrained sediments (Hesp and Hyde 1996). In many blowouts, the deflation basin continues to erode until it reaches the water table or a less erodible surface, followed by scarping of the lateral walls, widening the feature (Carter et al. 1990). Due to topographic steering and acceleration, rates of sediment transport within blowouts can be significantly greater than potential flux rates calculated from regional or remotely sensed wind data (Hesp and Hyde 1996).

Pressure differences within a trough blowout versus the open beach draw airflow in and accelerate it via streamline constriction and topographic forcing. When wind approaches the entrance of a blowout at incident angles normal to the foredune crest, flow acceleration along the central axis yields the highest wind speeds and maximum potential for erosion (Carter et al. 1990; Hesp 2002). During oblique to shore-parallel incident wind angles, topographic deflection results in large helical vortices altering the location of maximum erosion away from the centreline axis to a lateral wall (Byrne 1997; Fraser et al. 1998; Hesp 2002).

The evolution of blowouts is varied, as it is dependent on wind speed and directional variability, vegetation types and potential for re-vegetation, and the magnitude and frequency of beach/dune erosion. Blowouts may advance through

stages of evolution from erosional notches and incipient blowouts to large active blowouts to decaying, revegetated blowouts (Hesp 2002). During their active lifespan, blowouts act as conduits, accelerating airflow and sediment transport, thereby enhancing sediment delivery from the beach and backshore to landward of the foredune crest.

2.2.3 Parabolic dunes

Parabolic dunes, named for their shape, are characterized by vegetated, trailing ridges that connect to U-shaped depositional ridges downwind (Hesp 1999). Parabolics can develop by disruption and activation of older vegetated sand deposits, or, with continued sediment supply, the depositional lobe of a blowout may become mobile (Figure 2.3) (Hesp 1999). As the depositional lobe transgresses downwind over terrain, trailing arms are formed as migrating sands are trapped by marginal vegetation (Hesp and Thom 1990). Between the trailing arms, a deflation basin may continue to erode until a non-erodible surface is met (e.g., water table, layer of pebbles or shells) (Hesp 1999).

Unless relict and highly stabilized by vegetation, the heads of active parabolic dunes consist of a windward slope with bare sand and a steep, convex, vegetated lee slope (Robertson-Rintoul 1990), as well as convex outer slopes of the trailing arms. Parabolic dunes can range from tens to thousands of metres in

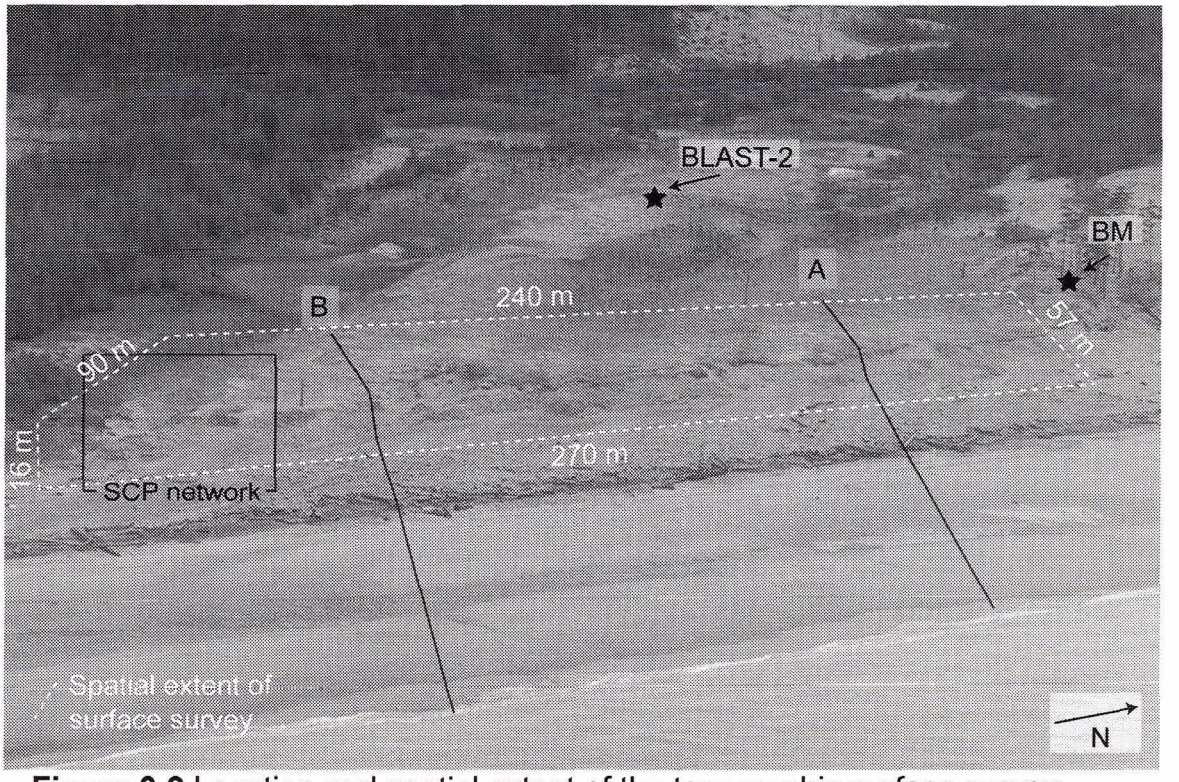

Figure 3.2 Location and spatial extent of the topographic surface survey, approximate location of cross-shore profiles A and B and the location of the SCP network used to assess the morphodynamics of a foredune-trough blowout complex. BM is the established benchmark used for recurrent surveying.

the driftwood, at topographic highs and lows in June 2002, June 2003, February 2004 and June 2004.

For this analysis, only two transects were selected to describe the morphological changes of the foredune, backshore and beach shown in Figure 3.2. These profiles were selected based on quality of the data, with 98% of all data points within 4° of the actual transect line of 118° (i.e., 2° on either side of the transect) (Figure 3.3). It is recognized that there is topographic variation within 4° of the transect over its length, approximately 200 m; however, this variation is believed to be minor compared with the scale of the analysis. Profiles were plotted as horizontal distance (HD) from the pin versus ellipsoidal elevation (Z)

This term is applied generally to many coalesced, migrating dune types including blowouts and parabolic dunes. More specifically, the term transgressive dunefield is used to define a coastal dune type that is characterized by a moderate- to large-scale active sand sheet migrating over terrain (Hesp and Thom 1990).

Transgressive dunefields may range in size from hundreds of metres to many square kilometres (Hesp et al. 1989). Their morphology is characterized by extensive, laterally continuous deflation basins, and an unvegetated to partially vegetated sand sheet terminating in a landward sinuous ridge (Hesp et al. 1989; Hesp and Thom 1990). The deflation plains of transgressive dunefields may host a variety of other dune types, including barchan dunes, transverse ridges, and coppice and shadow dunes (Hesp 1999). Transgressive dunefields generally develop when there is moderate to high onshore sand supply, strong onshore winds and limited pioneering plant growth (Hesp and Thom 1990).

2.3 Regional models of aeolian activity and dune mobility

The previous sections discussed the processes of aeolian sediment transport and the evolution and morphology of coastal dunes. One of the major challenges in aeolian geomorphology is linking the micro-scale process of aeolian sediment transport to the meso-scale morphological landforms it creates (Bauer and Davidson-Arnott 2002). To assess aeolian activity without detailed process-based wind measurements, a multitude of regional scale models have been developed that use standard meteorological data. Three models of this type that will be applied and critiqued for HG are: i) Fryberger's (1979) sediment drift

potential, ii) Lancaster's (1988) dune mobility index, and iii) Tsoar and Illenberger's (1998) modified dune mobility index. This section briefly introduces these models.

2.3.1 Fryberger's (1979) sediment drift potential

The Fryberger (1979) sediment drift potential model was developed to characterize desert dune morphology from standard meteorological data and broad coverage Landsat satellite imagery. Fryberger (1979) developed this model as part of a study on Global Sand Seas (McKee 1979) for the United States Geological Survey in coordination with the U.S. National Aeronautics and Space Administration to assess wind energy and sand transport potential in relation to dune form.

The Fryberger (1979) model uses standard wind data recorded at 10 m height to calculate the maximum regional sediment drift potential (DP) using a modified Lettau and Lettau (1978) (Equation 5) sediment transport equation:

$$DP = \frac{V^2(V - V_t)}{100} t \tag{6}$$

where V is mean wind speed measured at 10 m (in knots), V_t is the threshold of sediment transport (i.e., 12 knots, or 6 m/s) also measured at 10 m, and t is the time wind blew expressed as a percentage of the period of analysis. DP values are calculated for each wind direction, and through vector addition, the magnitude and direction of predominant drift are determined through the resultant drift potential (RDP) and resultant drift direction (RDD), respectively, which are expressed graphically by a sediment drift rose – a circular histogram.

Fryberger (1979) did not express DPs and RDPs as a measure of sediment flux (e.g., kg $m^{-1}s^{-1}$). Rather he created a unitless measure of sediment transport potential called vector units, or VU, which is typically expressed as a volume of sediment transported per width per year (e.g., m^3 m^{-1} a^{-1}) (Fryberger 1979; Bullard 1997). Vector units can be converted to proper flux values if the wind speed units are converted to m s^{-1} and an appropriate value for the bulk density of sand is used (Bullard 1997).

Through an assessment of over 130 sites distributed across Africa and Asia, Fryberger (1979) created a classification of wind regimes and aeolian landforms. To do this, he used DP as a measure of total transport potential and the RDP/DP ratio to characterize the directional variability in the wind regime (Table 2.1). The RDP/DP ratio, equivalent to the unidirectional index of Wilson (Wilson 1971), ranges from zero to one, where higher values indicate a uni-modal regime and lower values reflect a more complex or multidirectional wind regime.

Table 2.1 Fryberger's (1979) classification of wind energy environments using total DP and RDP/DP ratios.

Drift Potential Ranges (VU)	Energy of wind environment	Directional variability (RDP/DP)
<200	Low	< 0.3 Complex to obtuse bimodal
200-400	Intermediate	0.3 to < 0.8 Obtuse to acute bimodal
>400	High	>0.8 Wide to narrow unimodal

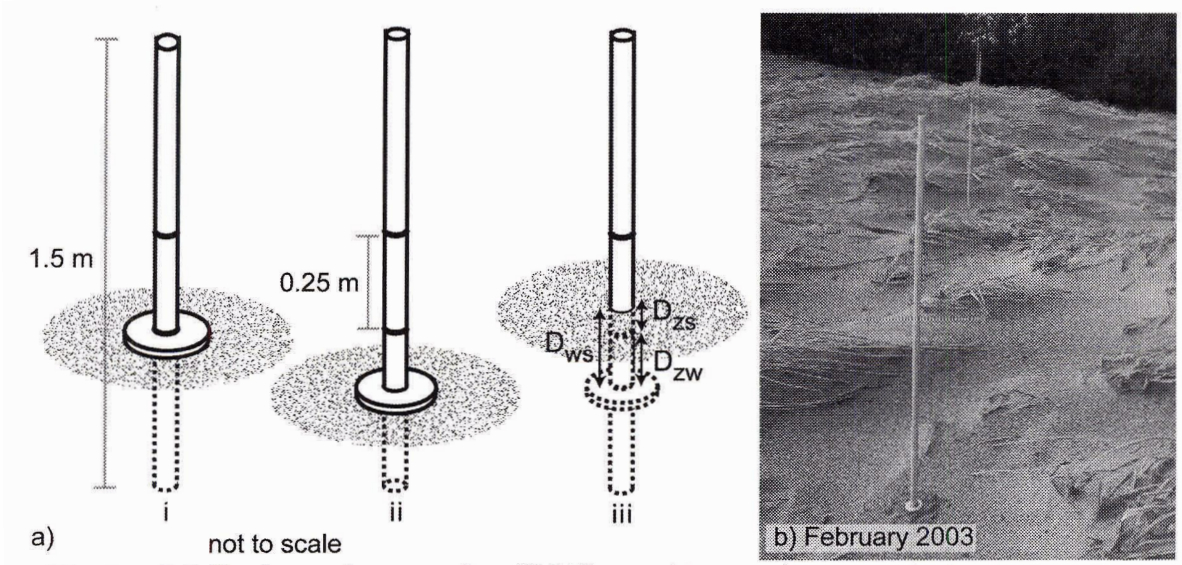

Figure 3.5 Surface change pins (SCP) used to monitor morphological and volumetric change of a trough blowout. At installation and reset (b), pins are set to the lower line with the washer at the surface (i). Washer and surface at the same height indicate only erosion (ii). Surface reworking occurs when the washer is deflated to some depth and redeposition occurs (iii). D_{ws} = distance from washer to surface, D_{zs} = distance from zero line to surface and D_{zw} = distance from zero line to washer.

Pins with washers are widely used to monitor depth of change in marine nearshore environments, where they are known as "depth of disturbance" (DOD) rods (e.g., Greenwood and Hale 1980, Greenwood and Sherman 1984). This research adapts this monitoring technique to a terrestrial sedimentary environment. The morphodynamics of a trough blowout-depositional lobe complex were assessed by plotting measurements of net surface change (D_{zs}), maximum deflation depth (D_{zw}) and redeposition (D_{ws}) on digital terrains maps produced from the 2002 topographic surface survey. To simplify the discussion, measurements from the SCP network are described by an ordinal classification (Table 3.2). However, the interval between recurrent measurements of the SCP network varies between three to eight months, and these measurements have

areas are active when values range between 100 and 200, and dunes are fully active when M is greater than 200 (Lancaster 1988). Through empirical assessments in predominantly continental desert environments (Ash and Wasson 1983; Pye and Tsoar 1990; Lancaster 1997b; Wolfe 1997; Lancaster and Baas 1998; Lancaster and Helm 2000; Knight et al. 2003), this model was shown to be a good indicator of dune mobility when used for longer-term monitoring over larger spatial scales. Attempts to calculate volumes or estimate rates of actual sediment transport over shorter time scales have failed, and this was not the intended use (Lancaster and Helm 2000).

2.3.3 Tsoar and Illenberger's (1998) dune mobility index

Tsoar and Illenberger (1998) argue that the mobility of an aeolian sedimentary environment is not accurately depicted by the P/PET ratio, as high infiltration rates in sand rapidly reduce the moisture available for vegetation growth. Instead, they suggest that dune mobility is best represented by the frequency, magnitude and directional variability of the wind, as wind provides the energy source for aeolian transport and limits vegetation growth on sand. They also suggest that the Fryberger (1979) model represents well the sediment drift potential of wind in aeolian environments and should be used to assess dune mobility. They provide the examples of an environment with low DP and high direction variability (lower RDP/DP ratio) where the potential for vegetation growth is greater as wind attacks are shared among the dune's slopes; whereas

in unidirectional environments there is more attack on one slope, thus less ability for vegetation to grow on that slope (Tsoar and Arens 2003).

From their analysis of 40 sites of aeolian dunes, Tsoar and Illenberger (1998) developed a dune mobility index by plotting DP versus RDP/DP values as follows:

$$M = \frac{DP}{1000 - (750\frac{RDP}{DP})} \tag{8}$$

where annual average values of M greater than 1 suggest sedimentary environments in which dunes are unvegetated and likely mobile (Tsoar and Illenberger 1998; Tsoar 2002). As of yet, this model has not been widely tested, and the sites from which it was derived are not provided.

3.0 Research Methods

This chapter describes the methods used to conduct a geomorphic assessment of the coastal dunes on East Beach, HG, to obtain each of the three objectives outlined in Section 1.2.

3.1 Morphological assessment of East Beach

The aeolian geomorphology of East Beach is assessed through the qualitative description and classification of four geomorphically distinct sites that illustrate the morphological diversity of this coast. For each site, dune form and evolution are discussed using three air photo series (Table 3.1), aerial videos and oblique photos taken during each field season. Coastal retreat is measured from the air photos between 1966 and 1980, but due to the small scale of the 1997 series, common features were not distinguishable and retreat rates could not be determined. Aerial video and digital oblique photos of the study region were captured simultaneously during two survey flights in the summers of 2002 and 2003. As the exact elevation, azimuth and speed of the plane are unknown, these images could not be used for quantitative measurements but are used for qualitative description. To facilitate the interpretation of the landforms from the photos, bar scales and north arrows have been added to all images.

Table 3.1 BC provincial air photo series and scales used for a morphological assessment of dune form and evolution on East Beach, HG.

Air photo series	Series number	Date taken	Scale
1966	BC4362	May 30	1:15840
1980	BC80008	May 10	1:12000
1997	BC97036	August 9	1:40000

3.2 Calculating aeolian activity and dune mobility

3.2.1 Meteorological data

Meteorological data for this analysis were obtained from three stations along the east coast of HG (Figure 1.1). Two are Environment Canada (EC) stations, located at Rose Spit (ID-1056869) and Sandspit (ID-1057050), and the third is a specialized meteorological station established by the UVic Geography Boundary Layer Airflow and Sediment Transport (BLAST) lab in June 2002, hereafter known as BLAST2 (Table 3.2).

The EC meteorological stations record wind speed and direction at the World Meteorological Organization's (WMO) standard height of 10 m. Wind data are recorded hourly but are not averages of the whole hour; rather, they are 1-minute, or since 1985, 2-minute, averages recorded on the hour to the nearest whole kilometre per hour (1 km hr^{-1} ~ 0.278 m s^{-1}). Wind direction is recorded as the direction the wind blew from in degrees to true north to the nearest tens of degrees on a 36-point compass (e.g., 10 degrees represents winds from 5 to 15 degrees). Precipitation data are recorded as hourly totals in millimetres for a 29-year period (1971-1999) at EC-Sandspit. No precipitation data are available for EC-Rose Spit.

Due to harsh weather and the remote nature of the two EC stations, there are large gaps in the data, as maintenance is delayed when instruments malfunction. For the analysis of aeolian activity, the selection of years is based

Table 3.2 Metadata for meteorological stations.

	EC-Rose Spit	EC-Sandspit	BLAST2
Station location (latitude and longitude)	54.17^0 N 131.670 W	53.25^0 N 131.820 W	54.07^0 N 131.680 W
Station number	1056869	1057050	N/A
Tower height (m)	10	10	5
Units and precision of wind speed recorded	0 km h^{-1}	0 km h^{-1}	0.00 m s^{-1}
Wind speed recording	Average of 2 minute recording on the hour	Average of 2 minute recording on the hour	Hourly average of 1 Hz sampling
Wind direction grouping	Tens of degrees	Tens of degrees	No aggregation (hundredth decimal precision)
Precipitation (mm)	N/A	Hourly sum	Hourly sum
Period of data used	1995-1999	1971-2000	August 15, 2002 to June 3, 2004

N/A - not available

primarily on the availability and continuity of the data (i.e., the years with the lowest percentage of missing data).

BLAST2, the second source of meteorological data for this analysis, is located on the largest parabolic dune complex on East Beach, approximately 170 m inland from the foredune crest (Figure 3.1). The station is located at Site 2, also the location of the two-year geomorphic assessment of a foredune-trough blowout complex (Chapter 6). BLAST2 consists of a Campbell Scientific Inc. meteorological station recording hourly averaged wind speed (m s^{-1}) and wind

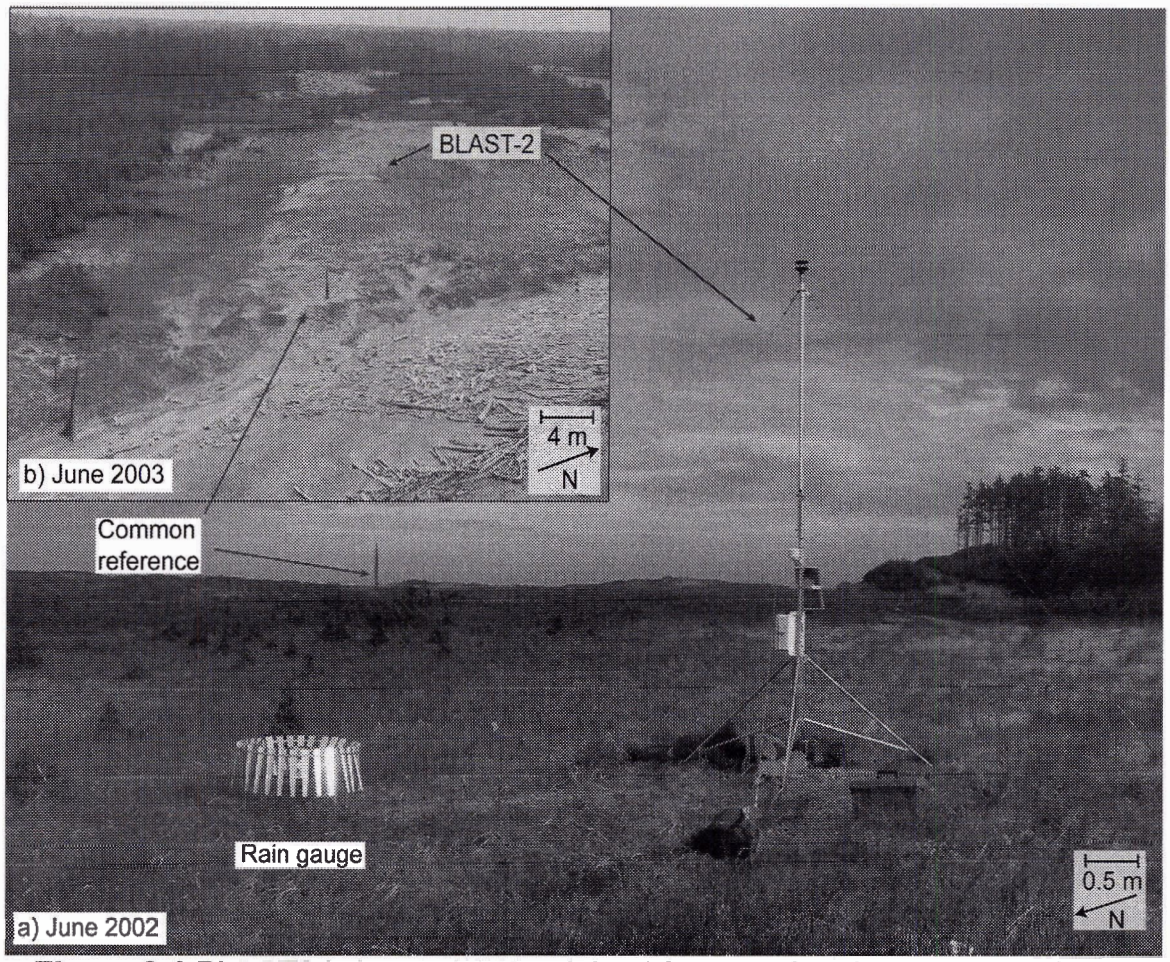

Figure 3.1 BLAST2 is located 170 m inland from the foredune crest on the longest parabolic dune complex on East Beach (Site 2 – Figure 1.1). This station measures on-site winds at 5 m and other meteorological variables including temperature, relative humidity, precipitation and atmospheric pressure. Tree snag indicates a common point of reference.

direction (degrees to true north) with no aggregation, from a Gill™ Windsonic ultrasonic anemometer mounted at 5 m. This instrument samples wind speed and direction at 1 Hz, then records an average for the whole hour. For logistical reasons, the BLAST2 wind speed data are recorded at 5 m, not at the WMO height of 10 m. To allow comparison between meteorological data and to apply the Fryberger (1979) sediment drift potential model (see below), the Law of the Wall (Equation 1) was applied, using an intermediate roughness length of 0.05 m

to characterize surface roughness of the vegetation (Touma 1977; Taylor and Lee 1984).

The BLAST2 station was installed to characterize the wind regime and conditions experienced by the dunes, rather than applying wind data from a remote station that may not reflect on-site conditions. However, the average wind speed from the BLAST2 station (4.8 m s^{-1}) compared with that from EC-Rose Spit (7.7 m s^{-1}) for the same period was markedly lower. This results from the location of the two stations as well as the height of their anemometers. BLAST2 is situated in the deflation plain of a large parabolic dune with low hummocky terrain and trees to the north and west, while EC-Rose Spit is completely exposed from all directions except the southwest, as it is situated on a spit.

As the BLAST2 station records wind speed at 5 m height, the conversion of wind speed from 5 m to that at 10 m required the application of the log-law, similar to Equation 1, which is sensitive to variations in surface roughness length and wind speed. For this analysis, a single intermediate value for roughness length (0.05 m) (Oke 1978) was chosen and used to convert all wind speeds, there by both under- and over-estimating the actual wind speed at 10 m.

3.2.2 Assessing regional wind regime

To characterize the wind regime in this region, one annual and 12 monthly average wind roses were produced using Golden Software Grapher™ 4.0 from a 5-year wind record from EC-Rose Spit (1995-1999). This period was selected as it contained the smallest proportion of missing data for wind speed and direction

at 2%, with annual percentages of missing data ranging from 0.48% to 4.66%. Only EC data were used for this characterization as BLAST2 had limited temporal coverage (i.e., less than two years).

Wind speed data were aggregated into four wind speed classes, with all non-transporting winds (< 6 m s^{-1}) in the lowest class, increasing at intervals of 6 m s^{-1} (i.e., 6-12, 12-18, >18 m s^{-1}). Wind direction data were aggregated into 12 direction classes centred on the major cardinal directions (north, east, south, west), each containing 30 degrees of the compass. To characterize the regional wind regime, the frequency and magnitude of winds, their directional variability and modality, and the proportion of winds above the threshold for sediment transport were assessed, both annually and monthly.

3.2.3 Calculating sediment drift potential

Fryberger's (1979) sediment drift potentials were calculated using wind data from both EC-Rose Spit and BLAST2. EC-Rose Spit data were used to characterize the long-term average regional wind regime, while BLAST2 data were only used to characterize aeolian activity experienced by the trough blowout complex during the two-year morphological study due to the limited temporal coverage. Wind data were processed into frequency tables consisting of six wind speed classes in knots (i.e., 12 - 16.99, 17 - 21.99, 22 - 26.99, 27 - 31.99, 32 - 36.99, >37 knots) and 36 direction classes, each containing 10 degrees and centred on north (0^{o}). Frequency of wind is proportional to the entire data set, including non-transporting winds, but only wind classes above the threshold of

sediment transport of 6 m s^{-1} (~12 knots) were used to calculate drift potential (DP). The Fryberger sediment transport equation (Equation 6) was applied to each wind speed and direction class using the wind speed class mid-point for V (e.g., for wind speed class 12-16.99, the mid-point is 14.5 knots), the threshold of transport (V_t) of 12 knots and t as the percentage of time wind blew in that wind class.

Directional DPs for each of the 36 direction classes were calculated by summing the six DPs in the direction bin. Subsequently, a total DP was determined by summing all directional DPs. The RDP and RDD were calculated through vector analysis using the mid-point of the wind direction class (e.g., for wind direction class 15-25° the midpoint is 20°). Sediment drift roses were plotted manually in a graphics program (i.e., Adobe Illustrator 10).

3.2.4 Calculating dune mobility

The Lancaster (1988) mobility index (M) was calculated for the study region using the 30-year EC climate normals (1971-2000) from the Sandspit meteorological station. These data were used due to the lack of precipitation data at EC-Rose Spit and the high percentage of missing precipitation data at EC-Sandspit during the 5-year period (1995-1999) used for the regional wind assessment. Although climate normals conceal inherent climate variability, they are the most complete record available and represent the average annual and monthly values for precipitation and temperatures under WMO standards.

Lancaster's (1988) dune mobility index (Equation 7) was applied using the annual wind competence (W), precipitation (P) and potential evapotranspiration (PET). Annual W was extracted from the 30-year wind record (1971-2000) from EC-Sandspit with a threshold value of 6 m s^{-1} (21.5 km hr^{-1}). For this period, there is a low average percentage of missing data for wind speed at 0.8%, with annual values ranging from 0% to 11.8%. Monthly precipitation and air temperature, from the 30-year climate normals, were used in combination with tables developed by Thornthwaite and Mather (1957) to calculate monthly PET values that were summed to yield an annual PET.

The Tsoar and Illenberger (1998) dune mobility index (Equation 8) was calculated using the annual DPs and RDPs from the 5-year (1995-1999) record from EC-Rose Spit.

3.3 Geomorphic monitoring

Since June 2002, a foredune-trough blowout complex on the highly energetic, retreating coast of East Beach was monitored through topographic surveys, cross-shore profiles and repeat measurements of an extensive surface change pin (SCP) network.

3.3.1 Topographic surveys

In June 2002, benchmark (BM) at 54°04.1'N by 131°40.7'W was established to the north of the site, marked by a 1.5 m rebar stake driven into the ground. A relative coordinate system was established at this BM oriented to

magnetic north with arbitrary coordinates of northing (N) = 1,000 m, easting (E) = 500 m and elevation (Z) = 50 m. All elevation values were recorded as distance below the arbitrary benchmark at 50 m and converted to ellipsoidal elevation. Ellipsoidal elevations are used throughout as they provide a good relative measure of elevation, whereas converting to mean sea level or chart datum on East Beach would introduce error and decrease accuracy. Measurement error, due to rod placement and sinking at the surface, is estimated to be ± 2 cm for points shot from the Topcon™ total station.

A detailed topographic survey of the foredune and foredune plain was conducted in June 2002 covering 270 m by 90 m with sampling density of 0.23 pts m^{-2} (5,700 points) (Figure 3.2). Re-measured in early July 2004, the survey was extended to include the driftwood jam on the backshore, with resulting coverage of 120 by 270 m with sampling density of 0.17 pts m^{-2} (5,260 points). The surface survey was conducted by running transects perpendicular to the foredune crest with point selection at significant changes in slope. Point resolution varies across the surface, with highest density along the topographically complex foredune crest and stoss slope, with decreasing point density seaward across the driftwood jam and landward over the foredune plain.

Morphological change of the beach-foredune complex was monitored through the recurrent survey of six cross-shore transects (118°) tied into the same coordinate system as the surface survey. Transects commenced at a rebar pin located approximately 80 m landward from the foredune crest to the waterline at the time of measurement. Measurements were taken of the sand surface, not

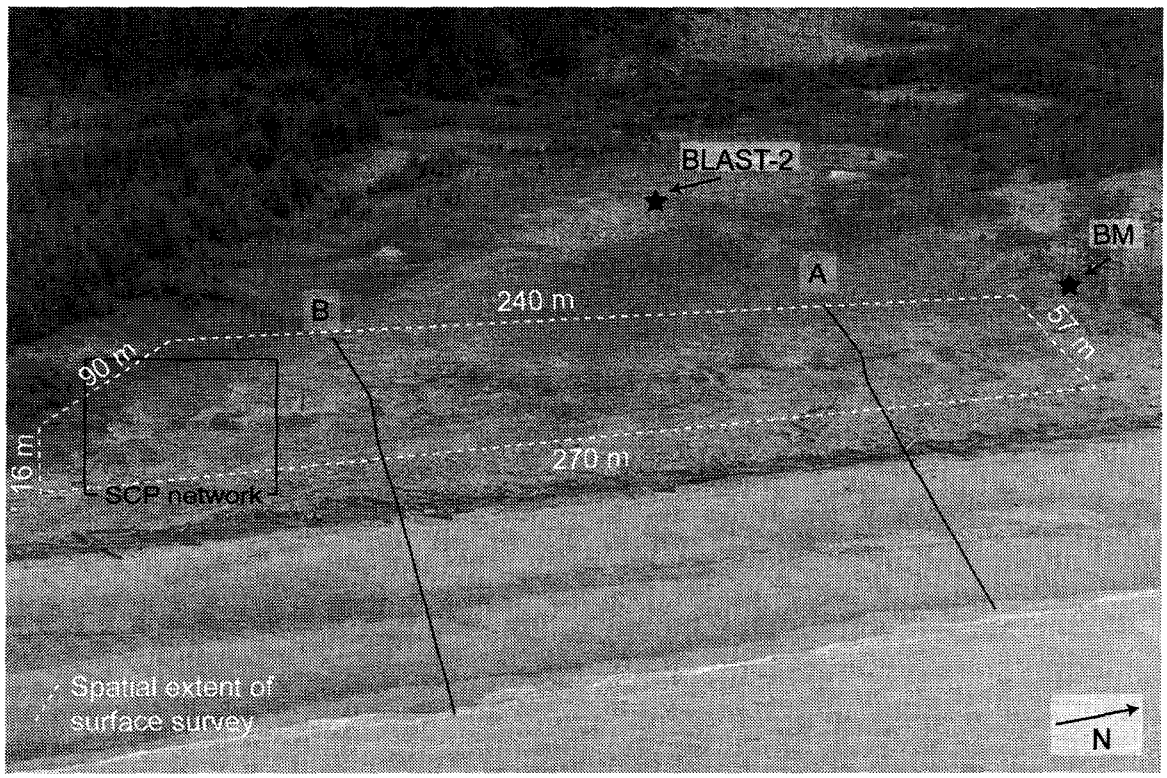

Figure 3.2 Location and spatial extent of the topographic surface survey, approximate location of cross-shore profiles A and B and the location of the SCP network used to assess the morphodynamics of a foredune-trough blowout complex. BM is the established benchmark used for recurrent surveying.

the driftwood, at topographic highs and lows in June 2002, June 2003, February 2004 and June 2004.

For this analysis, only two transects were selected to describe the morphological changes of the foredune, backshore and beach shown in Figure 3.2. These profiles were selected based on quality of the data, with 98% of all data points within 4° of the actual transect line of 118° (i.e., 2° on either side of the transect) (Figure 3.3). It is recognized that there is topographic variation within 4° of the transect over its length, approximately 200 m; however, this variation is believed to be minor compared with the scale of the analysis. Profiles were plotted as horizontal distance (HD) from the pin versus ellipsoidal elevation (Z)

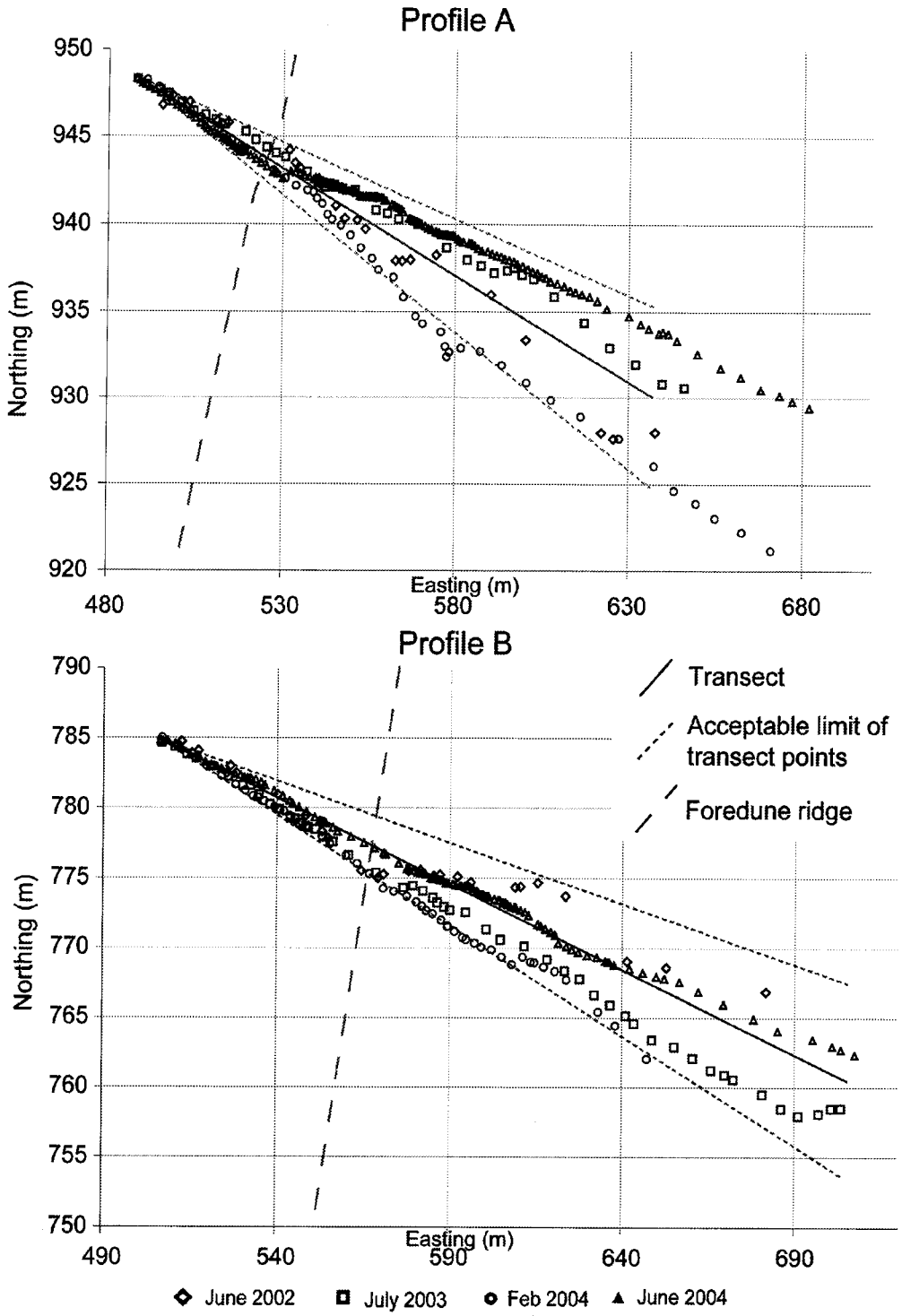

Figure 3.3 Near dune normal transects established in June 2002 and measured in June 2003, February 2004 and June 2002. The transect bearing is 118° (solid line) while the short dashed lines are 2° either side of the actual transect (i.e., transects are within 4°of acceptable error).

with three times vertical exaggeration. As they run near crest normal, profiles were rotated to dune normal so that the horizontal measurements were not exaggerated. These measurements, combined with photos taken during field visits, were used to describe morphological change during the two-year period of study.

3.3.2 Surface change pins (SCP)

To assess seasonal morphologic and volumetric change of a trough blowout-depositional lobe complex, a network of surface change pins (SCP) was established in June 2002. The SCP network was oriented parallel to the trough of the blowout, consisting originally of 174 pins spaced 2.5 m perpendicular to and 5 m parallel to the axis of the blowout (Figure 3.4). The network was expanded to 275 pins in June 2003 with pins added along the north and west edges to further include the depositional lobe (Figure 3.4). The location and elevation for each pin were tied into the referencing system presented above.

SCP are aluminum rods 1.5 m in length, each inscribed with a unique identification number and two lines: one at 50 cm and the other at 75 cm from the top of the pin (Figure 3.5). In February 2003, washers were installed on 70% of the pins and by September 2003, washers were installed on all pins. At initial installation and pin reset, SCPs were driven into the ground and set to the lower line (Figure 3.5 a). Pin measurements were conducted by measuring the height of the surface to the top of the pin or one of the measurement lines, while washer depths were measured to the surface with a measurement error of ± 2 mm.

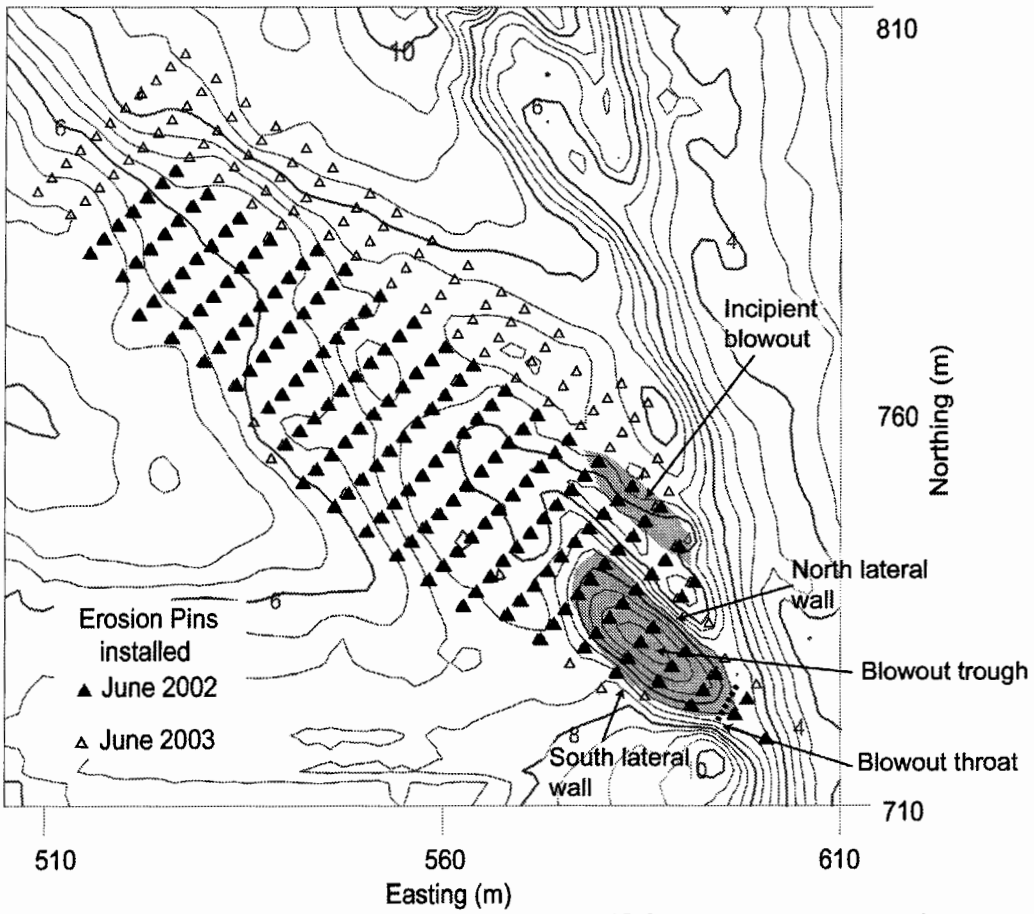

Figure 3.4 Location of surface change pins (SCP) within the trough blowout-depositional lobe compex. Components of the trough blowout are labeled to facilitate description of morphological change discussed in Chapter 6. Elevations are in metres above the ellipsoid with a 0.5 m contour interval.

Surface elevations were determined by associating the pin identification number with the location and elevation from the topographic survey measured as the height above the ellipsoid. Traditionally, SCPs or erosion pins have been used to quantify net surface change by measuring the distance from the zero line to the surface at time of measurement (D_{zs}) (Figure 3.4), a value that is positive for net accretion or negative for net erosion. With the addition of washers to the SCP network, a new dimension of geomorphic change can be monitored.

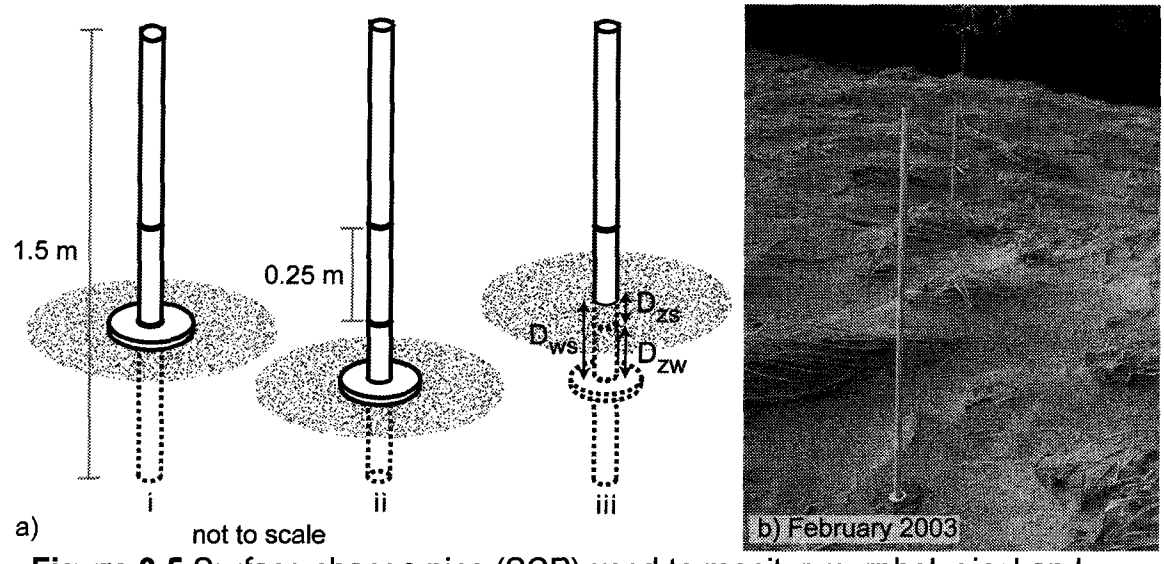

Figure 3.5 Surface change pins (SCP) used to monitor morphological and volumetric change of a trough blowout. At installation and reset (b), pins are set to the lower line with the washer at the surface (i). Washer and surface at the same height indicate only erosion (ii). Surface reworking occurs when the washer is deflated to some depth and redeposition occurs (iii). D_{ws} = distance from washer to surface, D_{zs} = distance from zero line to surface and D_{zw} = distance from zero line to washer.

Pins with washers are widely used to monitor depth of change in marine nearshore environments, where they are known as "depth of disturbance" (DOD) rods (e.g., Greenwood and Hale 1980, Greenwood and Sherman 1984). This research adapts this monitoring technique to a terrestrial sedimentary environment. The morphodynamics of a trough blowout-depositional lobe complex were assessed by plotting measurements of net surface change (D_{zs}), maximum deflation depth (D_{zw}) and redeposition (D_{ws}) on digital terrains maps produced from the 2002 topographic surface survey. To simplify the discussion, measurements from the SCP network are described by an ordinal classification (Table 3.2). However, the interval between recurrent measurements of the SCP network varies between three to eight months, and these measurements have

Table 3.2 Ordinal classification of SCP measurements.

Measurement range	Ordinal classification
Surface Change (m) - distance zero line to surface (D_{zs})	
>0.3 to 0.45	major deposition
>0.15 to 0.3	moderate deposition
>0 to 0.15	minor deposition
>-0.15 to 0	minor erosion
>-0.3 to -0.15	moderate erosion
-0.45 to -0.3	major erosion
Deflation (m) - distance zero line to washer (D_{zw})	
0	no deflation
>-0.05 to 0	minor deflation
>-0.15 to -0.05	moderate deflation
-0.45 to -0.1	major deflation
Redeposition (m) - distance washer to surface (D_{ws})	
0	no redeposition
>0 to 0.15	minor redeposition
>0.15 to 0.3	moderate redeposition
>0.3 to 0.5	major redeposition

not been temporally standardized. As such, the magnitude of surface change, deflation and redeposition must be considered as relative to the length of the measurement period.

3.3.3 Morphological and volumetric change

Raw topographic and SCP data were processed using Golden Software Grapher™ 4.0 and Surfer™ 8.0. These programs allowed the plan, cross-sectional and three-dimensional representation and spatial analysis of geomorphic change, as well as the calculation of volumetric change between surfaces.

For the volumetric change of the foredune complex, the two surface surveys were gridded by the default Kriging approach, with grid resolution set to

1.5 m. This resolution produced the lowest calculated residuals compared with 1 m and 2 m grid spacing. To calculate volumetric change between surfaces, the spatial extent of each survey was constrained to the same area, and the same grid size was used. The 2002 surface survey was then subtracted from that in 2004. Results of surface change were plotted on a contour map of the site, with blue as deposition and red as erosion.

Volumetric change for each measurement period of the SCP network was also determined by gridding each surface with the default Kriging approach but with 1 m grid resolution, which provided the lowest residuals. Each grid was spatially constrained by the area of the SCP network (i.e., pre-June 2003 versus post-June 2003). Once the grid size, spatial extent and reference elevations were the same, earlier surfaces were subtracted from later surfaces (e.g., June 2003 – February 2003) to yield negative surface values when erosion occurred. Volumetric results yielded a net positive surface, a net negative surface and a total surface change. Values of volumetric change were standardized both spatially (by dividing by the spatial area of the SCP network at that time of measurement) and temporally (by the number of months the measurement period covers), yielding a value with units of $m^3\ m^{-2}\ month^{-1}$ or surface change of $m\ month^{-1}$.

3.3.4 Aeolian activity

Volumetric change of the foredune and foredune plain were compared with estimates of potential sediment drifts calculated from the BLAST2 wind data

using the Fryberger (1979) model. This was conducted using the two years of BLAST2 data, with wind velocity measured in m s^{-1}, to yield an annual RDP. Using Line A from Bullard's (1997) conversion of DP in VU to rate of sand transport potential in m^3 m-$width^{-1}$ a^{-1}, the RDP was converted to a rate of sediment transport.

For each of the measurement periods of the SCP network, wind roses were plotted using BLAST2 data. To assess and compare wind energy between measurement periods, the Fryberger (1979) sediment drift potential model was applied using BLAST2 wind data (see Section 2.2.3). To allow comparison, wind energies were temporally standardized by the number of months for each measurement period. As nearly two months of BLAST2 data were lost (late June through mid-August 2002) due to insufficient memory in the datalogger, this period was standardized by the number of months of wind data available, not the length of time between measurements of the SCP network.

4.0 Aeolian geomorphology of East Beach, HG

This chapter presents the environmental setting of the coastal dunes on East Beach, HG, including a discussion of: i) the Quaternary history, ii) the regional climate, iii) the wind, wave and current regimes, iv) the sediment source and properties, and v) the types and influence of various 'roughness elements,' including vegetation and driftwood. This is followed by the documentation and qualitative description of four distinct sites of aeolian dunes on this coast.

4.1 Environmental Setting

4.1.1 Quaternary History

HG has experienced a very different glacial history than mainland British Columbia, yielding a complex and dynamic landscape (Clague 1982). The Cordilleran ice sheet reached its maximum in this region after 21 ka BP (C^{14} years) but before 15 ka BP (Blaise et al. 1990). At its greatest extent, it did not cover HG. Instead, HG was covered by independent piedmont and ice-cap glaciers that originated in the Queen Charlotte Mountains to the south (Barrie and Conway 2002). These glaciers retreated from HG much earlier (13.5 – 13 ka BP) than the Cordilleran ice sheet from the mainland (10 ka BP), resulting in varied isostatic response.

Relative sea levels on HG during the Holocene have been influenced by isostatic depression, eustatic sea-level changes and tectonic activity, although over the last 100 years tectonic activity effects on sea-levels have been negligible (Larsen et al. 2003). When the Cordilleran ice sheet retreated from

northern Hecate Strait (13 ka BP), a forebulge of 50 to 100 m magnitude developed in response to crustal depression of the mainland (Hetherington and Barrie 2004). As a result, HG uplifted, producing a sea-level low stand of 150 m below present levels (Hetherington and Barrie 2004). During this period, the eustatic sea level was rising, but at a much slower rate.

The eustatic sea-levels continued to rise throughout the Holocene but sometime after 12.4 ka BP, subsidence of the glacio-isostatic forebulge yielded a rapid sea-level transgression (Barrie and Conway 2002). By 9.1 ka BP, sea levels reached current levels and continued to rise to a high stand of 13 to 16 m above current levels by 8.9 ka BP (Clague 1982; Fedge and Josenhans 2000). Since 3.8 ka BP, the sea level has regressed, leaving relict, prograding beach and dune ridges on the north coast, most of which are formed by or capped with aeolian sands (Walker and Barrie 2004) (Figure 1.2b). On East Beach, the relict dune ridges are separated by low-lying inter-dune areas that are presently being transgressed as the coastline retreats at 1 to 3 m a^{-1} (Barrie and Conway 2002). This rapid rate of retreat, combined with high wind energy, is creating a landscape of highly active Holocene dunes interspersed with eroding Pleistocene cliffs.

4.1.2 Climate

The Köppen classification system designates HG as having a marine West Coast cool (C_{fb}) climate, where *C* is a moist, subtropical, mid-latitude climate, *f* signifies no period of precipitation deficiency, and *b* signifies a median

range of temperature where summers are cool and winters are mild. Moderated by the Pacific Ocean, temperatures are mild year-round, with an annual average of 8.3°C, and a seasonal variation with daily means from 3.2°C in January (high 5.6°C, low 0.7°C) to 15.0°C in August (high 17.9°C, low 12.1°C) (EC-CMC 2002) (Figure 4.1). Freezing temperatures are infrequent in this region, with an average of 4.7 days a^{-1} below 0°C for 1971-2000, a notable decrease from the previous climate normals for 1969-1990, with 38 days a^{-1}.

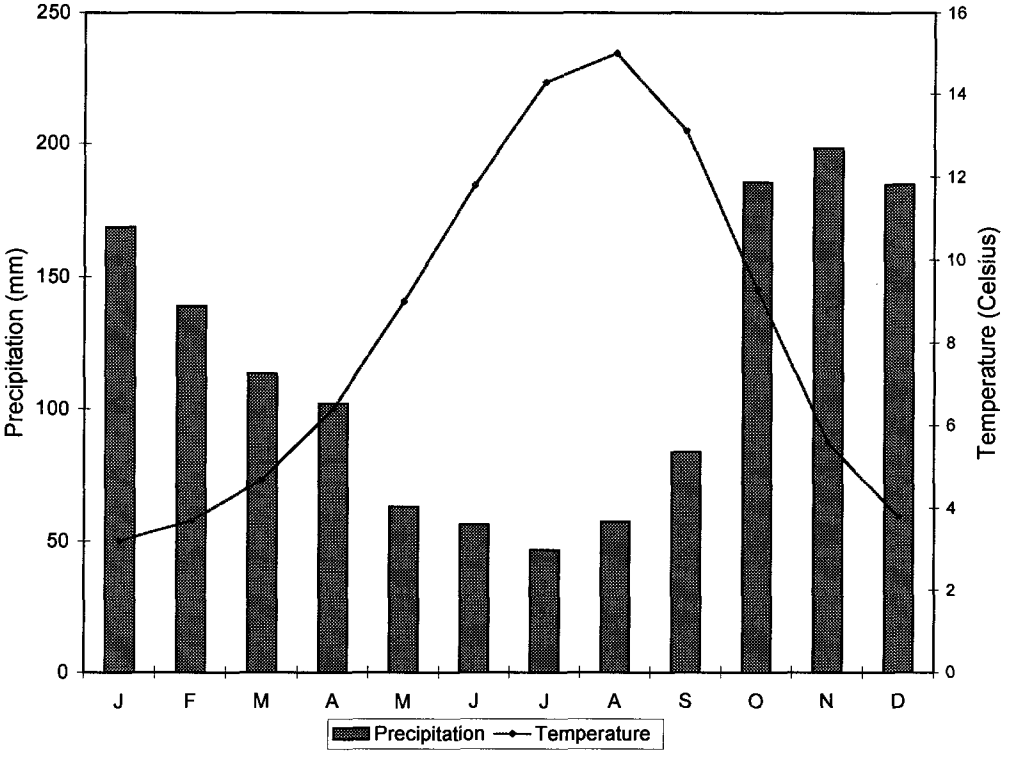

Figure 4.1 Monthly 30-year climate normals from EC-Sandspit (1971-2000) illustrate the seasonality of both temperature and precipitation. Values shown for precipitation (mm) represent total monthly average values of both rain and snow. Values for temperature (°C) represent average monthly temperatures determined by calculating the mean from the highest monthly high and lowest low.

HG experiences high year-round precipitation, with a total annual average of 1,398.4 mm recorded at EC-Sandspit (1971-2000). Of the total precipitation,

53% falls in four months from October through January, with markedly less (11%) precipitation during the summer (June through August) (Figure 4.1). November experiences the greatest monthly average precipitation (198.2 mm), while the least is received in July (46.6 mm). Snowfall may occur during the winter months (December through March) but is short-lived and constitutes only 4% of the total precipitation.

4.1.3 Wind regime

The prevailing winds in the northeast Pacific are controlled by the location and intensity of the Aleutian Low (AL), centred over the Gulf of Alaska, and the Pacific High (PH), generally centred at 35°N and 150°W (Thomson 1995). During winter months, the AL deepens, resulting in the development of storms that track northward along the west coast of British Columbia, intensifying rapidly as they approach the centre of the pressure system. These storms bring strong moisture-laden winds exceeding 30 m s^{-1} from the south to southeast over Hecate Strait. In May, the AL dissipates and retreats, while the PH intensifies and generates west to northwest winds from June to August. During summer months, however, HG still experiences frequent gale-force (i.e., 18 m s^{-1}) southeast storms as low-pressure systems migrate over northern waters.

The annual average wind regime on East Beach is oblique bimodal (Figure 4.2). The strongest and most frequent winds blow from the southeast (obliquely onshore), while a secondary mode of winds of lower magnitude blow from the west to northwest (offshore). The average annual wind speed recorded

at EC-Rose Spit for 1995-1999 is 8.5 m s^{-1}. For this period, 62% of winds recorded were above the threshold of sediment transport (i.e., 6 m s^{-1}), with calm conditions recorded less than 1% of the time. For a detailed annual and monthly assessment of the wind regime, see Section 5.1.

Prominent sources of inter-annual variability in weather patterns and storm events in the Pacific Northwest are known climate phenomena such as the El Niño Southern Oscillation (ENSO) and the Pacific Decedal Oscillation (PDO) (Viles and Goudie 2003). Positive, or warm, phases of the ENSO result in deeper than normal Aleutian Lows during December through February (Shabbar et al. 1997). In negative, or cool, phases of the Southern Oscillation (La Niña), a high-pressure area forms south of Alaska that blocks the deepening of the Aleutian Low, thus moderating storm activity. During warm phases of the PDO, warmer water is observed along the west coast of North America and the Aleutian Low is enhanced in the winter months, while the cool phase shows roughly the opposite conditions (Zhang et al. 1997). A warm phase of the PDO will enhance an ENSO event. El Niño events occur every three to seven years (Allan and Komar 2002), while the PDO shifts from warm to cool phases approximately every 25 years (Gedalof and Smith 2001).

Recent El Niño events have produced enhanced storm waves and wind events along the Pacific coast of North America from California to Washington (Storlazzi et al. 2000; Allan and Komar 2002). During the 1997-98 El Niño, when

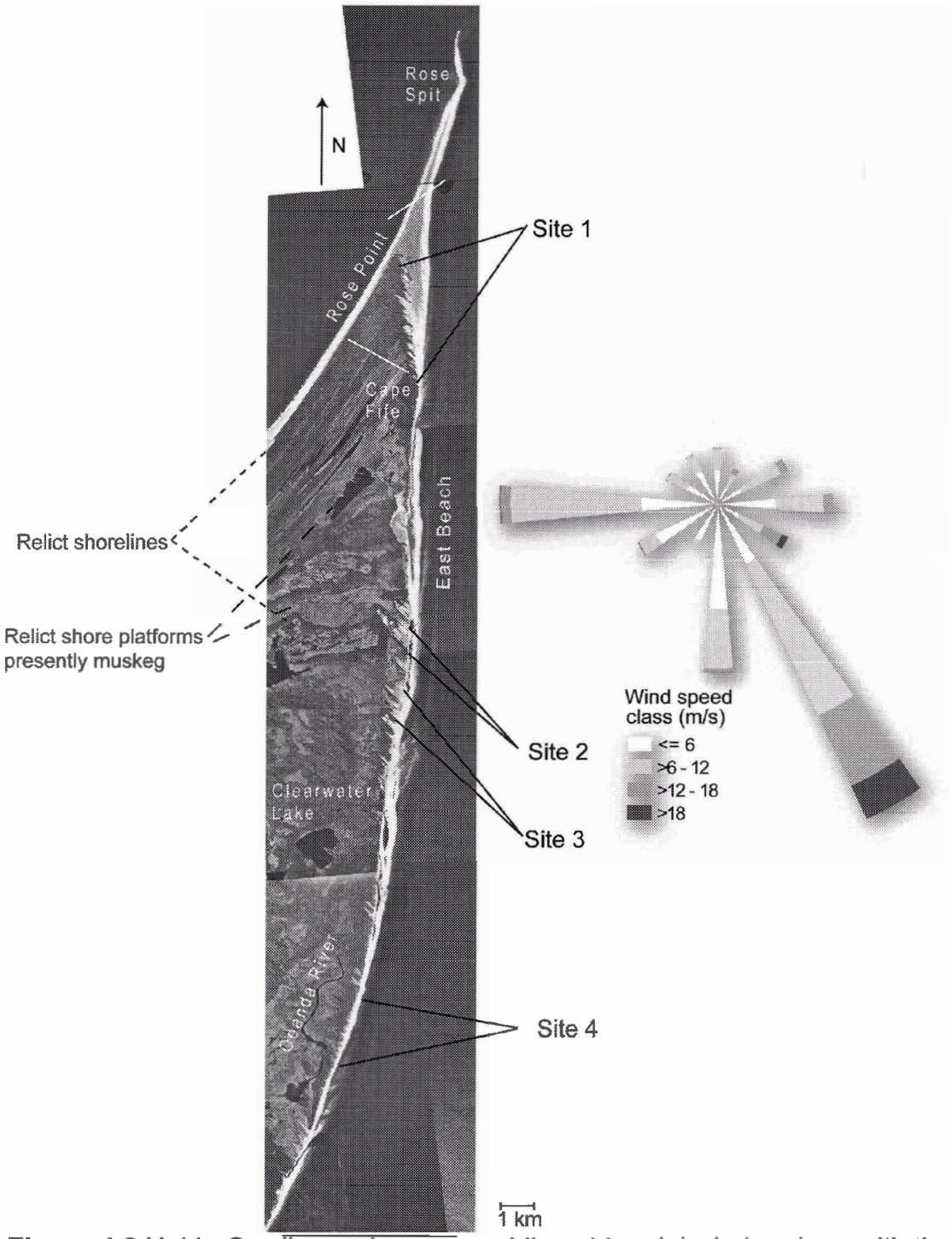

Figure 4.2 Haida Gwaii experiences an oblique bimodal wind regime, with the predominant wind direction from the southeast blowing obliquely onshore to East Beach, and a second mode of winds from the west blowing offshore (EC-Rose Spit 1995-1999). Photo mosaic from BC provincial airphotos BCB97035_4,6,12,14,184,187,189)

regional sea level rose 0.4 m, Barrie and Conway (2002) observed 12 m of coastal retreat. To date, the full extent of influence of these two modes of climate variability on HG is unknown, though preliminary results from Abeysirigunawardena and Walker (unpublished data) show strong linkages between storm winds and the PDO. From their analysis, storms characterized by strong winds from the east and the south have become more frequent in response to the sharp regime shift in the PDO in the mid 1970s from negative to positive, supporting the recent observations of increased storminess in this region.

4.1.4 Tide, current and wave regime

The tidal regime in this area is mixed semi-diurnal and macrotidal ranging from 4.5 to 7 m, with HHWMT exceeding 7 m. As the east coast of HG is sheltered from Pacific swell, waves experienced on this coast are typically generated locally by wind, therefore the waves follow a similar seasonal regime. The annual average significant wave height (H_s) is 1.8 m, rising to an average H_s of 2.8 m during the winter months of November through January, with a maximum observed H_s of 14.3 m in December (Eid et al. 1993).

Waves and currents produced by southeast winds run oblique to East Beach, driving a strong northerly longshore sediment drift (Harper 1980). This active littoral system transports sediments in the nearshore and creates multiple, migrating shore-attached sand bars along the northern section of East Beach (Barrie and Conway 1996) (Figure 4.3). These bars often become exposed at low

tide, allowing wind to transport sediment onshore to the beach and backshore (Walker and Barrie 2004).

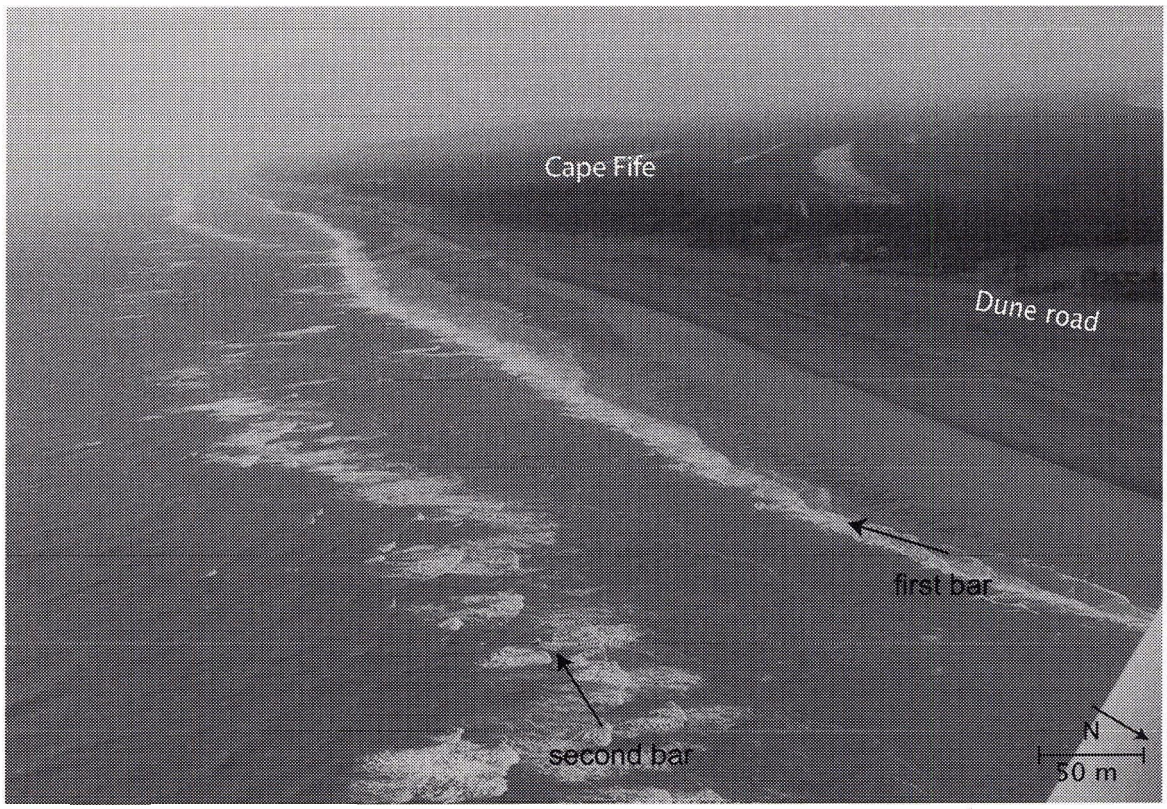

Figure 4.3 Sediments are stored in the nearshore and transported alongshore in multiple-shore parallel and shore attached bars maintained by tidal currents and storm driven wind-waves.

4.1.5 Sediment characteristics and source

The Naikoon Peninsula is a relatively flat plain of unconsolidated Quaternary glacio-fluvial sands (Barrie and Conway 1996). Sediments were deposited during the last glacial retreat and have subsequently been reworked into the current landscape of relict shorelines, bars and offshore deposits. Samples from a foredune on East Beach show that the aeolian sediments on this coast are mainly quartz sands with traces of magnetite and shell fragments.

Sediments have an average grain size of 1.65 ϕ (i.e., 320 μm), and thus are slightly larger than Bagnold's (1941) standard grain size (i.e., 250 μm), are well-sorted (standard deviation = 0.44) and are finely skewed (skewness = 0.27).

The sediment supply for the dunes on East Beach is from the nearshore, and the glacio-fluvial and Holocene aeolian sands eroding from bluffs like those of Cape Ball (Figure 4.4a and b) and Cape Fife (Figure 4.4c and d). These bluffs experience frequent wave attack, resulting in retreat of the bluff as sediments are transferred to the nearshore littoral system. Intense swash action and strong alongshore tidal currents transport sediments northward in shore-parallel bars that become shore-attached along the north of East Beach (Figure 4.3). These bars become exposed at moderate to low tides, greatly enhancing the supply of sediments to aeolian processes and the backshore dune systems.

Walker and Barrie (2004) observed heightened erosion of the beach and bluff systems at the heads of these bars. Nearshore bars dissipate storm surge energy, but at the heads of the bars, wave energy appears to be focused, thereby enhancing erosion. Subsequently, as the bars migrate northward, the sediment supply to the backshore is enhanced, allowing increased delivery of aeolian sands to the backshore, thereby infilling wave-cut scarps and feeding the dunes.

4.1.6 Vegetation

The vegetation on the backshore and dune systems of East Beach is predominantly American dune grass (*Elymus mollis*) (Figure 4.5a) and several

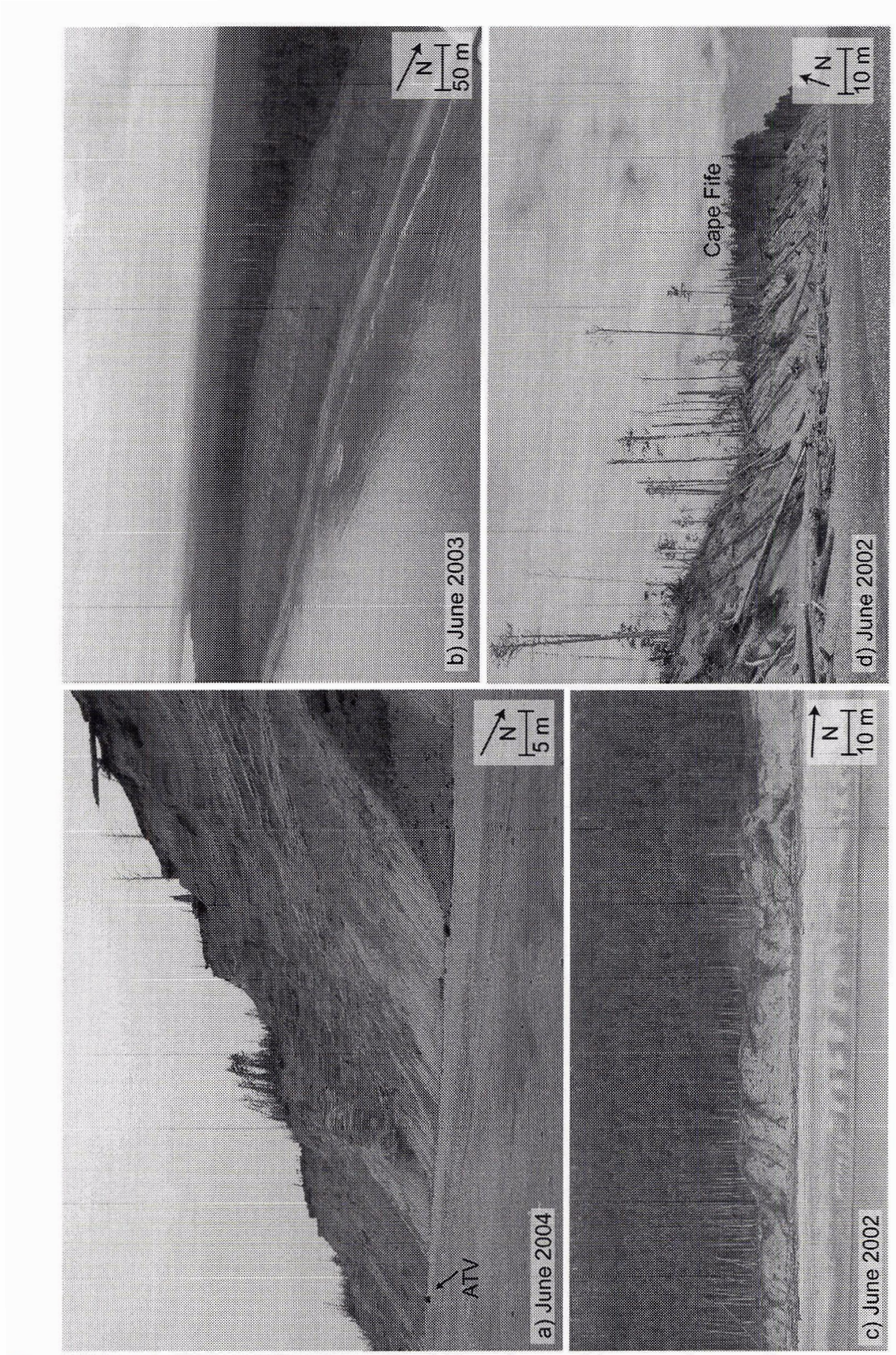

Figure 4.4 Eroding cliffs along East Beach provide a major sediment source for the dunes on this coast. Cape Ball (a and b) and Cape Fife (c and d) have minimal driftwood stored at the base, thus they are exposed directly to wave attack at high tide and during storm surge.

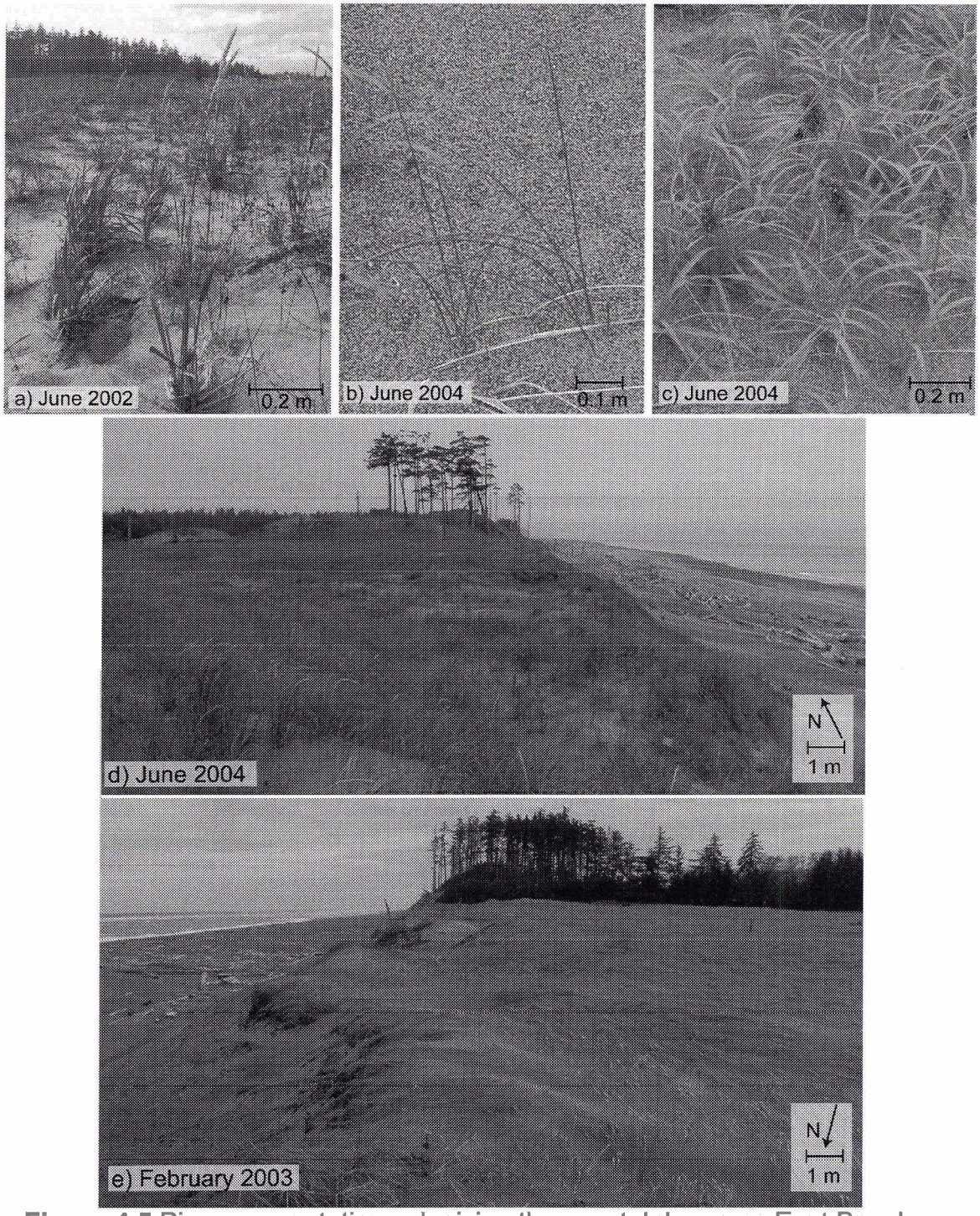

Figure 4.5 Pioneer vegetation colonizing the coastal dunes on East Beach, HG: a) American Dune grass (*Elymus mollis*), b) various species of rush (*gn. Jenus*), c) large-head sedge (*Carex macrocephela*). d) vegetation cover on a foredune as seen in summer compared with (e) winter, when grasses and rushes die back.

species of rush (genus *Juncus*) (Figure 4.5b), as well as the large-head sedge (*Carex macrocephala*) (Figure 4.5c) (Wiedemann et al. 1999). All are robust, perennial species that thrive in sandy and salty environments, exposed to full sun, and are resistant to water-level changes and aeolian abrasion and deposition (Pojar and MacKinnon 1994). These grasses provide a surface roughness that promotes deposition of aeolian sediments and dune stabilization.

The predominant tree species on the dunes of East Beach is Sitka Spruce (*Picea sitchensis*), a coastal species that thrives in moist environments and is resistant to transporting sand and sea spray (Cooper 1958). Other tree species include Red Alder (*Alnus rubra),* Western Hemlock (*Tsuga heterophylla*) and Red Cedar (*Thuja plicata*) (Pojar and MacKinnon 1994).

During the spring and summer, with increased daylight and warmer temperatures, vegetation cover increases on the backshore and foredunes, with grass heights up to 1 m and densities as high as 95% (Figure 4.5d). During winter months, when aeolian activity is greatest, surface roughness is dramatically reduced as vegetation dies off and becomes buried by aeolian sands (Figure 4.5e), promoting increased aeolian activity (Hesp 2002).

4.1.7 Driftwood

Driftwood along the backshore of East Beach plays an important geomorphic role. Comprising mostly felled timber, driftwood distribution varies along the coast, ranging from several scattered snags at the base of the capes (Figure 4.4a and b) to extensive driftwood jams up to 200 m wide (Figure 4.6a).

Driftwood along this coast has been recognized by Walker and Barrie (2004) to serve three important geomorphic functions.

First, driftwood jams act as 'accretion anchors' on the backshore. As a roughness element, driftwood interrupts the airflow, causing localized turbulence and jetting. As the wind encounters this roughness, much of the entrained sediment load transported from the beach is deposited. During storm wave attack, these sediment-laden driftwood jams act as buffers, releasing and reworking sediments and logs instead of eroding the foredunes. There is evidence, though, of scarping at the bases of the established foredunes behind extensive logjams, suggesting that, historically, these jams have been completely removed, exposing the foredune to direct wave attack (Figure 4.6a). Although driftwood in the backshore can provide protection, if mobilized in nearshore currents, driftwood can also locally enhance erosion of foredunes as logs become 'battering rams' thrust up against the base of the bluffs and foredunes by the waves.

The second geomorphic function of driftwood is to provide nuclei for incipient dune formation. As aeolian sediments are deposited within the driftwood jam, they may form shadow dunes around individual logs (Figure 4.6b and c) (Walker and Barrie 2004). Provided continued supply of sediments and low frequency of destructive wave attack, the driftwood matrix will continue to fill with sand to develop into an incipient foredune (Hesp 2002). With a mild climate and high year-round precipitation, the environmental conditions of HG promote high vegetation growth rates, which promote stabilization of these new

Figure 4.6 a) Sediment laden driftwood jam along the base of a scarped foredune, creating a buffer against future wave attack. b) Driftwood jam infilled with sediment and stabilized by vegetation. c) Shadow dunes develop around individual logs. d) Lakes formed on the backshore as creeks and streams from the wetlands are dammed by driftwood jam.

foredunes. Unlike incipient foredunes developing in backshore vegetation described by Hesp (2002), the size, morphology and stability of incipient 'driftwood' foredunes on this coast are determined by the characteristics of the driftwood matrix, not the density, distribution and species of vegetation.

Third, driftwood jams along East Beach dam wetland and stream discharge, creating lakes at the base of the established foredunes (Figure 4.6d). These lakes reduce the sediment available for aeolian transport onshore into the dune systems and reduce the intrusion of salt water into the coastal freshwater table. These lakes are subject to rapid drainage when the driftwood jams are breached by wave attack, and to infilling by aeolian sediments (Walker and Barrie 2004).

There is wide spatial and temporal variability in the density and distribution of driftwood along East Beach. While the controls on this variability are not well understood (Amos et al. 1995), one factor is the frequency and magnitude of storm surge. There is likely greater erosion at the base of the foredune if a high spring tide and moderate onshore wind event are experienced after multiple swash events that have already depleted driftwood jams than if such an event occurred with no preceding wave scarping. Although there have been no investigations into the influence of increased logging during the last century on the amount of driftwood on this coast, it is highly likely that the amount of driftwood on East Beach has increased during that time.

4.2 Aeolian geomorphology of East Beach

East Beach is host to highly active, aggrading Holocene dunes interspersed with eroding cliffs of Pleistocene sediments (Conway and Barrie 1994). During the last sea-level regression from the high stand 16 m above current levels, relict shorelines were abandoned, interspersed with low-lying shore platforms (Figure 4.2b). The poorly drained areas of muskeg were transgressed during the late Holocene by large parabolic dunes. Currently, the stabilized features that developed over the Holocene are being eroded and reworked due to high rates of coastal retreat on East Beach (i.e., 1 to 3 m a^{-1}).

The average orientation of the coastline is 12° to true north, with foredunes aligned roughly with the coastline. The parabolic dunes on this coast have an average alignment of 336 ± 8° to true north, oblique to the shoreline but closely aligned with the predominant southeast wind direction (Walker and Barrie 2004).

The following section documents and describes the aeolian geomorphology of four sites along East Beach: Site 1 – Parabolic and blowout dunes, Rose Point East; Site 2 – Foredune-parabolic dune complex; Site 3 – Locally prograding foredunes south of Lummi Creek; and Site 4 – Eroding relict parabolic dunes (Figure 4.2). This selection of sites demonstrates the morphological diversity of aeolian features along this coast.

4.2.1 Site 1 - Parabolic and blowout dunes, Rose Point East

From the ocean landward, Site 1 consists of a narrow driftwood jam, a low, discontinuous, established foredune at the vegetation boundary, and a vegetated dune plain backed by blowouts and parabolic dunes (Figure 4.7). This site has experienced differential retreat of the driftwood jam, with the northern portion around Rose Point retreating 43 m from 1966 to 1980 (3.1 m a^{-1}), while the southern portion, just north of Cape Fife, retreated only 12 m (0.9 m a^{-1}) (Figure 4.7). By 1997, the driftwood line on the backshore had retreated approximately 10 m further.

Site 1 has a relatively narrow beach (< 50 m), with the seaward extent of the backshore demarcated by a laterally discontinuous longshore driftwood jam (Figure 4.8). In June 2004, the driftwood jam was sediment-laden, with multiple linear depositional lobes aligned with the southeast winds. Exposed driftwood is present as much as 200 m inland from the beach, and has experienced infilling by aeolian sediment and stabilization by vegetation. The vegetated plain between the driftwood jam in the backshore and Dune Road comprises buried driftwood and a complex array of hummock, coppice and shadow dune features. Along the vegetation boundary, a discontinuous established foredune is present that resembles a Stage 1 of Hesp's (1999) morphological classification (Figure 2.1). This feature is at a Stage 1 on the erosional cycle as it is a low foredune, newly vegetated with increasing stabilization during the last 20 years, and is located on a stable portion of this coast (Figure 4.8a and b). It is not currently subject to wave erosion events as the driftwood jam provides a buffer. The vegetated plain

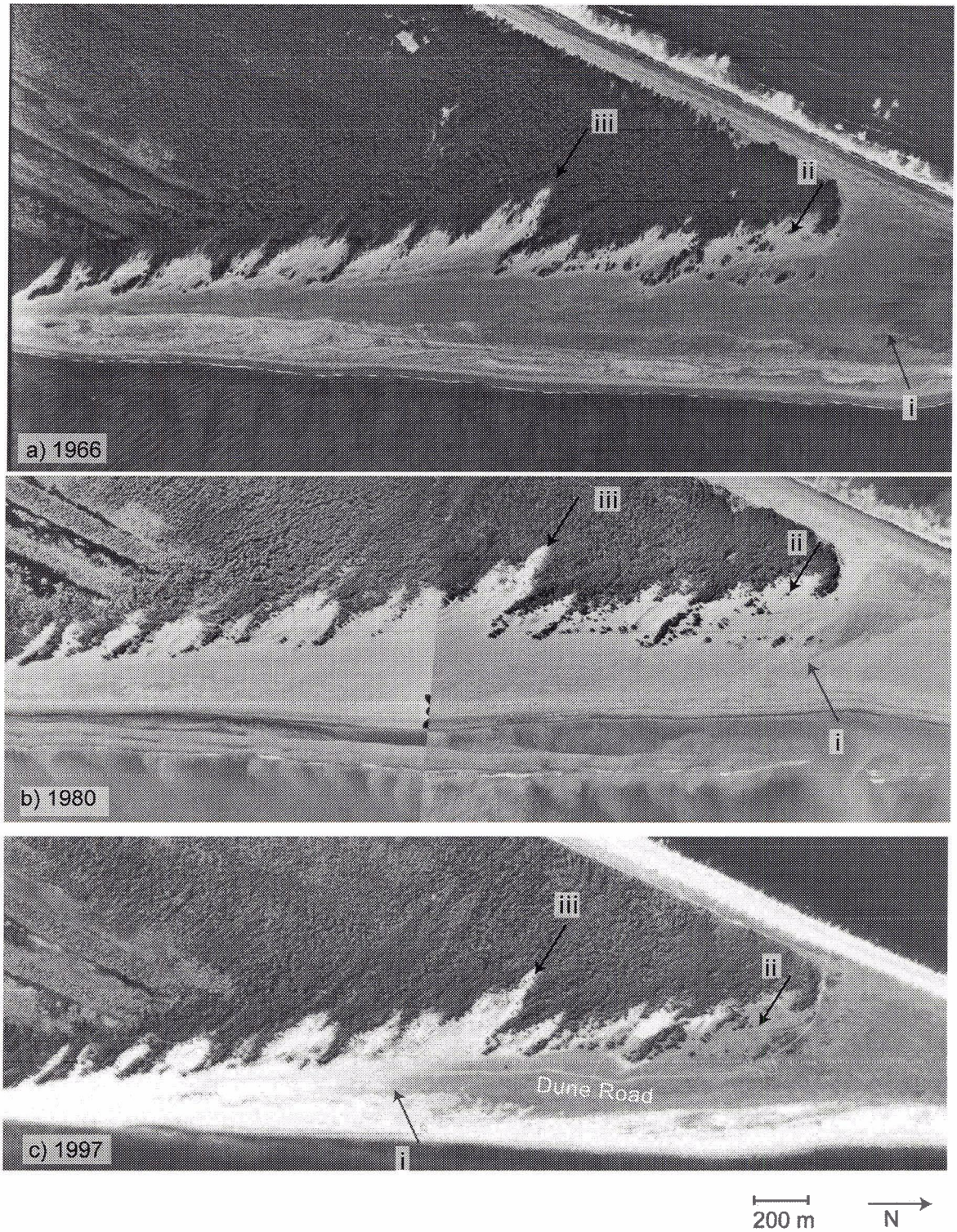

Figure 4.7 Site 1 is host to a wide driftwood jam, a discontinous established foredune, a vegetated dune plain backed by a suite of blowout and parabolic dunes. The coastline at this site has retreated 43 m between 1966 and 1980. Roman numerals indicate common features discussed in the text. a) BC4362_222 1966, b) BC80008_228 and 230 1980, c) BCB97035_4 1997.

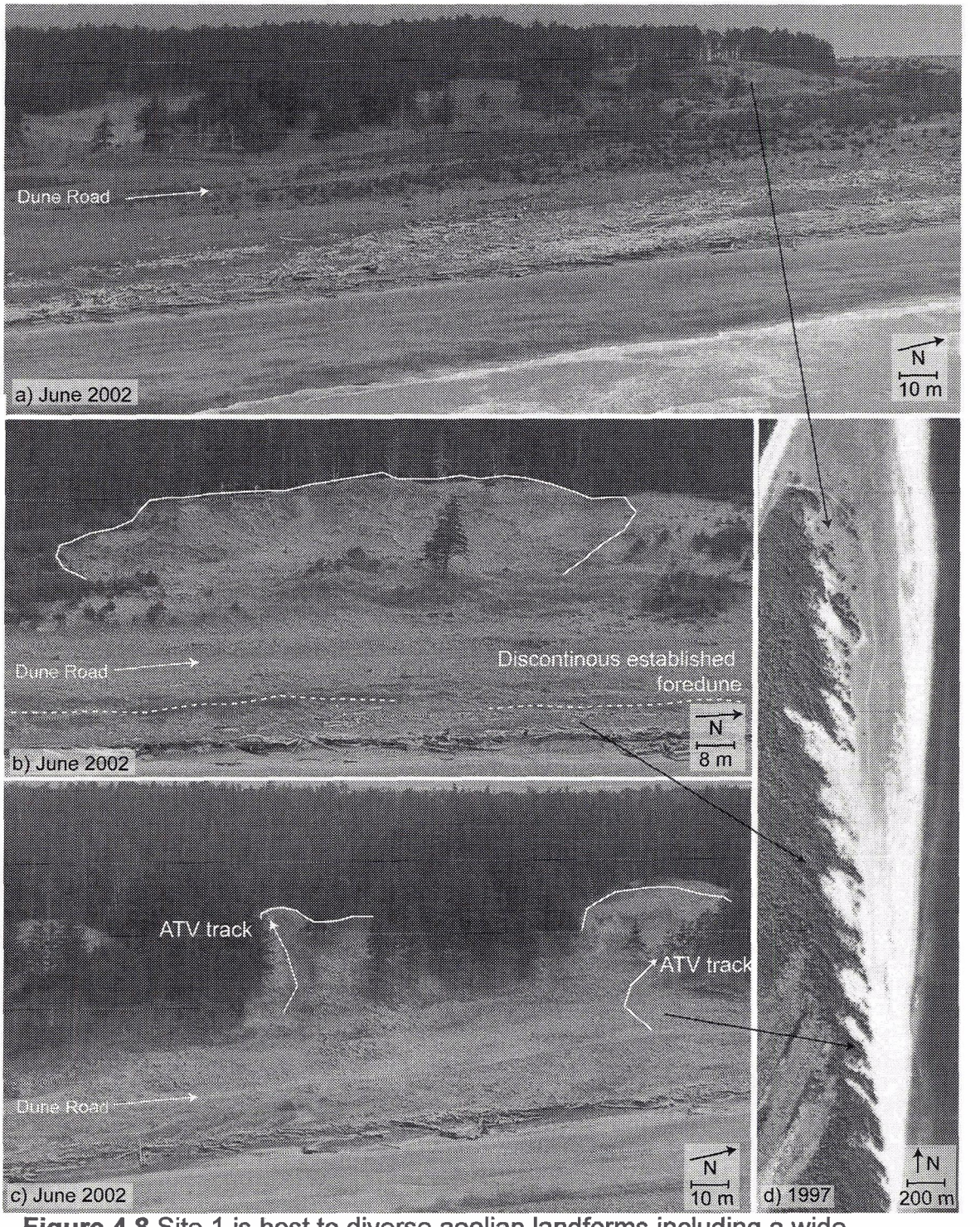

Figure 4.8 Site 1 is host to diverse aeolian landforms including a wide vegetated dune plain backed by a suite of blowout and parabolic dunes reactivated by recreational vehicle traffic. (d) Airphoto BCB97035_4 1997 highlights the location of features found in a, b and c.

narrows from the northern part of Site 1 to the south, where the established foredune disappears completely just north of Cape Fife (Figure 4.8c).

During the 31 years of airphotos assessed (1996 to 1997), vegetative cover has increased, reducing the sediment availability. In 1966, the vegetation line (Figure 4.7a i) was located just to the north of Rose Point. In 1980, the vegetation line has receded northward (Figure 4.7b i), suggesting an increase of aeolian sediment supply. By 1997, vegetation covered the entire dune plain landward of the driftwood jam (Figure 4.7c i) and the parabolic blowout dunes on the north of Rose Point (Figure 4.7c ii). These air photos were taken during different months (i.e., 1966 and 1980 in May, while 1997 was taken in August, see Table 3.1), which might, to some extent, account for the enhanced vegetation cover observed in 1997. However, during field visits between 2002 and 2004, increased complexity of vegetation species on this dune plain, from pioneering grasses and reeds to flowering plants and patches of Sitka Spruce saplings was observed, suggesting this plain currently maintains vegetation cover year round and has for many seasons (Figure 4.8a).

Landward of Dune Road, parabolic dunes with active deflation basins exist (Figure 4.8b and c). The parabolic dunes along the central portion of this site have densely vegetated, steep lee slopes, as sediments transported from the deflation basins are deposited landward and avalanche down the slope into full forest stands. These features are not actively migrating but have very tall and steep depositional lobes. Figure 4.8b shows ghost forests in the deflation plains of these dunes, where stumps remain *in situ* after the migrating sands have

transgressed and killed the trees. The deflation basins of these parabolic dunes remain active, as evident from the exposed erosional scarps on the lateral walls and the lack of vegetation (Figure 4.7).

As Hesp (1999) suggests, distinguishing between blowouts and parabolic dunes is difficult but may be done by determining the presence or absence of trailing arms. At this site, the broader shaped features in the central portion of the site are parabolic dunes, while the features close to Cape Fife appear to be blowouts. The blowouts have narrower shapes with bare sediment deflation plains and steep lee slopes. These features may be a younger evolutionary stage of the parabolic dunes in the central portion of this site.

The southern blowout in Figure 4.8c is aligned approximately 10° to the west of all the parabolic and blowout dunes at this site. This slight shift in the dune trend is likely a result of anthropogenic influence, as ATV tracks can be seen up the central axis of this dune. Site 1 experiences human disturbances such as ATV and other vehicle traffic, as Dune Road, which provides access from North to East Beach, transects this site. Vehicle traffic kills vegetation, destabilizes slopes and reactivates dune sands. There are extensive trails and tire tracks observed not only landward of the established foredune (i.e., at Dune Road) but up the face and over the heads of the blowouts and parabolics. This is the case with the head of the parabolic dune highlighted in Figure 4.7 iii, which has migrated landward slightly during the last 31 years.

4.2.2 Site 2 – Foredune-parabolic dune complex

Site 2 hosts the longest (1.2 km) parabolic dune complex on East Beach (Figure 4.2), fronted by a discontinuous established foredune and wide (> 50 m) backshore driftwood jam. This discussion will be limited to two parabolic dune heads that share a common trailing arm to the south. To simplify description, these two features have been labelled A and B (Figure 4.9), where A is the longer parabolic and B is the shorter.

The trailing arms and heads of these features are densely vegetated on the outer slopes, predominantly by Sitka Spruce (Figure 4.10). The southern arm and western portion of the north arm have steep, convex outer slopes (25-30°) with muskeg at the base (Figure 4.10). The northern arm is not visible, as the deflation plains of two other parabolic dunes to the north have coalesced.

The head of Parabolic Dune B is at the same landward extent as the parabolic dunes to the north and the south of this site, while Parabolic A extends approximately 300 m further inland (Figure 4.9). There are exposed stumps and ghost trees in the deflation plain and on the sides of the arms of the dune where the surface has been deflated. The relict shoreline just to the south of these parabolic dunes is dated to 5240 years (sample ID SAW03-20, Lat. 54° 04' 20" Long. 131° 41' 32", Wolfe and Walker unpublished data).

Currently, Parabolic A remains active, as observed during field visits in June 2002 and 2003, with exposed sand throughout most of the deflation plain at the head of the parabolic. During the 31 years of air photo records (Figure 4.9), vegetation cover has increased along the northern edge of the parabolic complex

Figure 4.9 Site 2 hosts the longest parabolic dune complex on East Beach. This site has experienced rapid retreat of the coastline (34 m between 1966 and 1980) while increased vegetation growth on the parabolic dune complex has stabilized the inland dunes. a) BC4362_227 1966, b) BC80008_221 1980, c) BCB97035_184 1997.

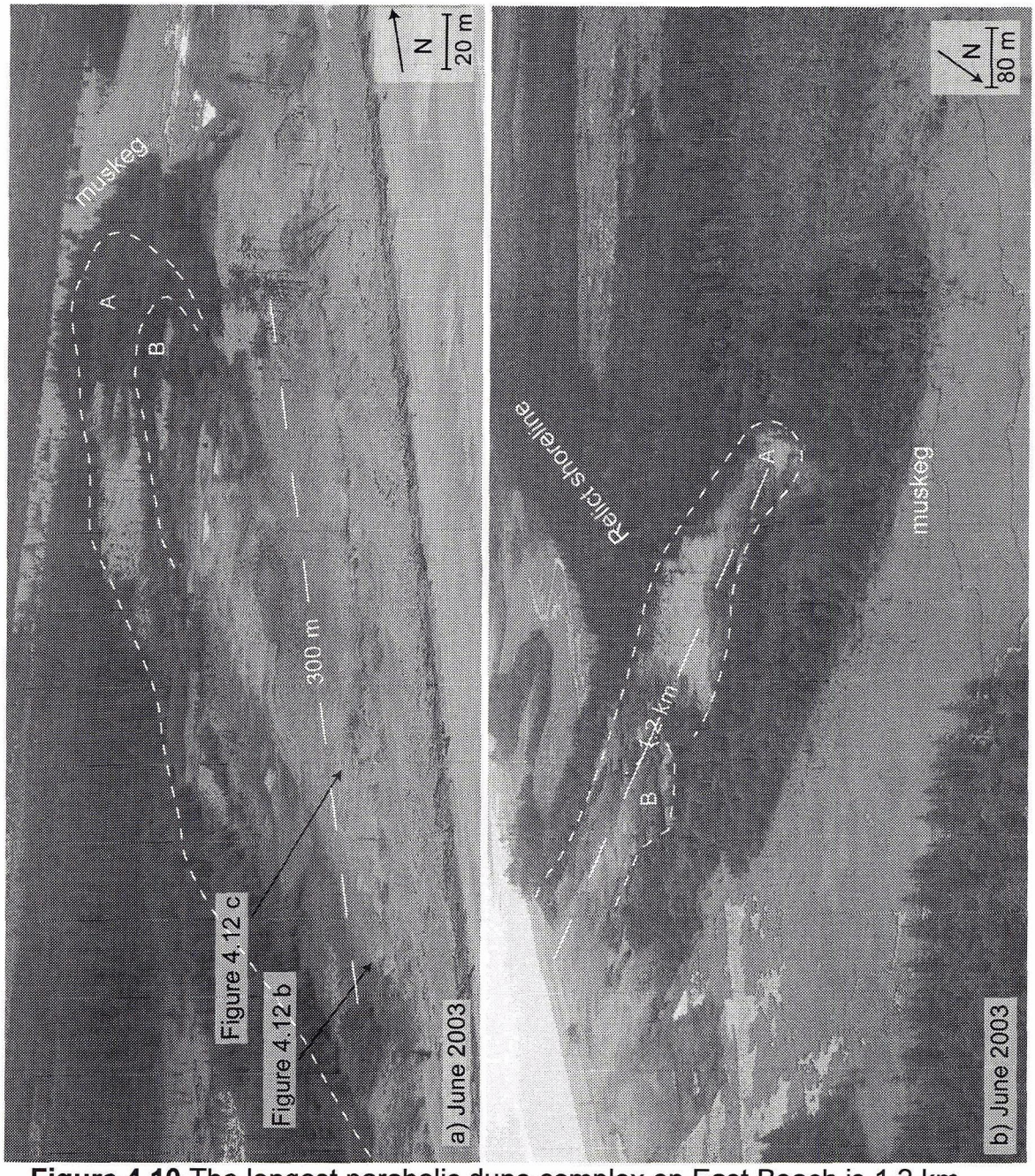

Figure 4.10 The longest parabolic dune complex on East Beach is 1.2 km long and 300 m at the seaward margin. It comprises two distinct heads located at A and B. These parabolics have transgressed relict interdune areas that are currently muskeg.

and in the deflation plain, suggesting increased stabilization since 1966 (Figure 4.9 ii).

There has been significant retreat of the established foredune at this site since 1966 (Figure 4.9 i and ii). Between 1966 and 1980, the foredune retreated approximately 34 m (2.4 m a^{-1}). Evidence of further retreat between 1980 and 1997 can be seen at the grouping of trees highlighted at i in Figure 4.9 and along the bluff to the south at ii in Figure 4.9, where the width of the densely vegetated ridge has decreased.

In 2002, there is a single established foredune ridge, with no evidence of wave scarp, breached in several locations by erosional hollows (Figure 4.11a). Some of these hollows have developed into full blowouts of both trough (Figure 4.11b) and saucer shape (Figure 4.11c), while others remain as small depressions that may develop into blowouts in the future (Figure 4.10a). The trough blowout in Figure 4.11b is the site of the detailed morphological assessment in Section 6.3. This feature has a long (30 m), narrow (11.5 m) trough 4 m deep with a depositional lobe extending 25 m landward of the blowout rim. The saucer blowout, located approximately 100 m north along the foredune ridge, is a shallow, broad deflation basin with a linear depositional ridge through the centre that has developed during the last two years (Figure 4.11c). The ridge is aligned to the southeast and is a continuation of a linear depositional ramp built up at the foredune toe (seen in Figure 4.11c).

As the established foredune at this site has a single dune ridge breached in several areas with blowouts, both incipient and fully developed, this foredune

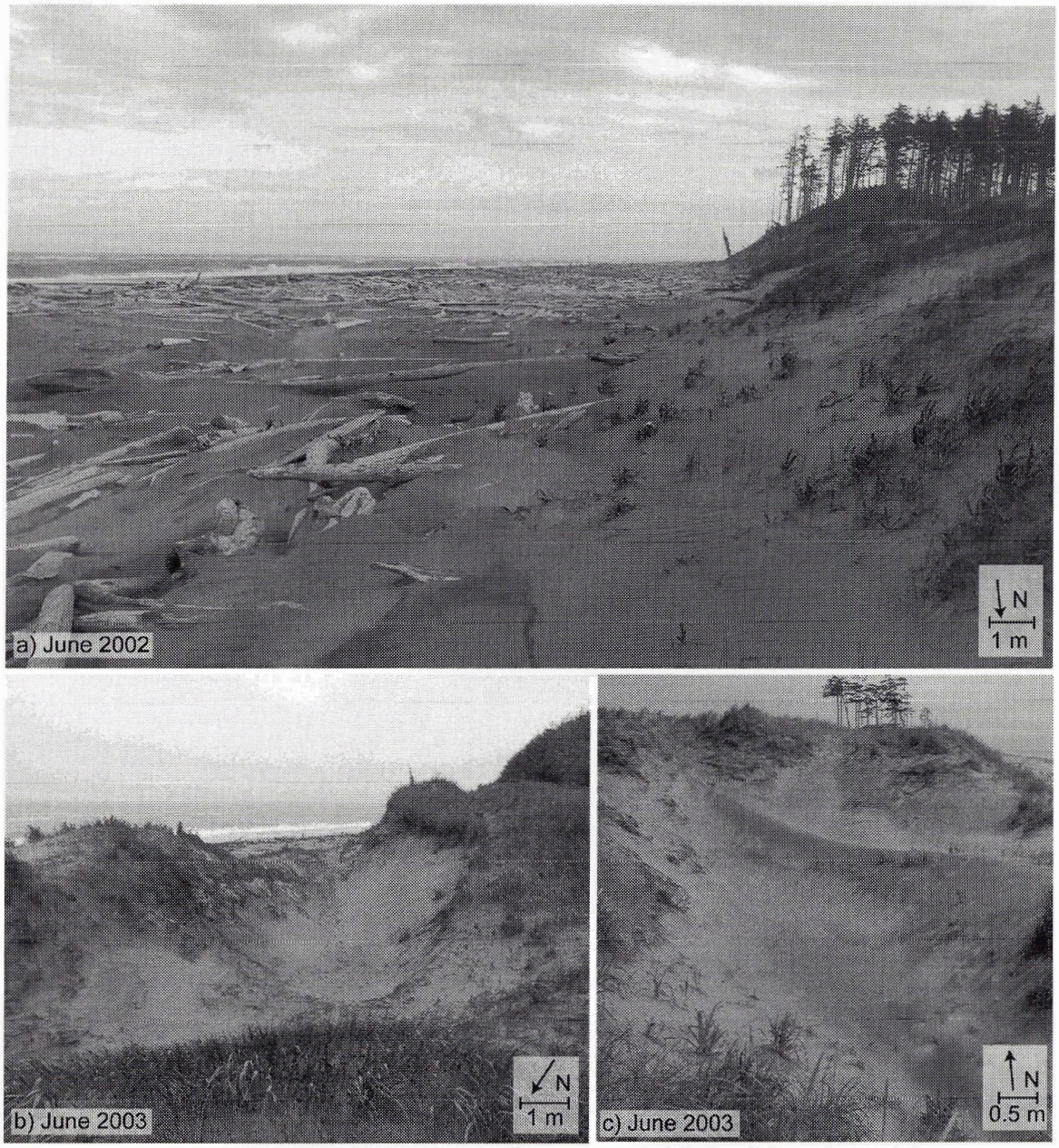

Figure 4.11 Site 2 is host to a discontinuous established foredune (a), breached in several places by blowouts of both trough (b) and saucer (c) shape. In June 2002, a wide (> 30 m), sediment filled, backshore driftwood jam is present at the toe of the established foredune.

resembles a Stage 3 on the erosional cycle of Hesp's (1999) morphological classification (Figure 2.1). There is no wave scarp or evidence of multiple generations of foredune growth. The backshore at this site hosts a sediment-filled driftwood jam extending more than 50 m from the foredune toe in June 2002, with an incipient foredune developing at the seaward margin (Figure 4.11a).

At the base of the foredune, behind the driftwood line, a lake has formed as seen in the 1997 air photo (Figure 4.9c). This lake receives water from the wetlands over which the parabolic dunes have transgressed. Over the period of study, this lake has varied in size throughout the seasons, getting smaller during the summer then enlarging during the fall and winter with increased precipitation. By the summer of 2003, the driftwood jam had been breached, the lake completely drained and by summer 2004, this region had been infilled with aeolian sands.

This site is prone to episodic reworking or removal of the driftwood jam as seen in the 1980 air photo, where waves have removed most of the driftwood from the base of the foredune. Currently, there is no wave scarp present at the base of the foredune, unlike other sites, suggesting that the driftwood jam is able to sufficiently buffer against wave attack or that the onshore aeolian sediment transport allows for the rapid recovery of the backshore.

4.2.3 Site 3 – Locally prograding foredunes south of Lummi Creek

Site 3 comprises four parabolic dunes with coalesced deflation plains and multiple generational established foredunes with locally prograding incipient foredunes (Figure 4.12). Between 1966 and 1980, the foredune at this site retreated 52 m (3.7 m a^{-1}), while between 1980 and 1997 the foredune retreated significantly less (Figure 4.12 i and ii), while progradation occurred in the backshore driftwood jam.

The heads of the parabolic dunes at this site are bordered by Lummi Creek, which meanders along the landward extent. In 1966, there are two places where the parabolic dunes have transgressed the creek (Figure 4.12 iii and iv). No further landward migration of the parabolic dunes is observed by 1980; instead, these features appear to have become increasingly stabilized with vegetation. By 1997, the heads and trailing arms of the parabolic dunes have significantly increased vegetation cover, with predominantly Sitka Spruce saplings and Red Alder (Figure 4.12 v). Vegetation cover on the deflation plain has also increased during the 31-year record with pioneering grasses and Sitka Spruce saplings (Figure 4.12).

The backshore driftwood jam at this site underwent significant change during the 31-year record (Figure 4.12). In 1966, the driftwood jam along the north of the site is approximately 30 m wide, narrowing to 10 m on the south. In 1980, the driftwood jam extends over 100 m along the northern section, while the southern area has a driftwood-dam lake at the toe of the foredune, with driftwood

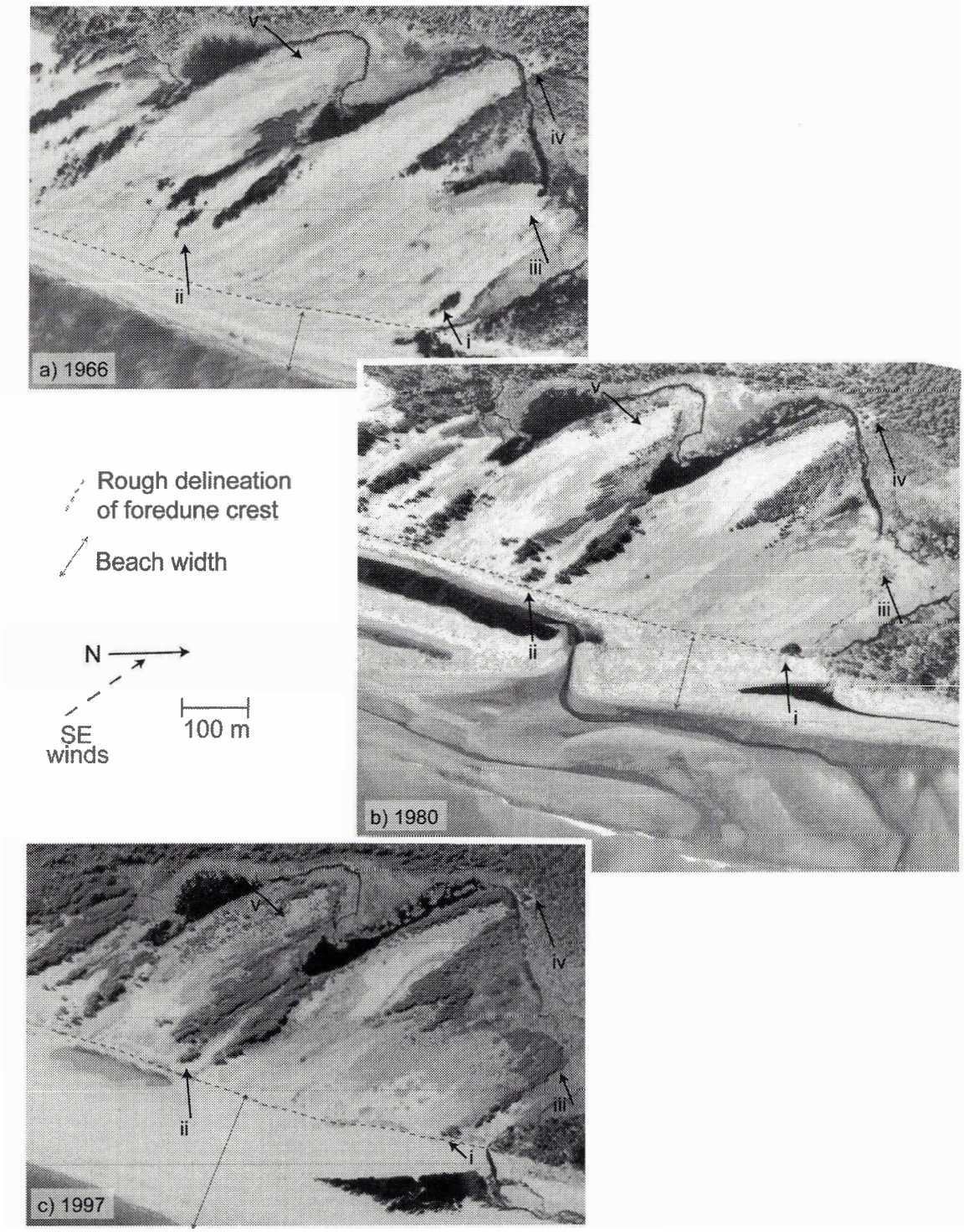

Figure 4.12 Site 3 host four parabolic dunes with coalesced deflation plains with increasing vegetation cover since 1966 suggesting increased stabilization. The foredune at this site has retreated 52 m between 1966 and 1980. Roman numerals locate several points of discussion in the text. a) BC4362_227 1966, b) BC80008_220 1980, c) BCB97035_187 1997.

on the seaward edge of the lake. By 1997, the lake to the south has mostly drained, and the driftwood jam is not distinguishable on the small-scale air photo.

In 2003, the driftwood jam is relatively narrow adjacent to the outfall of Lummi Creek, rapidly widening to the south (Figure 4.13a and b). Adjacent to the creek, the narrow driftwood jam is backed by an established foredune with a discontinuous ridge breached in many places by blowouts of both trough and saucer shape (Figure 4.13a and 4.14a). As this foredune is highly erosional, it is classified as a Stage 4 on Hesp's (1999) morphological classification (Figure 2.1). Along the southern portion of this site, there are multiple generations of incipient and established foredunes (Figure 4.14b).

An incipient foredune can be seen developing in the seaward extent of the driftwood jam just landward of the storm scarp (Figure 4.13 i). This is backed by a region of sediment-laden driftwood and a second driftwood line with some pioneering American dune grass (Figure 4.13 ii). An interdune depression exists between points ii and iii in Figure 4.13 where sparsely vegetated depositional ramps have formed at the base of the established foredune (Figure 4.14b). There are three distinct generations of growth on the established foredune (Figure 4.13b iii, iv and v), likely resulting from the presence of the driftwood-dam lake in the backshore evident in 1980 (Figure 4.12b). After the lake drained, the backshore has infilled with aeolian sediments at the base of the established foredune (Figures 4.13b and 4.14b). Currently, the established foredune along the southern portion of this site resembles a Stage 4b on the accretional portion

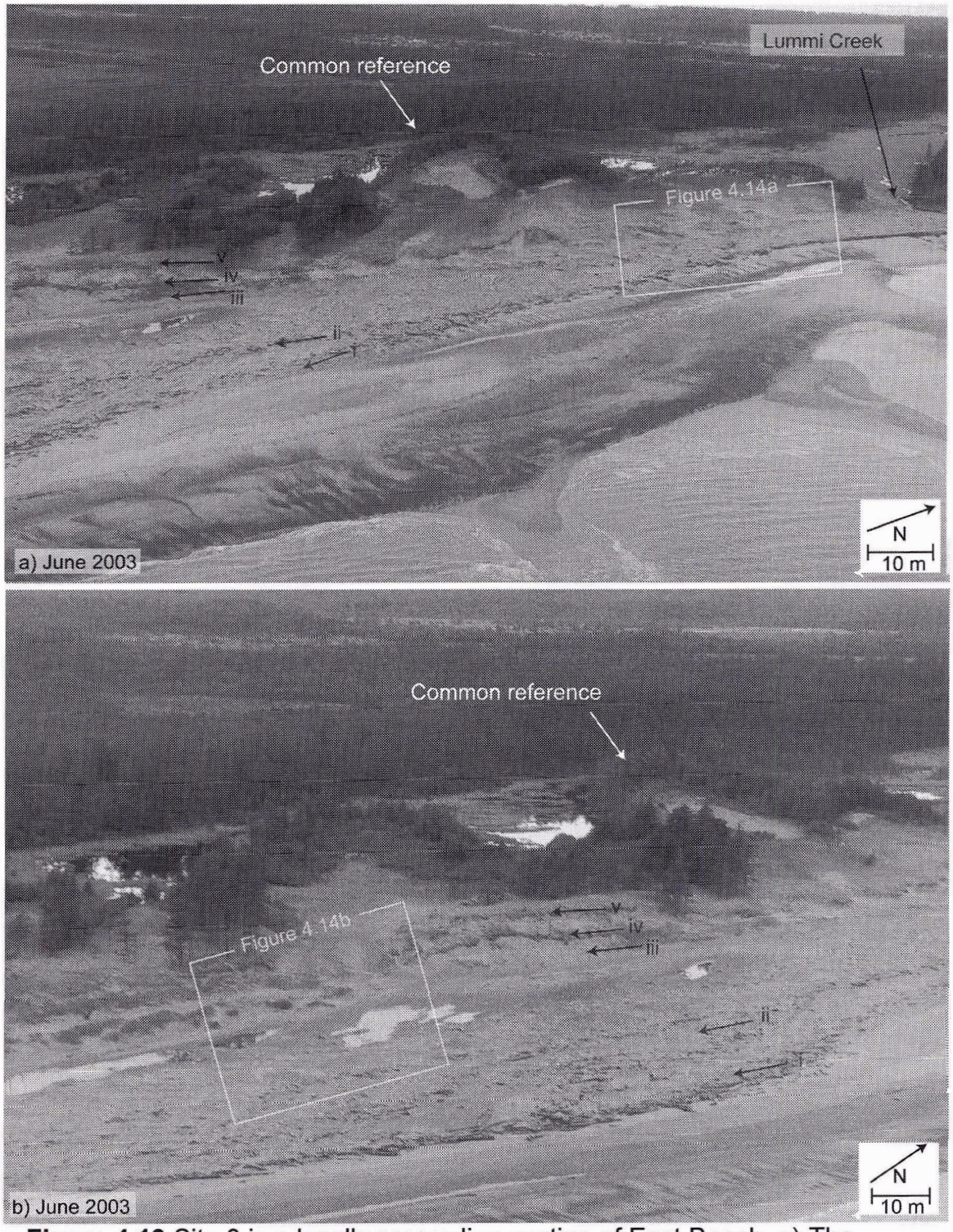

Figure 4.13 Site 3 is a locally prograding section of East Beach. a) The northern portion of Site 3 has a single established foredune breached by blowouts of both trough and saucer shape. b) The southern portion has a wide driftwood jam and multiple generations of incipient and established foredunes.

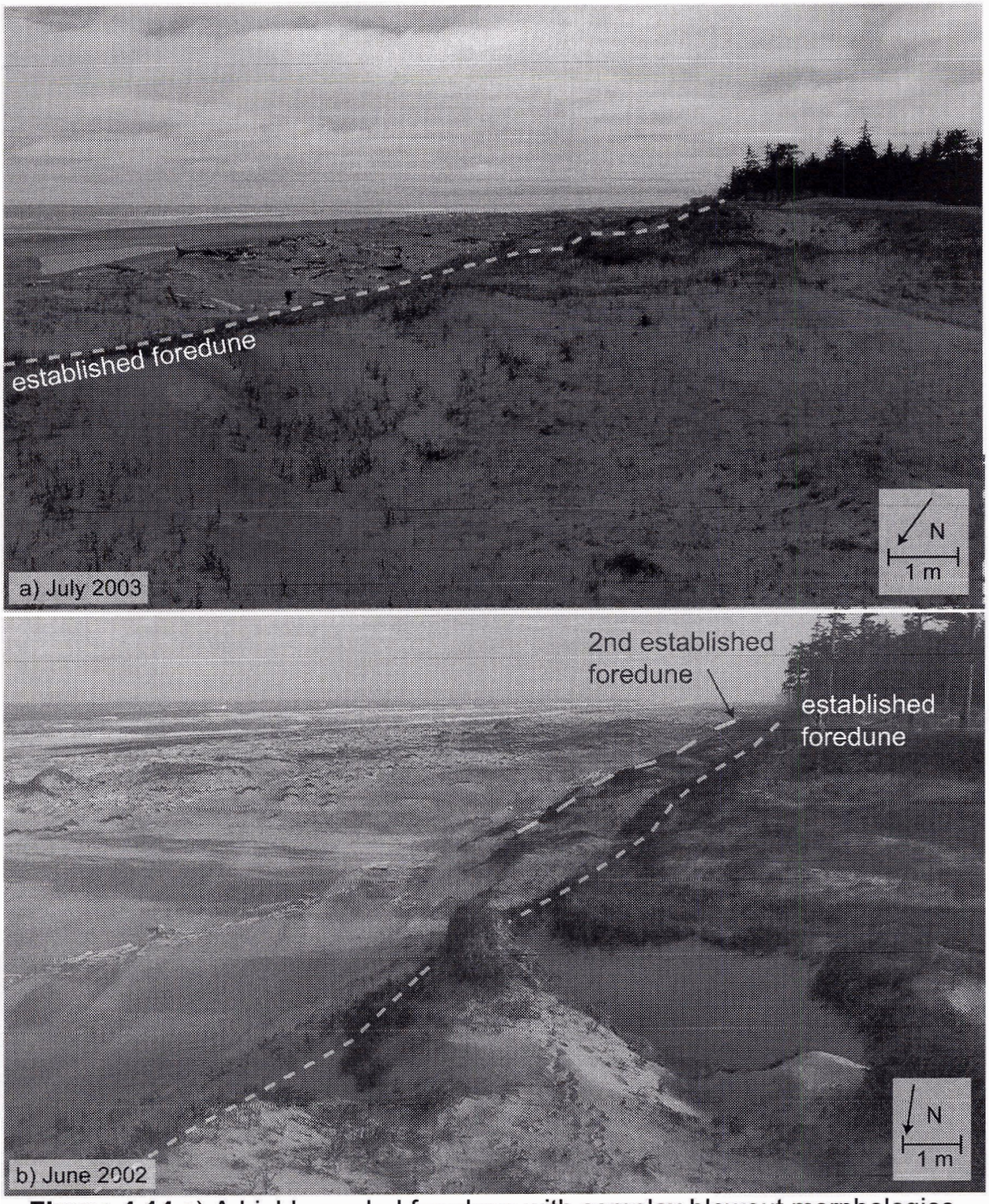

Figure 4.14 a) A highly eroded foredune with complex blowout morphologies. b) Multiple generations of foredune growth stabilized by vegetation. The dash grey lines roughly delineate the incipient and established foredunes.

of Hesp's (1999) classification (Figure 2.1), as it is a locally prograding section of East Beach.

4.2.4 Site 4 – Eroding relict parabolic dunes

Site 4 comprises a relatively narrow beach and backshore with a rhythmic sinuous dune ridge from the truncated portions of relict parabolic dunes highlighted in Figure 4.15 i. The heads of four relict parabolic dunes, currently stabilized with dense woody vegetation (predominantly Sitka Spruce and hemlock), extend 450 to 600 m inland from the current shoreline aligned from southeast to northwest (Figures 4.15 i).

Between 1966 and 1980, the shoreline, defined by the base of the dunes, retreated 48 m (3.4 m a^{-1}). By 1997, the shoreline retreated farther but the backshore increased in width with the presence of a nearshore bar. In 1980, the head of a nearshore bar can be seen in the centre of Site 4 (Figure 4.15b). By 1997, the head of the bar has migrated northward but the bar remains in the nearshore (Figure 4.15c).

The erosional features at this site appear to be the truncated arms of relict parabolic dunes. As the shoreline retreats, wave attack erodes the base of the dunes, causing slumping and removal of sediment to the nearshore. Recent observations show that wave scarps are present along this entire site, but most have partially recovered through infilling of aeolian sands (Figures 4.16 and 4.17). The exposed arms of the relict parabolics are currently being eroded by aeolian process, behaving much like blowouts. These features have active, non-

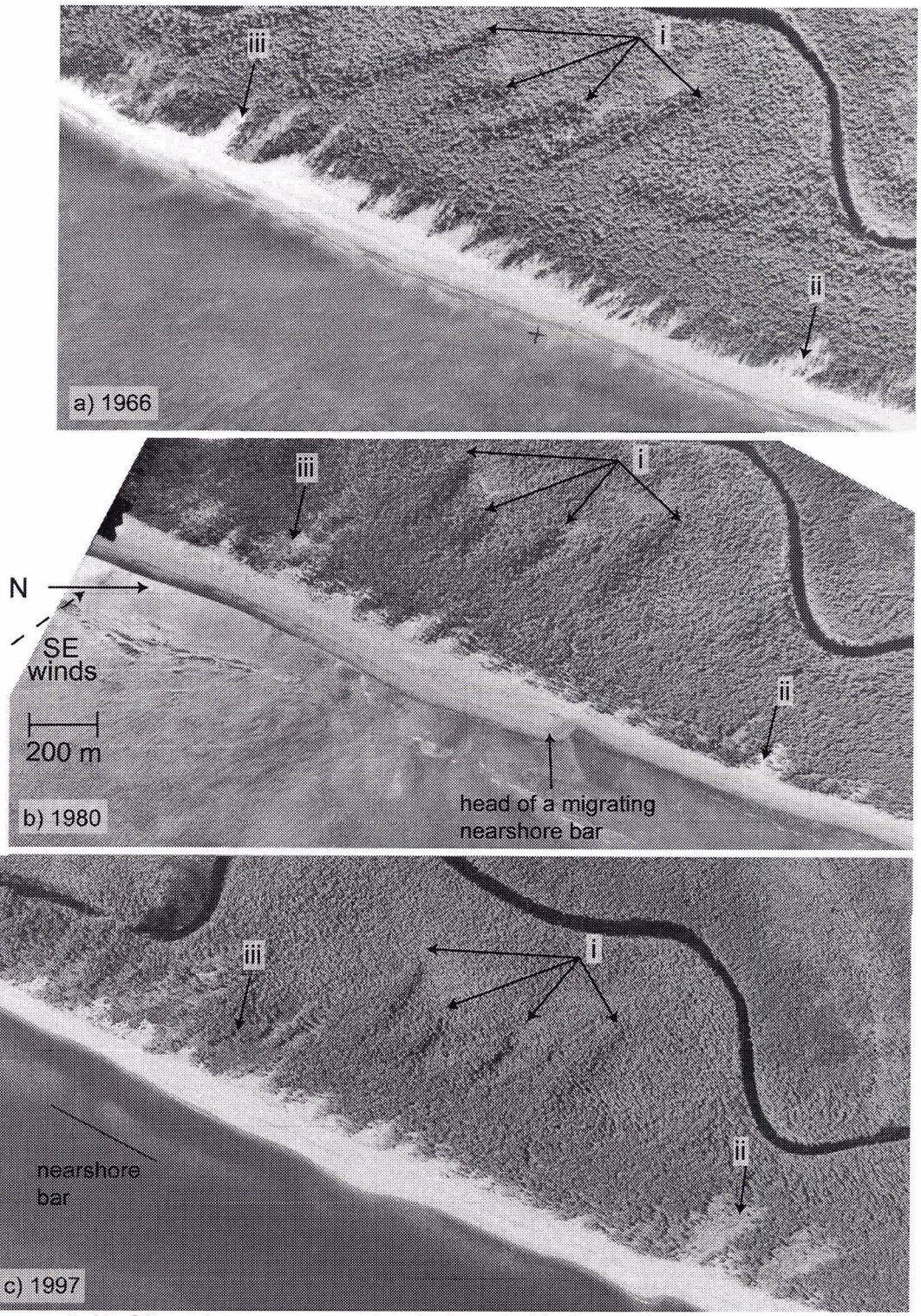

Figure 4.15 Site 4 has a narrow backshore with the relict heads of parabolic dunes (i). The truncated relict arms are being exposed as the coastline retreats (measured retreat of 48 m between 1966 and 1980). a) BC4362_233 1966, b) BC80008_207 1980, c) BCB97035_14 1997.

Figure 4.16 The truncated arms of relict parabolic dunes are being exposed as the coastline rapidly retreats. The short white dashes delineate the dune ridge, while long white dashes highlight the depositional lobe, where visible.

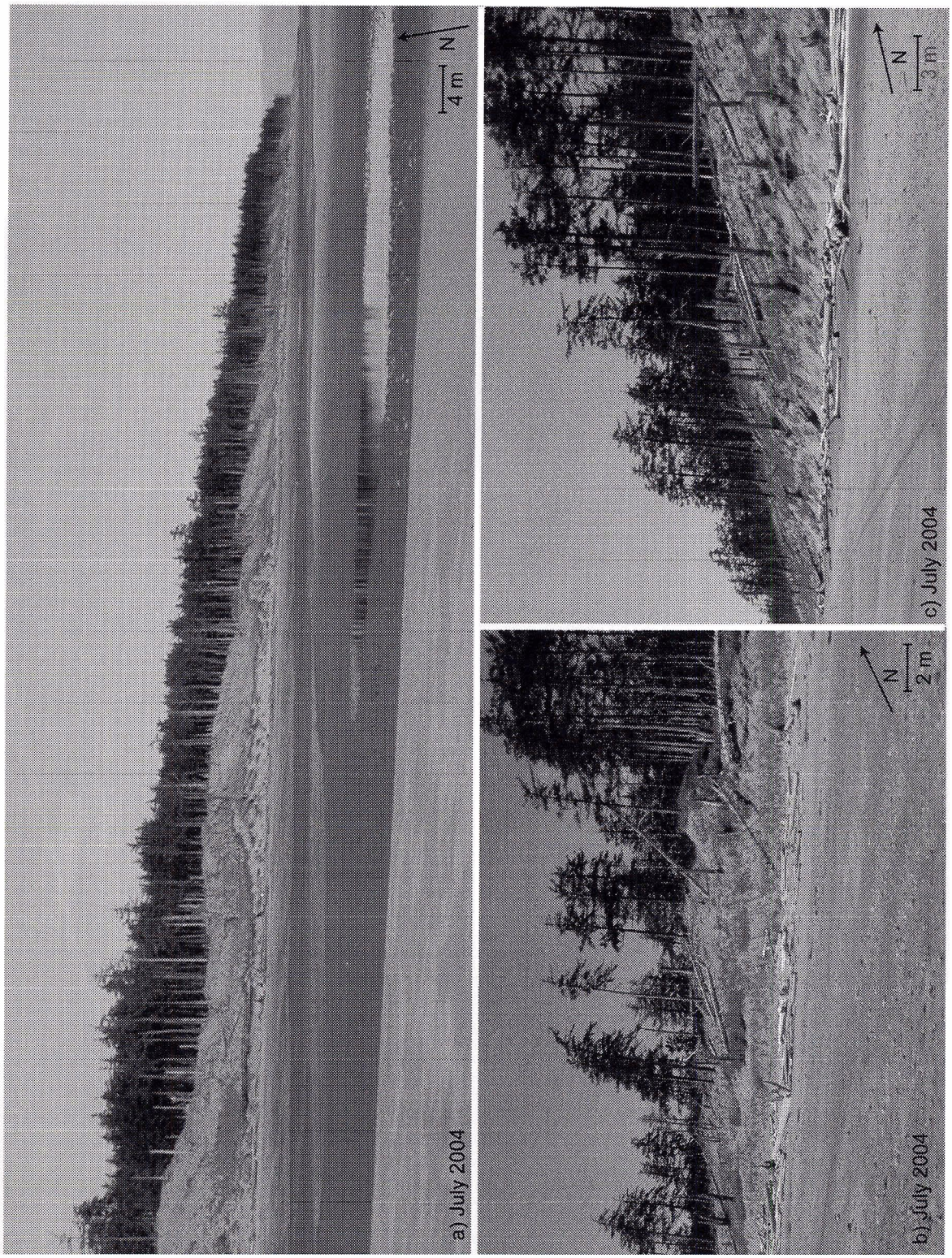

Figure 4.17 Site 4 hosts a narrow backshore with minimal driftwood that is accumulating aeolian sediments. Wave scarps are evident along most of this site, although incipient foredunes are developing in the driftwood as sediment accretes.

vegetated deflation plains that supply sediments to be transported landward to densely vegetated depositional lobes.

Figure 4.16 shows that the depositional lobes are vegetated with tall Sitka Spruce trees, but the understorey of these forests directly downwind of the blowout ridge does not comprise complex vegetation. Instead, the depositional lobes appear to be covered with pioneering grasses similar to those found along the wave scarp and on the backshore. This suggests that aeolian sands are being eroded from the deflation plain, transported by onshore winds and deposited just landward of the blowout ridge. As sediments are eroded from the deflation plains, ghost forests are being exposed (Figures 4.16 and 4.17).

Figure 4.15 ii shows localized stabilization of a blowout through increased vegetation cover between 1966 and 1980, followed by significant retreat (> 100 m) by 1997, while in Figure 4.15 iii, a blowout has continually stabilized with increased vegetation cover since 1966. Therefore, the blowouts at this site are responding to localized controlling conditions such as airflow, surface moisture, vegetation growth and sediment supply.

Site 4 has a much narrower beach and backshore than the other three sites, with minimal driftwood (Figures 4.15 and 4.16). As it lacks the buffer provided by an extensive sediment-laden driftwood jam, this site is highly susceptible to storm surge attack. During field research in June 2003 and 2004, there were scattered patches of driftwood with minimal sediment accretion, while wave scarp(s) were visible along the base of the dunes (Figures 4.15 and 4.16).

As observed during field visits in June 2003 and 2004, the wave scarp at the base of the dunes was infilled with aeolian sediments and was moderately covered with pioneering grasses (Figures 4.16 and 4.17). This process is similar to that presented by Hesp (1999) in the Box D wave erosion event (Figure 2.1). There is no established foredune at this site comparable to those in the erosional and accretional cycles of Hesp's (1999) classification. There is incipient foredune development along the backshore driftwood at this site, with pioneering vegetation growing, but no features appear to have persisted to develop into an established foredune (Figure 4.17).

4.3 Summary and Conclusions

Of the four coastal dune types described by Hesp (1999), three are found on East Beach: foredunes, blowouts and parabolic dunes. These features are maintained by strong, year-round winds and an abundant supply of sediment transported from nearshore bars to the beach-dune systems, despite high precipitation. Primarily due to the high vegetation cover and high annual precipitation, fully established transgressive dune fields are not found on this coast. Within each of the three coastal dunes types (Hesp 1999), East Beach displays a wide morphological diversity.

All four sites have incipient foredunes developing on the backshore, with driftwood acting as accretion anchors (Walker and Barrie 2004). These dunes are not dependent on the presence of vegetation to initiate growth, but vegetation does provide long-term stability by protecting the dunes from aeolian erosion.

The morphology of these dunes is primarily dependent on the characteristics of the driftwood, including the width and height of the logjams, and the density and distribution of the wood within them. The logjams, and in turn the dunes, are further influenced by the frequency and magnitude of wave attack and storm surge as these processes erode the driftwood jams and recycle sediment back to the beach and nearshore.

By applying Hesp's (1999) (Figure 2.1) model of established foredune evolution, the morphological stages for the foredunes at three of the four sites were determined. Due to a narrow backshore and rapid retreat rate at Site 4, there is no established foredune, only evidence of wave scarp similar to that presented by the Stage D (Figure 2.1). At Site 1, a low-lying, discontinuous foredune resembles a Stage 1, as this portion of the coastline has been relatively stable, allowing a foredune to grow, while increased vegetation cover has been observed since 1980. Site 2 appears to be a Stage 3 on the erosional cycle with no evidence of recent historic wave scarp. There are numerous breaches in the foredune of aeolian origin, and the vegetation cover is moderate along most of the foredune except in the blowouts. The northern portion of Site 3 is a Stage 4 as it is a highly eroded, discontinuous foredune with many deep and wide blowouts and variable vegetation cover. However, there is no clear evidence of wave scarp. The southern portion appears to be a Stage 4b as there is clear evidence of historic scarping at the base of the foredune and subsequent accretion and revegetation of multiple generations of foredunes at this site while locally progradation occurs behind an extensive driftwood jam.

Blowouts also display wide morphological diversity on this coast. As the blowouts on East Beach are subject to similar climatic and biogeographical conditions (e.g., precipitation, vegetation type, wind regime), their size and morphology are primarily determined by the size and type of sedimentary landform on which they are developing and the process of initial disturbance or erosion. Blowouts from the four study sites range from small (< 1 m wide) incipient blowouts along the seaward face of the established foredune at Site 2, to broad (> 50 m) and tall (> 10 m) blowouts with exposed ghost forests in the deflation plains at Site 4 developing in the truncated heads of relict parabolic dunes.

Parabolic dunes on East Beach also display wide morphological diversity. These range from active landforms that have migrated into dense vegetation with currently active deflation plains at Site 1, to fully stabilized relict parabolic dunes at Site 4. The parabolic dunes at Sites 2 and 3 have transgressed low-lying muskeg, and over the last 31 years, the deflation plains have become increasingly stabilized with vegetation growth.

East Beach is subject to a highly energetic wind and wave regime resulting in a high rate of coastal retreat at 1 to 3 m a^{-1} and up to tens of metres in extreme years (e.g., 1997-98 El Niño) documented by Barrie and Conway (2002). This analysis has shown retreat rates the four sites between 1966 and 1980 ranging, 0.9 to 3.7 m a^{-1}. These values are similar to those calculated by Barrie and Conway (2002), but this assessment has shown that differential retreat occurs along this coast, producing varied morphological response of the

aeolian landscape. Site 3, for example, rapidly retreated during 1966 to 1997 but is currently prograding behind an extensive driftwood jam. While Site 2 has a wide backshore driftwood jam, this site does not have multiple generations of foredune development.

As this coastline retreats, the response of these aeolian features is of great interest. The dominant view of sedimentary shoreline response to landward retreat due to sea-level rise is described by the Bruun model (1962), with net loss of sediment from the upper beach to the nearshore at a rate proportional to the sea-level rise (S) ranging from 50 to 100S for most beaches. This model was recently challenged by Davidson-Arnott (2003), who stated that the failure to include the onshore sediment transfer and dune sediment budget into a model of coastal retreat is a conceptual weakness. He proposed an alternate model (the RDA model) that considers onshore aeolian transport of sediment to the beach-dune system from the nearshore, resulting in no net loss of sediment to the nearshore (Davidson-Arnott 2003). If this were the case, the response of a sedimentary coastline to sea-level rise would be the landward migration of foredunes.

The beach-dune systems on East Beach during the last 31 years demonstrate that this coast is retreating and that the foredunes are migrating, but that they continue to accrete, as does the driftwood jam on the backshore. The driftwood jams provide a sediment store, a matrix for incipient foredune development as well they provide a buffer against storm wave attack.

5.0 Aeolian activity of northeast Graham Island

This chapter presents a discussion of the aeolian activity of northeast Graham Island. First, the local annual and monthly wind regimes are characterized. Second, regional meteorological data are used to apply and critique three models of sediment drift potential and dune mobility: i) Fryberger's (1979) sediment drift potential model, ii) Lancaster's (1988) dune mobility index and iii) Tsoar and Illenberger's (1998) modified dune mobility index.

5.1 Wind regime

HG is exposed to high year-round wind energy, with an average annual wind speed of 8.5 m s^{-1}, infrequent periods (0.035%) of calm winds (i.e., < 0.5 m s^{-1}) and frequent (62%) transporting winds (i.e., > 6 m s^{-1}). The annual wind rose from EC-Rose Spit for 1995-1999, selected due to data quality (i.e., the least percentage of missing data at 1.86%), shows a strong bimodal wind regime with a primary mode from the southeast and secondary mode from the west (Figure 5.1). The southeast winds show the greatest frequency (27%), as well as the greatest magnitude, of winds with 3.5% of wind speeds greater than 18 m s^{-1}. The westerly component has a total frequency of 15% of the total record. However, the magnitude of the westerly winds is markedly less, with the bulk of the winds in the 6-12 class and with no recorded winds greater than 18 m s^{-1}. Other modes in the wind regime include moderate (6-18 m s^{-1}) winds from the south and east, as well as low frequency (i.e., < 2%) but high magnitude (> 18 m s^{-1}) winds from the east-southeast.

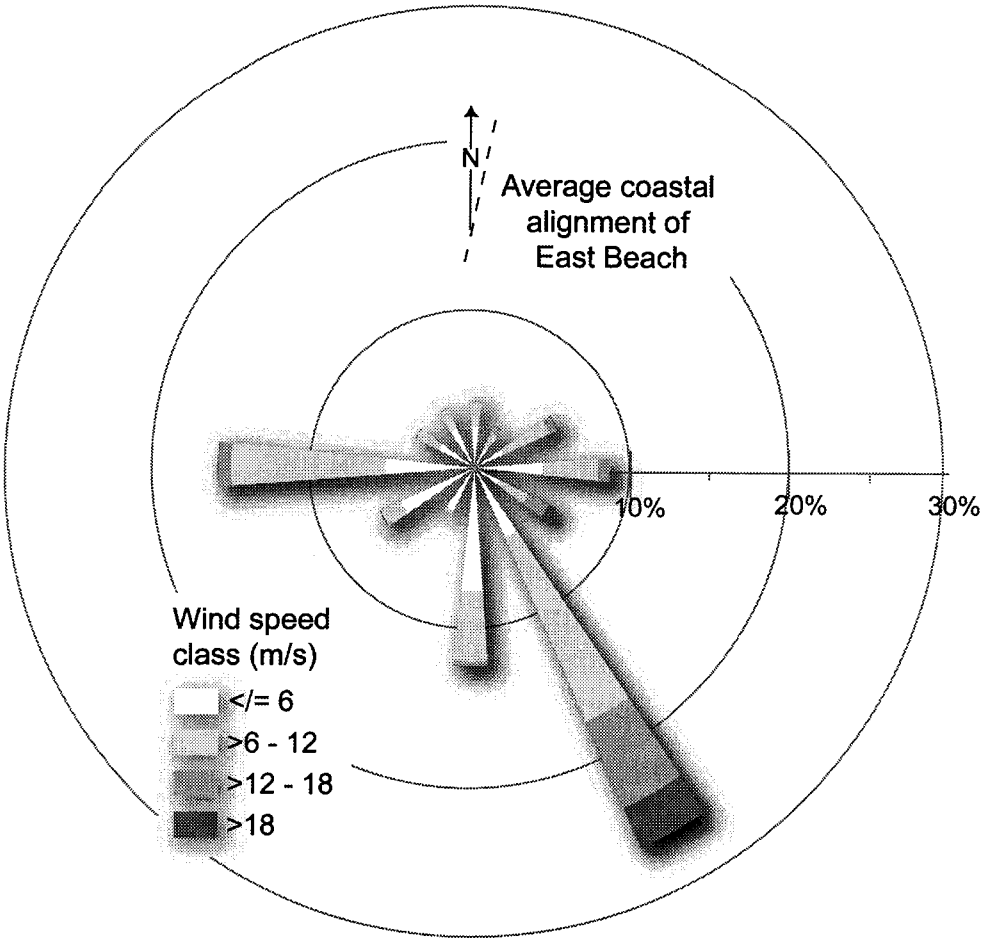

Figure 5.1 The annual wind rose from EC-Rose Spit (1995-1999) for HG shows the greatest magnitude winds from the southeast and a secondary mode of lower magnitude winds from the west.

The wind regime in HG is seasonally opposed, with the greatest magnitude winds from the southeast experienced from September to April (Figure 5.2). During May through August, westerly winds of lesser magnitude predominate, but southeasterly winds still show the greatest magnitude (Figure 5.2, Table 5.1).

Average monthly wind speeds range from 6.37 m s^{-1} in August to 9.68 m s^{-1} in December (Table 5.1). The annual pattern of the mean monthly wind speeds

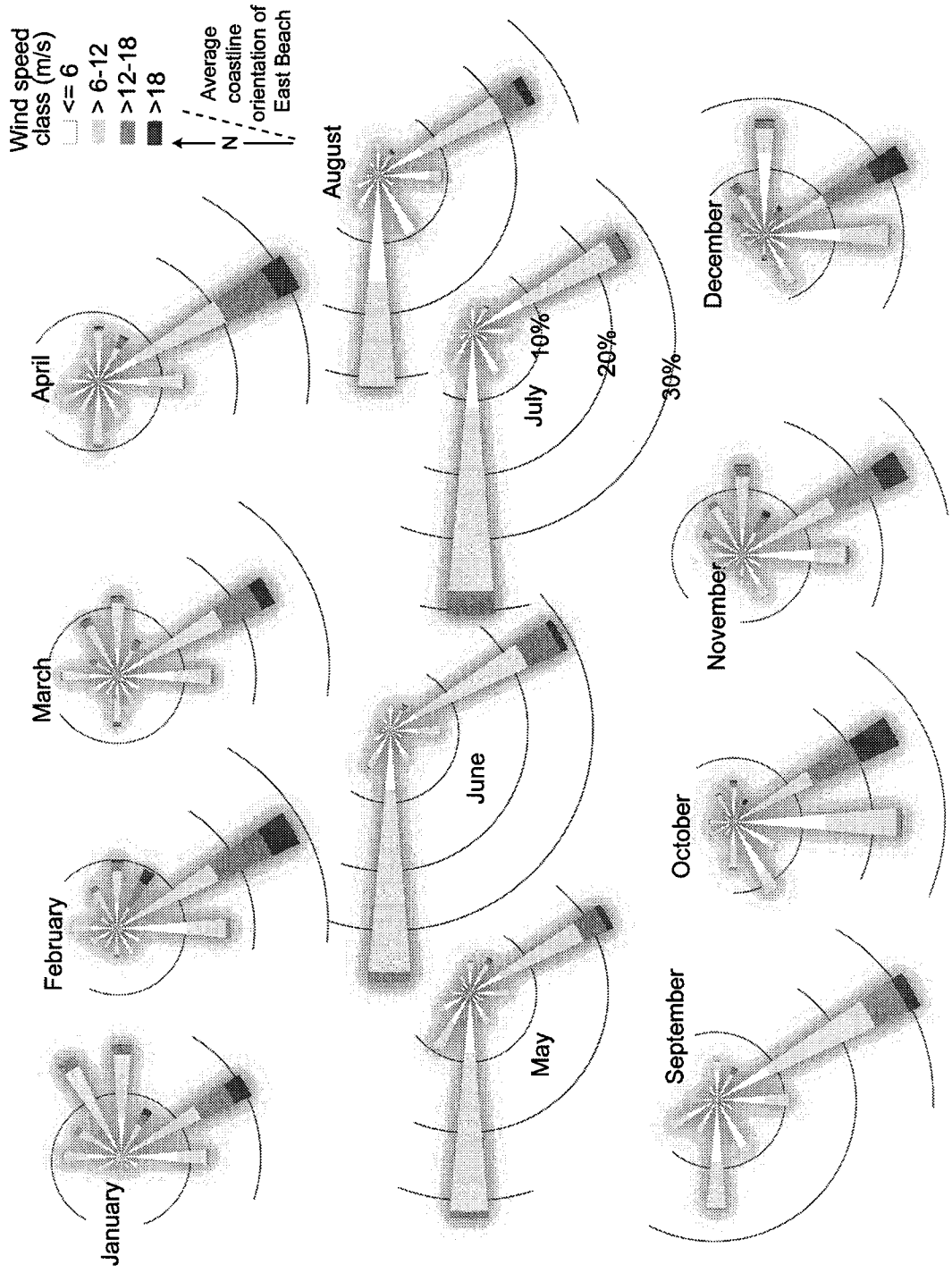

Figure 5.2 Monthly wind roses from EC-Rose Spit (1995-1999) show a seasonal shift in the wind regime. During the winter, fall and early spring, strong southeast winds are dominant, while during the late spring and summer, lower magnitude west winds dominate.

Table 5.1 Annual and monthly wind regime characteristics of northeast HG from five years of EC-Rose Spit wind data (1995-1999).

	Average wind speed (m/s)	Percent competent winds (>6m/s)	Primary directional mode	Secondary mode or range
Annual	8.10	62.3	SSE	W
January	8.71	69.4	SSE	ENE to ESE
February	9.17	68.6	SSE	S
March	8.37	65.5	SSE	S
April	7.97	59.0	SSE	S
May	7.48	62.9	W	SE
June	7.99	66.6	W	SE
July	7.03	57.4	W	SE
August	6.37	45.5	W	SE
September	6.97	51.6	SSE	W
October	8.69	62.2	SSE	S
November	9.08	69.6	SSE	S
December	9.68	70.6	SSE	E

is highest in December, decreasing through the spring until August, followed by a steep and steady increase through the fall into December (Figure 5.3). Throughout all months, the highest magnitude winds (i.e., > 18 m s^{-1}) are from the southeast, with the greatest proportion of these experienced in February and October (Figure 5.2).

The monthly trend for competent winds (i.e., winds above the threshold of sediment transport of 6 m s^{-1}) is similar to that of the monthly wind speeds, with the greatest percentage in December at 70.6%, and the lowest in August at 45.5% (Figure 5.3). Wind competence decreases steadily from a high in December through April, although a late spring maximum of 66.6% is experienced in June. A dramatic decrease in July and August is followed by a steep and steady rise of competent winds through the fall to December (Figure 5.3).

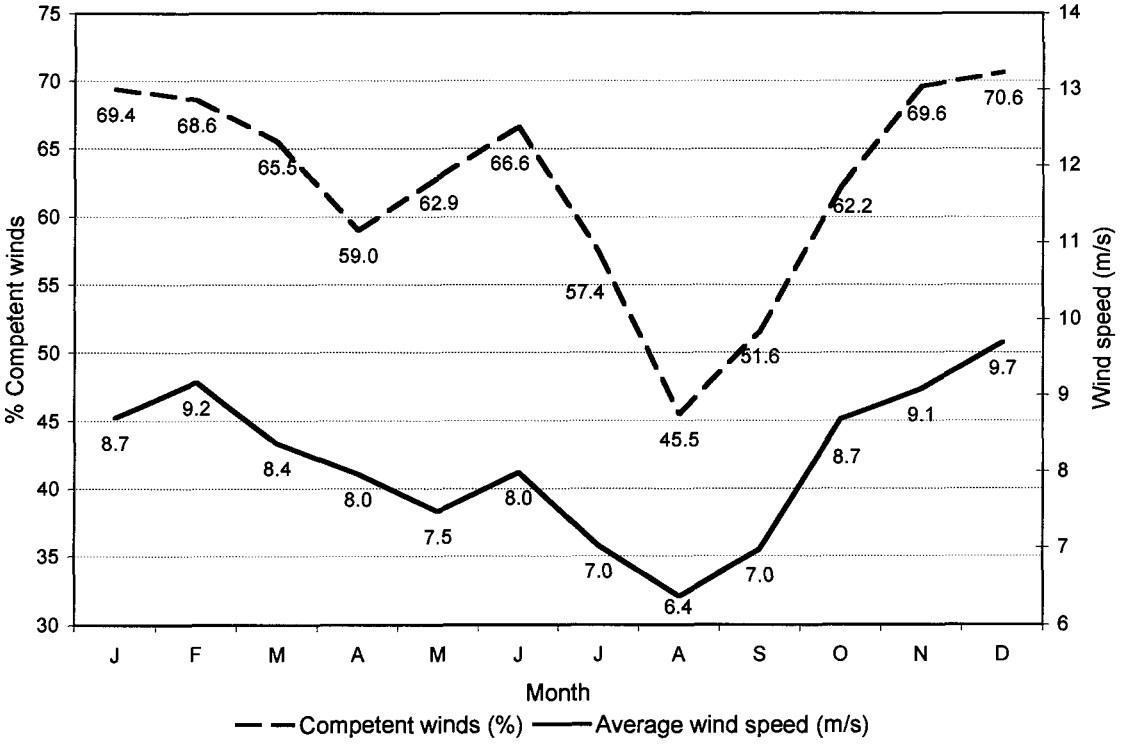

Figure 5.3 Mean monthly wind speeds and percent monthly wind competence from EC-Rose Spit (1995-1999) show a seasonal shift from high magnitude winds in the fall, winter and early spring while lesser magnitude winds during the summer.

5.2 Regional models of aeolian activity and dune mobility

To assess sediment transport potential and dune activity under these wind conditions, the same five-year period was used to calculate the results for two of the models under investigation (i.e., Fryberger (1979) and Tsoar and Illenberger (1998)), while the Lancaster (1988) model was calculated using the 30-year climate normals from EC-Sandspit (see Section 3.2.4).

5.2.1 Fryberger's (1979) sediment drift potential model

The Fryberger (1979) sediment drift potential model characterizes wind regimes and dune morphology using standard meteorological data. This model was originally developed using 134 predominantly arid sites to develop a classification of wind energies and aeolian landforms. From his work, Fryberger (1979) found wind energies ranging from 89 to 489, but subsequent work in both coastal and arid regions (Carson and Maclean 1986; Fryberger 1991; Nickling and Wolfe 1994; Anthonsen et al. 1996; Muhs and Wolfe 1999; Wolfe and Lemmen 1999; Tsoar and Arens 2003; Walker and Barrie 2004) shows a much broader range. For instance, the Great Sand Hills in the Canadian Prairies have DP values ranging from 863 to 1,395 VU (Wolfe and Lemmen 1999), the coastal dunes in IJmuiden, Netherlands have a DP of 1,224 VU (Tsoar and Arens 2003), and the highest calculated DP on Earth is found at Esperanza, Antarctica (Lat. 62° 24S; Lon. 56° 59W), with a DP of 10,246 VU (Pye and Tsoar 1990).

When applied to HG using five years of wind data from EC-Rose Spit (1995-1999, the Fryberger (1979) sediment drift potential model yields an annual average DP of 3,176 VU, an RDP of 1,826 VU to the RDD of 313° and an RDP/DP ratio of 0.58 (Figure 5.4). According to Fryberger's (1979) classification (Table 2.1), this environment is classified as high wind energy with an obtuse to acute bimodal regime. The drift rose illustrates the predominant sediment drift from the southeast, with a secondary vector from the west (Figure 5.4). There are also notable drift vectors from the east and northeast, but no drift vectors from the southwest.

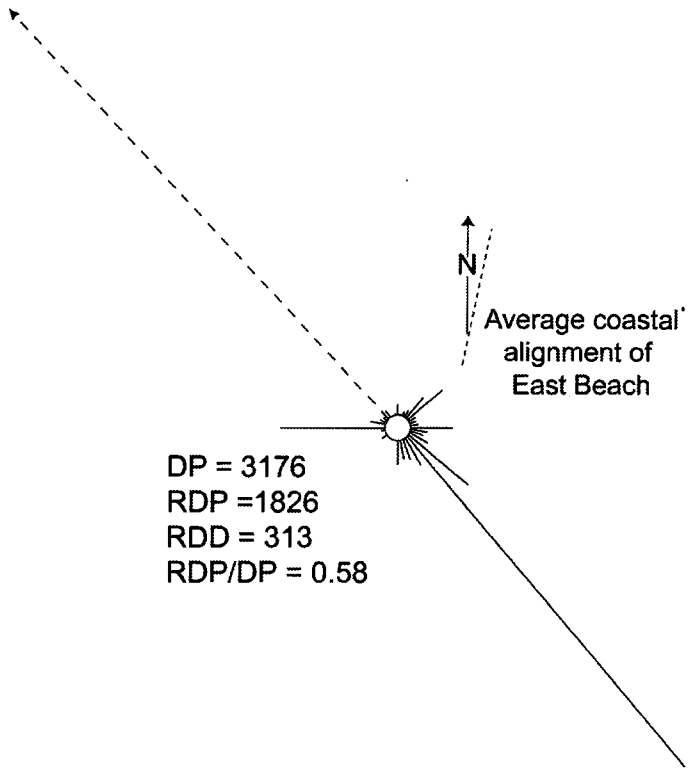

Figure 5.4 Annual Fryberger (1979) sediment drift potential, calculated from 5 years of wind data from EC-Rose Spit (1995-1999), shows significant drift toward the northwest.

Although this region experiences high annual DP due to the location and seasonal shift of the AL and PH, there is considerable seasonal variability (Section 4.1.3). The monthly drift roses in Figure 5.5 show that the greatest potential for sediment drift is experienced from September through February, when all DPs are greater than 200 VU, with a maximum of 364 VU in December (Table 5.2). During the spring months (March through May), while the AL dissipates, DP is reduced and directional variability increases (Table 5.2, Figure 5.5). In June, DP increases to 247 VU but then dramatically decreases to a minimum of 160 VU in August. This period of low DP occurs while the PH

Table 5.2 Summary of annual and monthly results for the Fryberger (1979) sediment drift potential model for HG.

	DP (VU)	RDP (VU)	RDD (degrees to true north)	RDP/DP
Annual	**3176**	**1826**	**317**	**0.58**
January	292	201	291	0.69
February	340	260	311	0.77
March	310	196	300	0.63
April	266	210	321	0.79
May	195	78	358	0.40
June	249	107	4	0.43
July	183	87	35	0.48
August	160	99	337	0.62
September	182	132	324	0.73
October	298	213	321	0.71
November	346	249	302	0.72
December	364	209	299	0.57

dominates the weather circulation of HG, and moderate westerly winds predominate.

Figure 5.6 shows the monthly RDPs ranging from a high of 260 VU in February to a low of 79 VU in May. During the period of May through August, the RDPs are lowest, ranging from 79 VU to 107 VU (Table 5.2, Figures 5.6 and 5.7). The greatest directional variability is observed in May, with an RDP/DP ratio of 0.4, and uni-modal winds are most frequent in April (RDP/DP = 0.79). From Fryberger's (1979) classification (Table 2.1), each month has a wind directionality of obtuse to acute bimodal, although April (RDP/DP = 0.79) and February (RDP/DP = 0.77) are closer to a wide uni-modal directionality.

The monthly RDPs trend closely to monthly DPs, with greatest RDPs observed in the fall and winter, decreasing through the summer (Figure 5.6). There are two notable deviations from this trend in April and December. In April, there is a peak in RDP, while the DP does not vary from its decreasing trend.

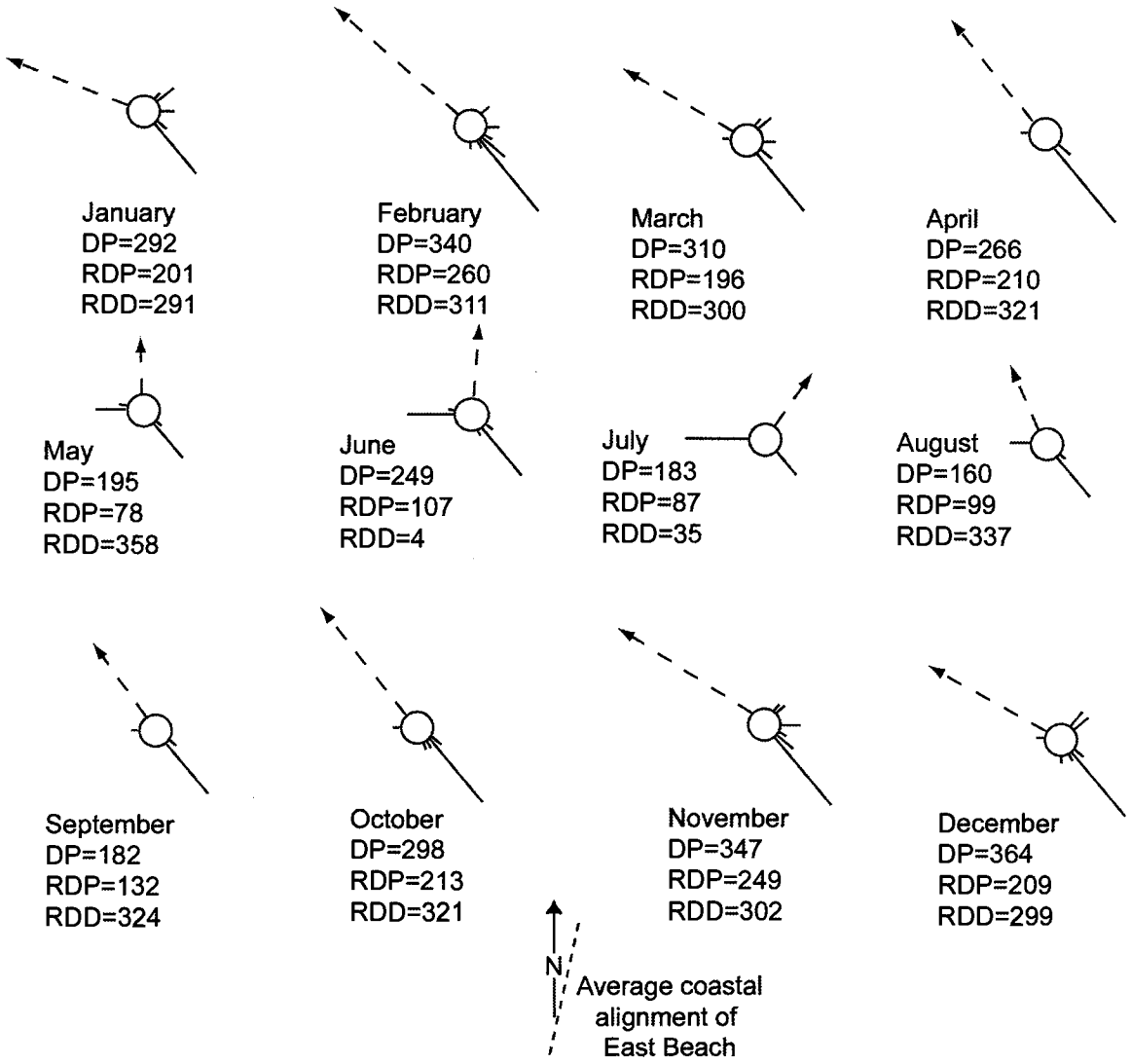

Figure 5.5 Monthly average DP and directional variability for EC-Rose Spit (1995-1999) show a distinct seasonal shift from the fall and winter to the summer.

This increase in RDP is explained by the high RDP/DP ratio of 0.79, which is the lowest observed directional variability. Under uni-modal wind directionality, predominant drift comes from only one direction, therefore the DP and RDP are very similar. In December, the opposite situation occurs. The observed DP is the greatest (367 VU), while the RDP decreases slightly. Again, this is explained with the reduced RDP/DP ratio showing an increase in directional variability.

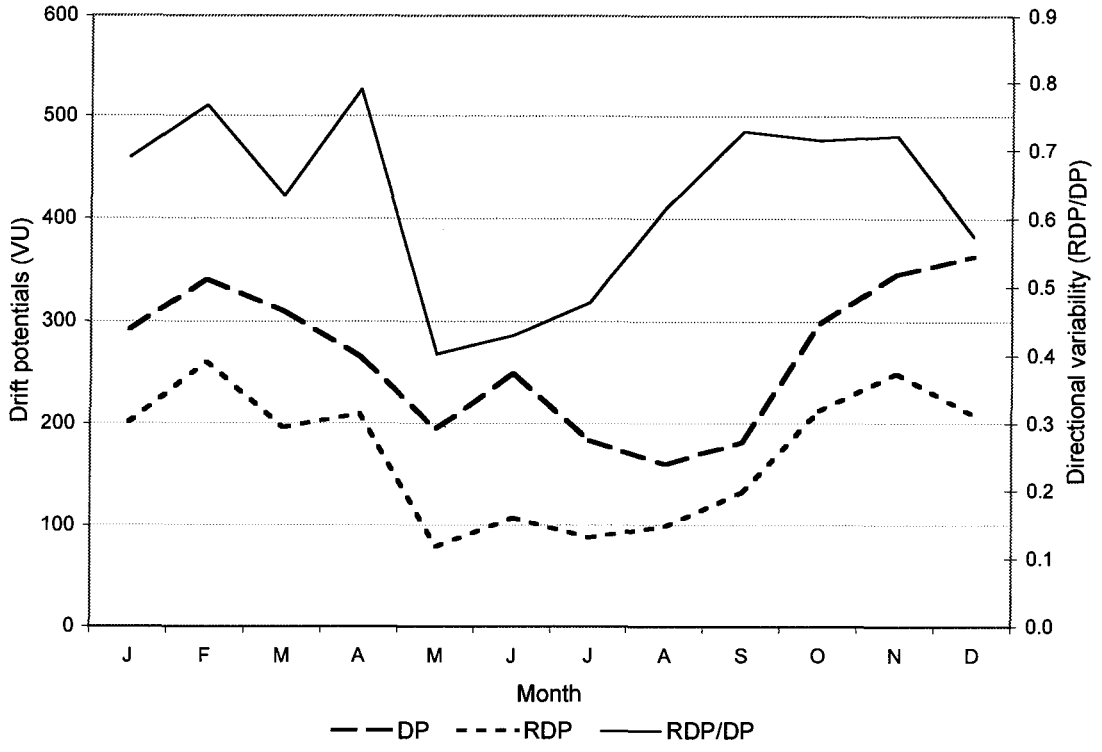

Figure 5.6 Monthly results of the Fryberger drift potential model for the QCI, EC-Rose Spit (1995-1999) show seasonal trend with greater drift potential in the winter and less in the summer, while directional variability increases (closer to zero) in the late spring to early summer.

At 313°, the annual RDD (Figure 5.4) is oblique onshore to East Beach and close to the average parabolic dune alignment of 336 ± 8° (Walker and Barrie 2004). Figure 5.7 shows monthly RDDs with oblique onshore drift fromJanuary through April, followed by a period of alongshore drift to slightly offshore in July, returning to oblique onshore through December. These results show that greatest aeolian drift potential occurs in the fall, winter and early spring months, which likely promotes major dune building. The winds in the late spring and summer months, which blow offshore but are of lesser magnitude, likely modify the dune form by reworking the heads of the dunes, but they do not the alter the dune trend.

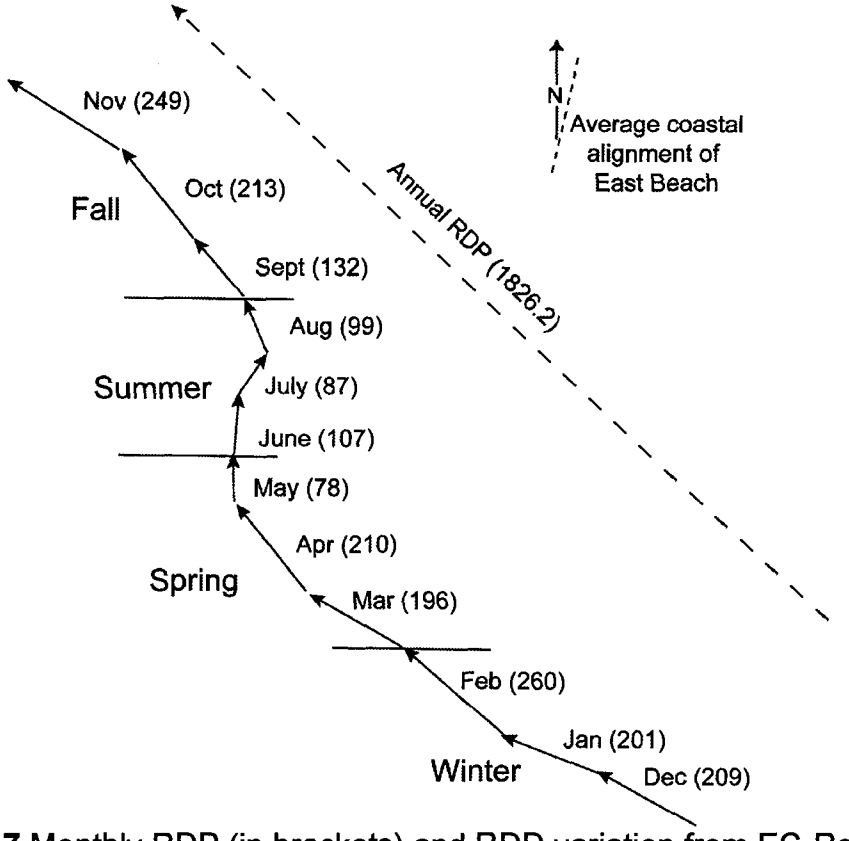

Figure 5.7 Monthly RDP (in brackets) and RDD variation from EC-Rose Spit (1995-1999) show a seasonal shift in drift direction from oblique onshore in the winter shifting to shore parallel in the late spring and obliquely offshore in the summer, then returning to onshore in the fall.

5.2.2 Lancaster's (1988) dune mobility index

Lancaster's (1988) dune mobility index was first derived and verified in a continental setting, where the primary variables controlling dune activity are considered to be the transport capacity of the wind and sediment availability. Lancaster's index provides an ordinal measure of dune activity using the relationship in Equation 7 with W, the percentage of time that wind speed is greater than the threshold of entrainment (i.e., 6 m s^{-1}), and the P/PET ratio, a surrogate measure for vegetation cover or moisture availability for vegetation

growth. In this respect, the Lancaster (1988) model considers the amount of sediment supply to be sediment available.

Applied in HG, the Lancaster (1988) model yields a dune mobility value of 16.5 calculated from the 30-year climate normals (1971-2000) from EC-Sandspit. According to Lancaster's (1988) index, this value suggests a dune system that is fully vegetated and inactive. From Section 4.2, the dunes in this region are partially to fully vegetated, yet dune activity is spatially variable and ranges from fully inactive in the inland regions and the heads of the parabolic dunes to highly active along the foredunes, in the blowouts and in the deflations of the parabolics. The active areas on this coast are predominantly those that are adjacent to the beach, as these areas have the additional supply of sediment from the littoral system and are subject to dune reactivation due to the rapid retreat rates of this coastline.

5.2.3 Tsoar and Illenberger's (1998) dune mobility index

Tsoar and Illenberger (1998) challenge the premise of Lancaster's (1988) index, suggesting that the P/PET ratio is not an effective measure of moisture availability for plant growth in sand due to the high infiltration rates in sand. They suggest dune mobility is more effectively determined by the frequency, magnitude and directional variability of the wind, as wind provides the energy source for aeolian transport and also limits vegetation growth (Tsoar and Arens 2003). Tsoar and Illenberger's (1998) model uses the Fryberger (1979) sediment

drift potential to assess vegetation cover and dune mobility by the relationship in Equation 8.

Annual results for the Tsoar and Illenberger (1998) mobility index for HG, calculated from five years (1995-1999) of wind data from EC-Rose Spit, yield an M value of 5.6. As this value is greater than 1, this index classifies the dunes in HG as mobile and unvegetated. Dune mobility and activity in HG is variable, from highly vegetated and relatively stable inland to moderate to low vegetation cover and highly active adjacent to the beach. Tsoar and Illenberger (1998) do not define "mobile" for their classification, but if it refers to actively migrating dunes, this is not the case in HG. The parabolic dunes are predominantly highly vegetated but not mobile. The foredunes may be considered to be mobile, but their landward migration results from coastal retreat combined with high onshore sediment supply and wind energy, not from wind energy alone, as this model suggests.

The Tsoar and Illenberger (1998) model does not differentiate between inland and coastal dunes. In fact, Tsoar and Illenberger (1998) do not provide the locations from which their original assessment was conducted, nor does Tsoar, in his subsequent work with this model (Tsoar 2002; Tsoar and Arens 2003), provide further detail regarding its derivation. The application of this model to assess the mobility of dunes is therefore very limited.

5.3 Discussion

The Fryberger (1979) model provides a measure of the potential drift of sediment based solely on wind data. It represents well the potential transport of sediments by wind as it recognizes the exponential increase in sediment drift with increase in wind speed (Equation 6). However, this model does not incorporate controls on the aeolian transport process such as surface moisture, vegetation, fetch length, topographic effects, or sediment supply or availability. As such, the magnitude of the DPs may not accurately predict sediment flux, but this model does provide a good relative measure of wind energy and a methodology for characterizing the wind regime both visually and quantitatively. Furthermore, Fryberger (1979) developed a morphological classification of aeolian sedimentary features by combining wind energy assessments with landform interpretations.

In Fryberger's (1979) original work, only one site of the 134 hosted parabolic dunes. This was at the Holloman Air Force Base, New Mexico, classified as a low-energy wind environment with considerable directional variability (RDP/DP=0.37), where both barchanoid and parabolic dunes were found (Fryberger 1979). This limited assessment of sites with parabolic dunes may be due to the scale and quality of satellite imagery used in 1979, in which parabolic dunes were not distinguishable, or perhaps, as Fryberger (1979) suggests, the limited temporal extent of his assessment restricts accurate landform interpretation. For example, Fryberger's (1979) methodology classifies the current wind regime and associates it with an interpretation of the aeolian

landforms. However, those aeolian features may be centuries or millennia old and perhaps were formed under a wind regime very different than that experienced today. In these instances, the morphological classification would incorrectly associate the morphology of a dune system with a wind regime. In coastal dune systems, the Fryberger (1979) morphological classification is further limited as it pre-dates the major research on coastal dune geomorphology conducted in the 1980s and '90s. As a result, there is insufficient supporting evidence in Fryberger's (1979) original work to accurately predict wind regimes where parabolic dunes might occur.

To extend the application of Fryberger's (1979) morphological classification to coastal systems, the wind energies and climatic conditions of four coastal sites with parabolic dunes are presented. These sites are: the Oregon dunes, the Greenwich dunes in Prince Edward Island, the transgressive dunes in Aberffraw, North Wales, and those on East Beach, Haida Gwaii, British Columbia. The Oregon coast is host to a wide range of dune morphologies including transverse dunes, barchanoid ridges and parabolic dunes (Cooper 1958; Fryberger 1991). These transgressive dunefields are currently mobile, migrating north-eastward at 3.8 m a^{-1} (Hunter et al. 1983). The Oregon coast has a temperate, rainy climate (average annual precipitation = 1,436 mm a^{-1}) with an obtuse bimodal wind regime (Hunter et al. 1983; Fryberger 1991). The higher magnitude winds occur during the rainy season (winter), but from the southwest (oblique onshore), while a secondary mode of lower magnitude wind from the northwest occurs during the summer. The wind energy in Oregon is low, with a

DP of 261 VU, an annual average wind speed of 4.1 m s^{-1} and an annual competence of winds at 22% (Table 5.3). The directional variability is obtuse to acute bimodal with an RDP/DP ratio of 0.63 (Table 5.3).

Table 5.3 Summary of wind regime characteristics for four coastal dune sites. DPs for Oregon and PEI are calculated by wind speed in knots by the same methodology outlined in Section 3.2.3. Data for Aberffraw are from Bailey and Bristow (2004).

	Haida Gwaii, BC, Canada	Greenwich Dunes, PEI, Canada	Oregon Dunes, USA	Aberffraw, north Wales, UK
Annual mean wind speed (m/s)	8.5	3.9	4.1	5.7-8
Annual wind competence (%)	62.3	12.8	22	N/A
Calm winds (%)	0.035	8.7	9.8	0.6
DP (VU)	3176	226	261	2084
RDP (VU)	1826	98	165	1657
RDP/DP	0.57	0.43	0.63	0.80
Annual precipitation (mm)	1399	1159	1436	1433
Data acquired	EC-Rose Spit	EC-Stanhope	~	*
Years of assessment	1995-1999	1995-2002	1982-1990	N/A

N/A - data not available
EC - Environment Canada
~ Data source: Samson surface met data (http://www.webmet.com/State_pages/SAMSON/24284_sam.htm)
* Data source: Bailey and Bristow 2004

The coastal dunes at Greenwich, PEI, also exist in a moist environment (annual average precipitation = 1,159 mm a^{-1}), but with lower winter temperatures (i.e., 73 days below 0°C), 25% of the total precipitation is received as snow (EC-CMC 2002). During the winter months, the dunes are typically snow covered, dramatically reducing the availability of sediment for transport (Hesp et al. 2004). The dunes in this area show a nearly continuous, well-vegetated foredune ranging in height from 4 to 10 m, with active blowouts backed by parabolic dunes with migration rates ranging from 0.8 to 13.5 m a^{-1} (Catto et al.

2002). From wind data from Stanhope, PEI, the wind energy is similar to that in Oregon with a DP of 226 VU, an annual average wind speed approximately half of that of HG, but similar to Oregon, at 3.9 m s^{-1}, and a low frequency of competent winds at 12.8% (Table 5.3). The directional variability in PEI is moderate, with an RDP/DP ratio of 0.43.

The coastal dunes at Aberffraw, North Wales, experience an annual average temperature of 12.6°C and high annual precipitation (1,433 mm a^{-1}) (UKMetOffice 2004). With a DP of 2,084 VU, an RDP of 1,657 VU, low frequency of calm winds (i.e., < 0.6%) and a low directional variability (RDP/DP = 0.79), the dunes in Aberffraw experience only two-thirds the wind energy affecting the dunes in HG (Table 5.3), yet they are highly mobile (Bailey and Bristow 2004). This site hosts a fully developed, transgressive dune complex 3 km long and 1 km wide, comprising two foredune ridges and three rows of compound parabolic ridges migrating at 1.3 m a^{-1} (Bailey and Bristow 2004). It is constrained on both edges by low headlands comprising Precambrian rock ridges that extend inland (Bailey and Bristow 2004).

To extend the Fryberger (1979) morphological classification, these four coastal sites could be added, as they indicate that parabolic dunes can also be found in intermediate to high wind energy environments (226 to 3,176 VU) with directional variability ranging from obtuse bimodal to narrow uni-modal (0.43 to 0.8).

Results of applying the Lancaster (1988) dune mobility index in HG using the 30-year climate normals (1971-2000) suggest that the dunes on East Beach

are vegetated and inactive. From the dune geomorphic assessment (Section 4.4), the heads and trailing arms of the parabolic dunes on East Beach are stabilized by dense woody vegetation (e.g., trees, shrubs), but the deflation plains remain only partially vegetated, with aeolian transport of sediment occurring. Furthermore, the foredunes and blowouts on this coast remain fully active. From the air photo assessment, stabilization, via vegetation cover, increased on the trailing arms and heads of the parabolic dunes on East Beach, while minimal migration is observed during the 31-year air photo record (1966-1997) (Section 4.4).

The use of precipitation and PET as a proxy for vegetation cover in the Lancaster (1988) model, and hence sand transport potential, simplifies the dynamics of vegetation growth and may provide a good estimate for inland or continental environments, but this ratio does not represent the conditions well for HG. Tsoar (2002) argues that the P/PET ratio oversimplifies the control of vegetation cover primarily because the water balance is not an effective measure in dune sands. Due to the large pore spaces in sand, precipitation infiltrates quickly, away from the surface, and is thus not readily available for plant growth unless precipitation occurs in frequent, low-magnitude events (Tsoar and Illenberger 1998; Tsoar 2002). In regions with very low precipitation (~0 mm), this model yields values that suggest infinite dune mobility, which is not possible (Knight et al. 2003).

In addition, this model uses the percent wind competence (W), thus the full effect of wind energy in dune mobility is poorly represented. The potential

transport of sediment by aeolian processes increases exponentially with an increase in wind speed (Bagnold 1941). Therefore, in regions that experience strong winds, the use of W grossly under-represents the effectiveness of aeolian activity. As suggested by Lancaster and Helm (2000), perhaps a different value for wind energy should be used that places greater weight on faster wind speeds, such as the cube of the mean wind speed.

Lancaster (1997a) recognized that the critical factors controlling dune mobility vary significantly from region to region. Lancaster and Helm (2000) found that mobility of the dunes in the Kalahari, the Great Plains, the Mojave and southern California deserts is controlled by vegetation cover, while mobility of the dunes in the Australian and Sonora deserts is controlled by wind strength. HG is subject to high wind energy and is not an arid environment. Precipitation and vegetation cover seem to have less influence on dune mobility in this region than wind energy.

The major limitation of the Lancaster (1988) mobility index in HG is that it was developed in a continental setting where sediment supply is equal to sediment availability. Therefore, it only accounts for changes in transport capacity and sediment availability through the P/PET ratio, not variations in sediment supply. When applied to dune systems that have a fixed sediment supply controlled by vegetation cover (e.g., continental dunes), this model performs well. As this model does not account for external sediment supply, if it is applied to a dune system in which the mobility is not controlled solely by transport capacity and sediment availability, it performs poorly. When applied in

HG, the Lancaster (1988) dune mobility index predicts well the dune mobility of the inland dunes that are removed from the external sediment source (i.e., the beach).

As this model was developed for inland dune systems, it does not consider the mode of dune reactivation. In continental settings, drought is the most likely control on dune mobility, which is accurately represented by this index. In coastal environments, dune mobility and reactivation are less controlled by variations in aridity but are more dependent on coastal erosion events as a result of sea-level variations coinciding with increased storminess (Tsoar and Arens 2003). Tsoar and Arens (2003) suggest this is the case for the coastal dune systems in western Europe and the northwest coasts of North America. From Section 4.2, this is also the case for East Beach, as the rapidly retreating coastline and high onshore sediment supply appear to control dune activity, not vegetation cover.

The application of the Lancaster (1988) model in HG to calculate long-term dune mobility is therefore cautioned, as it provides an overall assessment of dune mobility that is only partially accurate. The parabolic dunes have become increasingly stabilized by vegetation, but they are not inactive. Due primarily to the rapidly retreating coastline, in combination with high year-round wind energy, the foredunes and blowouts on this coast are highly active, as are the deflation plains of most of the parabolics. If this model were to be applied remotely to assess the mobility of the dunes on East Beach, the results would not be able to capture the complex activity of these features. However, understanding the

limitations of its application, this model does provide an accurate estimation of the propensity for coastal dunes to stabilize once they head inland and are removed from the beach sediment supply.

According to the annual results of the Tsoar and Illenberger (1998) model, the wind energy in HG is sufficient to hamper the ability of vegetation to grow, thereby creating highly mobile dunes. From the 31-year air photo record and morphological assessment in Section 4.2, the parabolic dunes on this coast are partially to fully vegetated, and although they are active, they are not mobile (Section 4.2) like the dune fields in Oregon and Aberffraw. However, the foredunes on this coast are active and migrating, primarily from rapid coastal retreat rates and continued onshore sediment supply, not from variations in vegetation cover.

When applied in HG, the Tsoar and Illenberger (1998) model incorrectly classifies this system as unvegetated and highly mobile. Tsoar and Arens (2003) propose that dune systems that deviate from the original model are likely stabilized artificially as part of anthropogenic sand dune management (e.g., the coastal dune systems of the Netherlands), or that the dunes were covered by vegetation in the past when the climate was different than current conditions and M was less than 1.

It is unlikely that either of these proposals explain the deviation in HG. Although some areas of East Beach were used in the early 1900s for homesteads, cattle grazing and gold mining (Dalzell 1989), there is no evidence of anthropogenic management of the dunes of northern East Beach. Vegetation

cover appears to have increased during the last 31 years, thereby stabilizing the inland portion of the dunes, while the foredunes remained active due to the external sediment source and high wind energy. These conditions are not differentiated in the Tsoar and Illenberger (1998) model and should be assessed in more detail in different environmental settings to determine if this model can in fact accurately determine regional dune mobility.

Tsoar and Illenberger (1998) proposed a dune mobility index that, unlike Lancaster's (1988), is not limited to certain environmental conditions. However, as the development and the interpretation of the model are not fully defined by the authors, further discussion and verification of its application in varying dune settings is required before it can be widely used. From its application in HG, this model does not provide additional information about dune mobility than can presently be assessed from the Fryberger (1979) model alone. In fact, the Tsoar and Illenberger (1998) model coarsens the results and removes valuable information that is provided by the Fryberger (1979) model. Therefore, the application of this model in HG is cautioned, and further assessment and clarification of its application is recommended.

5.4 Summary and Conclusions

The wind regime experienced in HG is seasonally bimodal, with the strongest and most frequent winds from the southeast and a secondary mode of lower magnitude winds from the west during the summer months. This wind regime results from the intensity and position of the Aleutian Low pressure

system and the anticyclonic circulation from the Pacific High in the summer. The seasonal shift of wind speed and direction is reflected in the monthly drift roses, with high onshore drift potential on East Beach in the fall, winter and early spring, decreasing and shifting to alongshore and slightly offshore in the late spring (Figures 4.5 and 4.7). The parabolic dunes align closely with the southeast winds, therefore the secondary modes in the wind regime make rework the dunes system but they do not alter the predominant dune trend.

From applying and critiquing the three models of dune mobility and sediment drift potential in HG, only two of the models appear to provide accurate results. The Fryberger (1979) model provides a good relative measure of potential sediment drift and illustrates that this site experiences comparably very high annual drift potential and moderate directional variability. The application of the morphological classification is limited in this environment; however, this study has presented four additional sites and a range of DPs and directional variability in which coastal parabolic dunes are found. Further assessment of parabolic dunes and the addition of coastal dune morphological assessment would greatly enhance the application of the Fryberger (1979) model.

The Lancaster (1988) model, as suggested by Lancaster and Helm (2000), was found to predict the mobility of dunes accurately when applied under the same conditions it was developed in (i.e., continental and arid). However, this model can not accurately predict dune mobility when the controls on the dune system are sediment supply from an external source rather than vegetation cover controlled by aridity. In HG, this model may be used cautiously to predict the

propensity of dune mobility for the inland portion of the dunes that are removed from the nearshore sediment source. This would require a greater understanding of the sedimentary system on this coast and the extent to which the beach sediment source influences the inland dunes.

This analysis has shown that the Tsoar and Illenberger (1998) model requires further discussion from the developers as to how it was developed and its interpretation. When applied in HG, the results do not provide any more analysis or insight into the aeolian activity of this sedimentary environment. In fact, the Tsoar and Illenberger (1998) model coarsens the results, hiding valuable information the Fryberger (1979) sediment drift model provides.

6.0 Morphodynamics of a foredune-trough blowout complex

This chapter presents a meso-scale examination of the morphodynamics of a foredune-trough blowout complex on East Beach (Site 2, Figure 4.12) over a two-year period (June 2002 to June 2004). This assessment includes a morphologic and volumetric analysis from a topographic survey, recurrent measurements of cross-shore profiles and a detailed assessment of morphological response of a trough blowout from a surface change pin (SCP) network.

The study site is a 270 m stretch of foredune at Site 2 (Section 4.2.2) extending from approximately 70 m up to 90 m landward of the foredune crest to the waterline, including the beach and an extensive driftwood jam in the backshore (Figure 3.2). No detailed airflow measurements were conducted at this site, therefore the discussion of morphological response of this foredune-trough blowout complex draws on relevant literature to describe the observed changes.

6.1 Geomorphic and volumetric changes in a foredune backshore driftwood jam complex

6.1.1 Topographic (surface elevation) change – June 2002 to June 2004

Figure 6.1 shows that the dominant surface change during the two-year period of study is positive, ranging from 0 to 3 m of aeolian sediment deposition. Landward of the foredune crest, the foredune plain accreted 0 to 2 m, while the greatest accretion occurred in the backshore at the foredune toe (2 to 3 m).

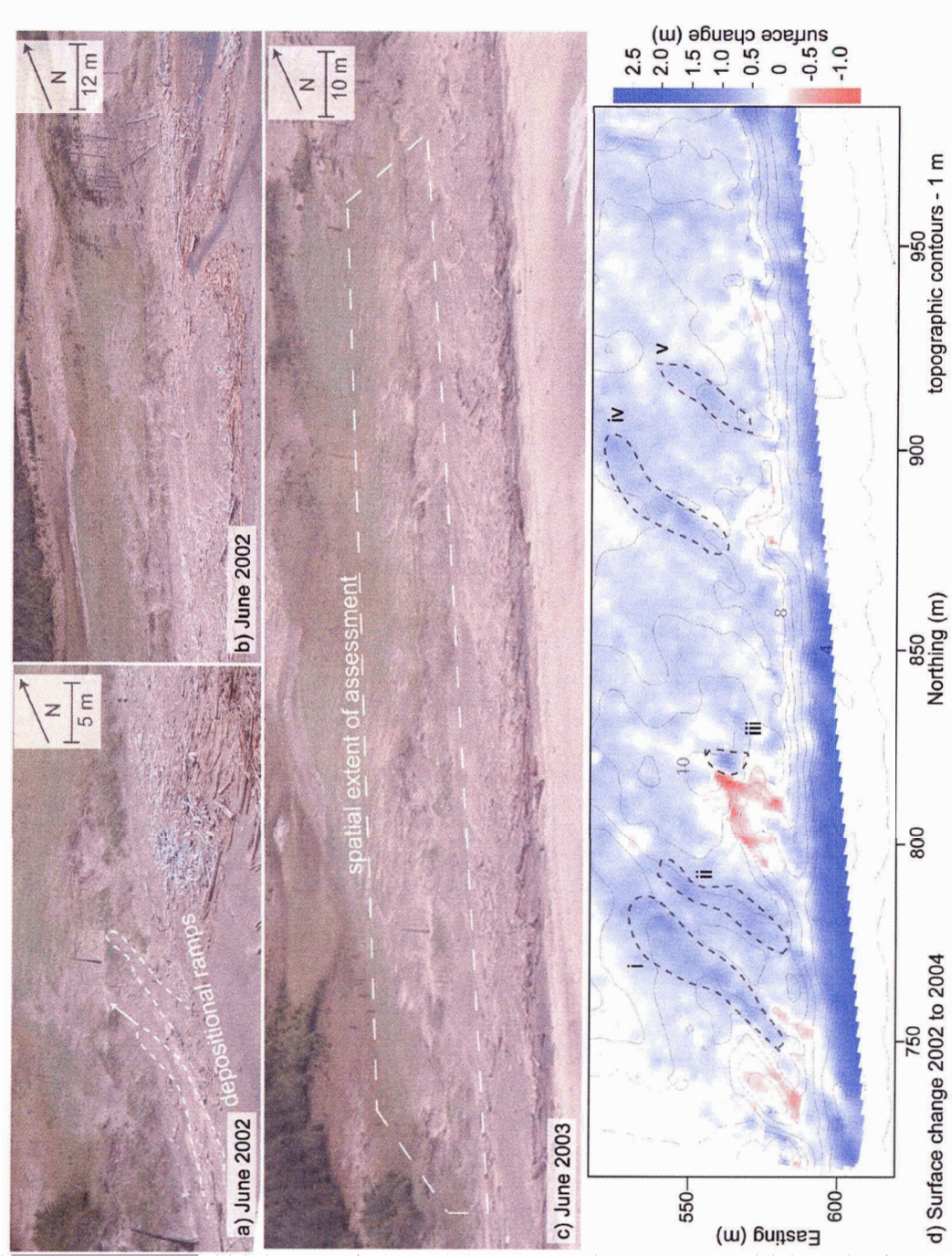

Figure 6.1 a) and b) Aerial photos of the study site in June 2002. c) Aerial photo from June 2003 with the spatial extent (34700 m^2) of topographic survey used to assess volumetric change of the foredune complex. d) Spatial representation of surface change measured from the recurrent topographic survey with 1 m grid spacing. Contour interval 1 m.

Figure 6.1d i, ii, iii and iv shows four linear lobes of enhanced deposition (> 1.5 m) along the foredune plain closely aligned with the southeast wind direction. The longest lobe (> 65 m) is located directly downwind from a small blowout in the foredune crest (Figure 6.1d i), and a second lobe, approximately 40 m long, is located 10 m to the north (Figure 6.1d ii). Both of these features are aligned with unvegetated sediment ramps at the base of the foredune (Figure 6.1a). There is a smaller depositional lobe landward and slightly to the north of the saucer blowout (Figure 6.1d iii), and two long linear depositional lobes (> 50 m) that are not visibly associated with other features on the foredune or in the backshore (Figure 6.1d iv and v).

Although the predominant surface change is depositional, localized erosion is observed in the deflation basins of the two large blowouts (Figure 6.1d) and at several areas along the seaward face of the foredune in small incipient blowouts. Interestingly, the foredune crest, in white, shows minimal vertical and horizontal change during the study period (Figure 6.1d).

The volumetric change at this site shows a net accretion of 29,692 m^3. The total deposition amounts to 30,474 m^3, while localized erosion accounted for 782 m^3. When standardized spatially, by beach width (270 m), and temporally, by the two years, this result yields +55 m^3 m^{-1} width a^{-1}. As the topographic survey only extends up to 90 m from the foredune crest, this flux value is an underestimate of the total volume of sand transported from the beach into the foredune plain. This is also supported by field observations of active sediment

transport and sediment ripples landward of the topographic survey that suggest aeolian sediments are being transported further inland than the grid monitored.

This flux value is compared with a calculated estimate of potential sediment drift using wind data from BLAST2 and the Fryberger (1979) model. Using Bullard's (1997) line A conversion of VU to sediment flux, the RDP calculated from the BLAST2 wind data in m s^{-1} yields a volumetric RDP of 21 m^3 m^{-1} width of beach a^{-1} (Table 6.1). This RDP was calculated for the same period as the topographic survey (June 2002 to June 2004). During this period, almost two months of meteorological data are missing from BLAST2 (June 26 to August 15, 2002), which has influenced the resulting RDP. However, as the missing data are from the summer months, in which westerly or offshore winds of lower magnitude predominate, the resulting error in the RDP is assumed to be minor.

Table 6.1 Summary of BLAST2 wind data and sediment drift potentials for August 2002 to June 2004. Volumetric change calculated using Bullard's (1997) Line A conversion of VU to sediment flux using RDP calculated from m s^{-1}.

Average wind speed (m/s)	4.8
DP (VU) from knots	1418
RDP (VU) from knots	1384
DP (VU) from m/s	155
RDP (VU) from m/s	148
RDD (degrees)	313
RDP/DP	0.96
Volumetric change from RDP (m^3/m/a)	21

As discussed in Section 2.2, models of sediment transport generally assume a transport-limited condition where a uniform, steady wind blows over a simple, dry surface with unlimited supply of sediments. Estimated rates from these models tend to overestimate actual rates of transport (Arens 1996b). However, at this site the actual transport observed is 60% greater than the estimated value. This likely results from under-sampling of wind speed due to the height, local topography and inland location of BLAST2, as well as enhanced sediment transport from the beach into the foredune due to topographic steering and airflow acceleration over the foredune, which can not be captured by a meteorological station 170 m inland.

6.1.2 Seasonal cross-shore profile change

Figures 6.2 and 6.3 show cross-shore profiles A and B, respectively, both established in June 2002, then measured in June 2003, February 2004 and June 2004. From Profile A, the beach face decreased by 0.7 m, and the backshore driftwood jam receded 38 m and increased in height by 2.2 m (Table 6.2). The stoss slope of the foredune and the foredune plain experienced minimal change during this period (Figure 6.2). Profile A in February 2004 contains a minor deviation in positioning (2 m), which results in a shift of the dune crest (see Figure 3.3a).

In June 2002, a sediment-laden driftwood jam (Figure 6.1b) extended approximately 50 m from the toe of the established foredune to an incipient

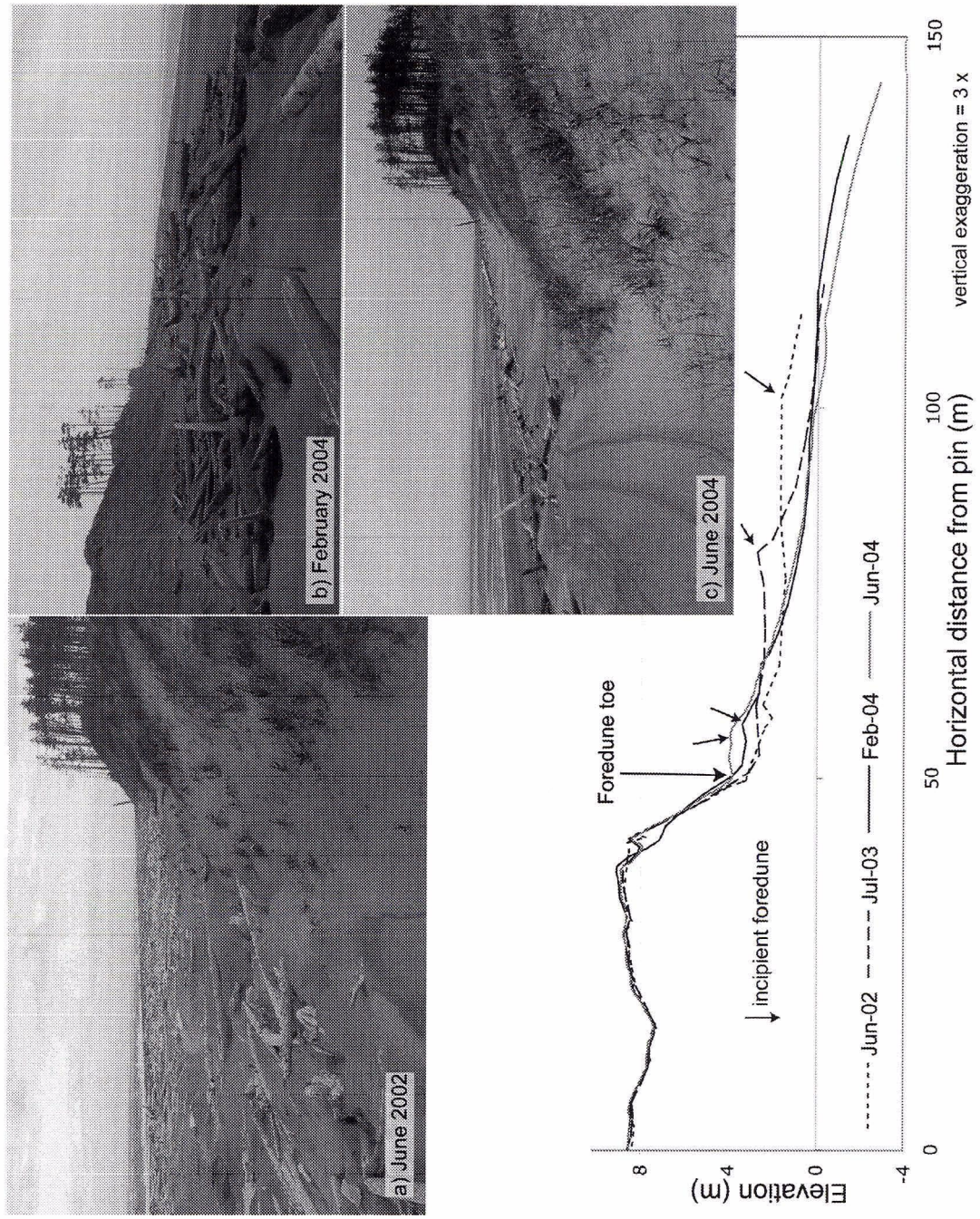

Figure 6.2 Profile A measured in June 2002 (a), June 2003, February 2004 (b) and June 2004 (c). a) Extensive sediment-laden driftwood jam is seen with incipient foredunes. b) In February 2004, most of the driftwood jam was removed. c) By June 2004, the driftwood jam infilled with aeolian sediments and an incipient dune is forming. Photos a) and c) are looking south, while b) is looking north.

Table 6.2 Horizontal and vertical change between profiles of the backshore driftwood jam and beach from cross-shore profiles A and B.

Measurement period	Horizontal change of the backshore driftwood jam (m)	Vertical change of the backshore driftwood jam (m)	Vertical change of the beach seaward of driftwood jam (m)
Profile A			
June 2002 to June 2003	-23	1	-0.7
June 2003 to February 2004	-15	0.7	0
February 2004 to June 2004	1	0.5	-0.1
Profile B			
June 2002 to June 2003	-12	0.6	-0.6
June 2003 to February 2004	-15	0.2	-1
February 2004 to June 2004	-1	0.2	N/A
N/A - not available	(positive values = seaward change)	(positive values = accretion)	(positive values = accretion)

foredune at the seaward scarp (Figure 6.2a). Landward of the incipient foredune, the driftwood jam decreased slightly in elevation (i.e., < 1 m), then rose to the established foredune, creating an interdune depression. By June 2003, the backshore driftwood jam retreated landward 23 m and the depression infilled with aeolian sediments, thereby increasing in elevation by 1 m (Table 6.2). The beach face seaward of the driftwood jam decreased in elevation by 0.7 m during this period.

Between June 2003 and February 2004, the driftwood jam retreated 15 m landward while increasing in height by 0.7 m (Table 6.2). Much of the aeolian sediment in the driftwood jam was removed, while accretion of sediment was observed at the base of the foredune (Figure 6.2b). From the February 2004 profile, the development of a new incipient foredune within the driftwood jam was observed as a slight increase in elevation at the toe of the foredune. By June

2004, the previously exposed driftwood on the backshore was buried by sediments, raising the base of the foredune a further 0.5 m while widening the backshore by 1 m (Figure 6.2c). In June 2004, an incipient 'driftwood' foredune had formed at the seaward extent of the driftwood jam with no vegetation cover (Figure 6.2c).

From Profile B, a similar pattern of change was observed, although the magnitude of change was less (Figure 6.3). From June 2002 to June 2003, the driftwood jam eroded 12 m and increased in height by 0.6 m, while the foredune and foredune plain experienced minimal change (Figure 6.3a). From June 2003 to February 2004, the driftwood jam eroded landward 15 m, the same as Profile A during that period, while accretion of aeolian sediments increased the elevation at the foredune toe by 0.2 m (Figure 6.3b). By June 2004, the backshore at Profile B had moved landward 1 m further and increased in elevation slightly by 0.2 m (Figure 6.3c).

During the year between June 2002 and June 2003, the backshore experienced differential retreat (i.e., 23 m from Profile A and 12 m along profile B). This was due to the presence and subsequent draining of the backshore lake (Figure 6.1b and c). In June 2002, the driftwood jam was much wider along the north of the study site than the southern portion, but during that year the driftwood jam was breached, draining the lake and straightening the seaward extent of the driftwood jam (Figure 6.1c). From June 2003 to February 2004, 15 m of landward retreat was observed along both profiles. As of June 2004, the

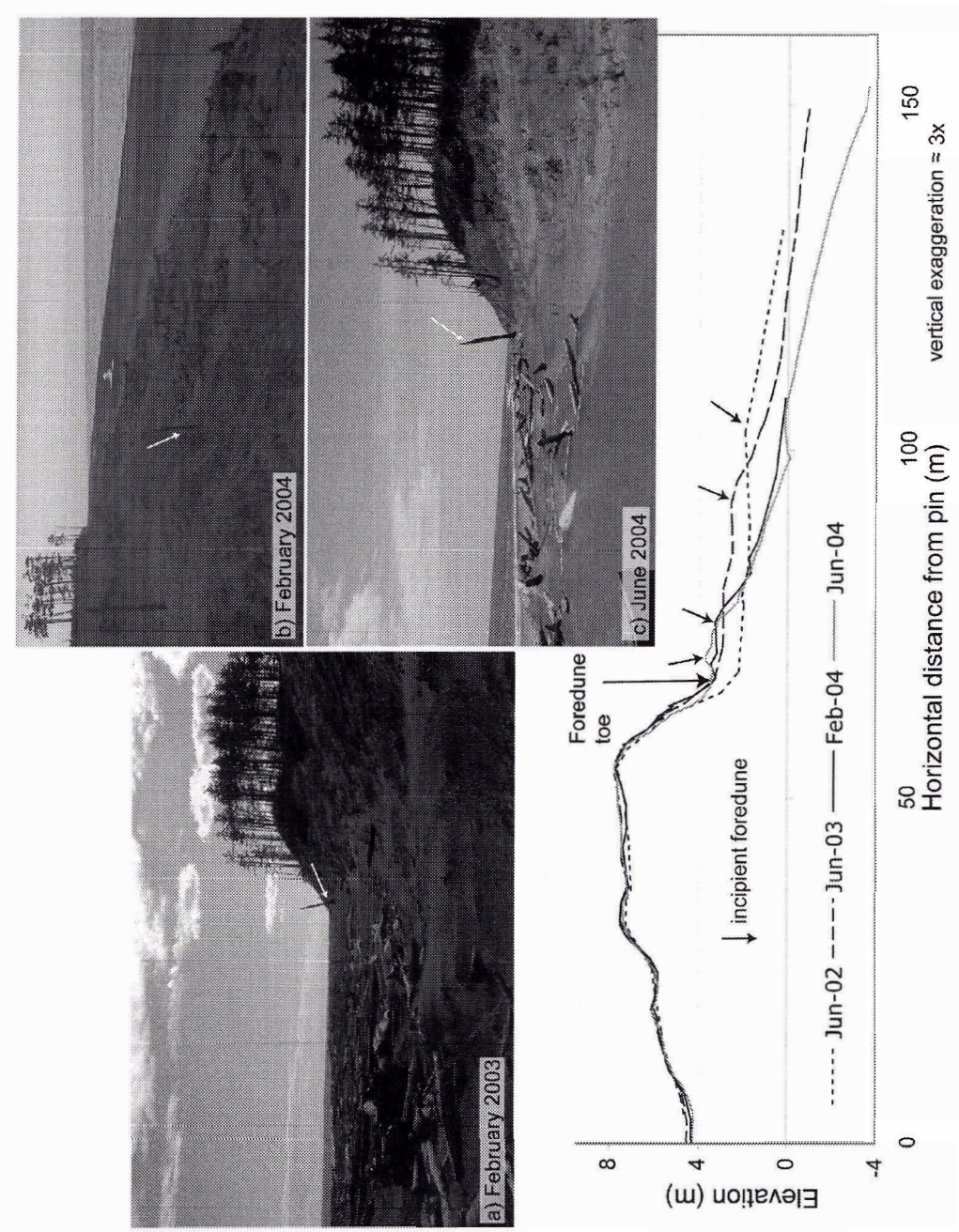

Figure 6.3 Profile B measured in June 2002, June 2003, February 2004 (b) and June 2004 (c). Although no measurement was taken in February 2003, photo a) illustrates well the morphology of the backshore from June 2002 to June 2003. Minimal change is seen on the foredune plain and stoss slope, while major retreat occurred in the backshore. Photos a) and c) are looking south, and b) is looking north. The white arrows show the same snag for reference.

backshore driftwood jam was approximately 10 m wide from the base of the foredune (Figures 6.2 and 6.3).

During this two-year study, HG was subject to a strong southeast storm event (i.e., 25 m s^{-1}), resulting in a 100-year-record water level of 8.1 m in Queen Charlotte City (Figure 1.1). This event occurred on December 24, 2003, and caused major erosion along the east coast of Graham Island. At the study site, during the measurement period that included this event (i.e., June 2003 and February 2004), the backshore retreated 12 m, largely in response to the Christmas Eve storm surge.

6.2 Seasonal morphologic and volumetric change in a trough blowout-depositional lobe complex

The trough blowout under investigation is approximately 30 m long from throat to back rim, with a maximum width of 11.5 m and maximum depth of 4 m (Figure 6.4a). A depositional lobe extends 30 m inland from the trough, while a larger depositional plain extends 45 m further landward of the lobe. The spatial extent of the surface change pins (SCP) network (Figures 3.4 and 6.4a) was established to cover this erosional landform and depositional lobe (Section 3.3.2). The blowout trough is aligned well with the predominant southeast winds and lacks vegetation, while the blowout rim and depositional lobe have moderate to high vegetation cover in the summer (Figure 6.4). During the fall and winter, vegetation cover is reduced as the grasses and reeds die and are buried by aeolian sands (Section 4.1.6).

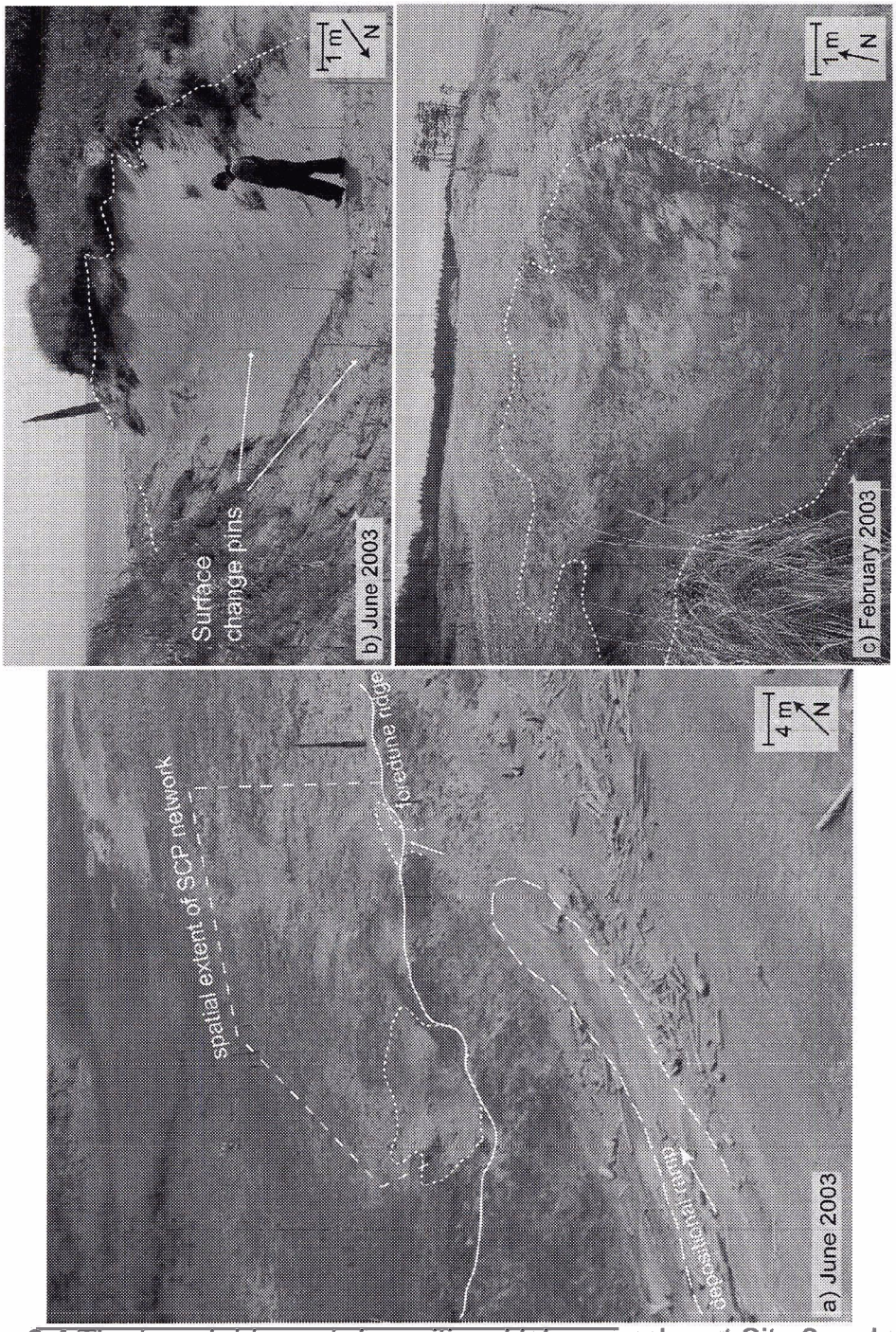

Figure 6.4 The trough blowout-depositional lobe complex at Site 2 under investigation shown in both summer (a and b) and winter (c). Short dashed lines mark the rim of the main trough blowout and two incipient blowouts to the north. The long dashed line highlights a depositional ramp at the base of the foredune that is topographically steered into the northern incipient blowout.

Due to the remote nature of this research site, measurements of the SCP network were conducted only once or twice a year, not at the beginning of each of the four seasons, precluding a true seasonal analysis. However, from the five measurements of the SCP network, a distinct seasonal morphological response is observed between the summer and winter months, as well as between the winter-summer (including spring months) and summer-winter (including fall months) (Table 6.3).

Table 6.3 Volumetric change and sediment drift potential for each period of measurement of the SCP network. Surface change is standardized both spatially (by the area of SCP network) and temporally (by the number of months during the measurement period). Drift potentials are also temporally standardized by the number of month of wind data during the measurement period.

Period of measurement	Summer-winter (June 02 - Feb 03)	(June 03 - Feb 04)	Winter-summer (Feb03- June03)	(Feb 04- June 04)	Summer (June03- Sept03)	Fall - winter (Sept 03- Feb04)
Volumetric change from surface change pin measurements						
Positive volume change (deposition) (m^3)	221	571	119	135	83	506
Negative volume change (erosion) (m^3)	17	10	14	15	3	19
Total volumetric change (m^3)	203	561	105	120	80	487
Standardized surface change (10^{-2} m/month)	1.5	2.0	1.2	0.8	0.7	2.8
Percent erosional surface	9%	2%	13%	12%	4%	4%
Potential aeolian activity						
DP (VU/month)	243	131	264	210	99	282
RDD (degrees)	313	314	315	311	310	314
RDP/DP	0.97	0.95	0.96	0.96	0.98	0.94

For all periods, the net surface change is positive (i.e., sediment accretion) in the blowout-depositional lobe complex. Maximum erosion over the two-year period at any one pin is -41.2 cm (February to June 2003), and the greatest deposition recorded at one pin is 42.3 cm (September 2003 to February 2004).

To assess the morphodynamics in this trough blowout, the patterns of surface change (D_{zs}), the surface deflation from the washer depths (D_{zw}) and the magnitude of redeposition (D_{ws}) are plotted and discussed with seasonal comparisons made (Figure 6.5 to 6.10). When assessed in combination, these three measurements from the SCP network highlight a process that can be termed reworking, where the surface is deflated, and then redeposition occurs. To compare aeolian activity during each measurement period, wind roses and drift roses are presented. To facilitate the description of results, Figure 3.4 locates the descriptive labels assigned to morphological components of the blowout.

6.2.1 Summer - winter

Figure 6.5 shows the wind rose, drift rose and surface elevation change measured for an eight-month period between June 2002 and February 2003. Major surface erosion is evident along the central axis of the blowout trough, with moderate erosion along the base of both lateral walls. One pin in the trough shows major deposition on the western edge of the north lateral wall. The depositional lobe exhibits predominantly accretion, except for one pin located on a northwest-facing slope directly downwind of the blowout (Figure 6.5). Minor deposition is observed on the depositional lobe within 20 m of the blowout trough, while enhanced deposition is observed in a linear lobe farther than 25 m from the blowout rim (Figure 6.5 i). This area is closely aligned with the trough of the blowout, the resultant drift direction (RDD) and predominant southeast winds.

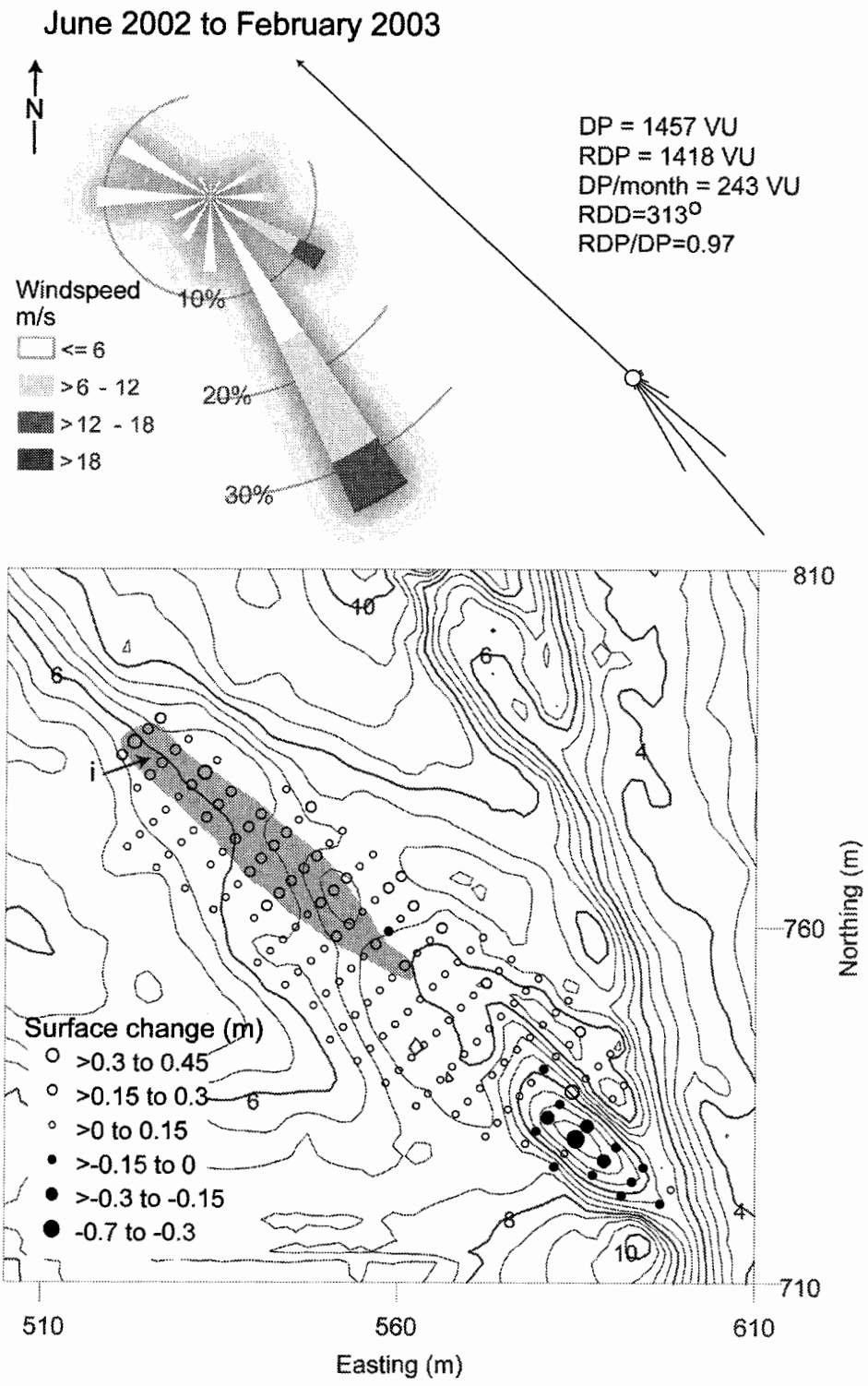

Figure 6.5 Wind rose from BLAST2, Fryberger (1979) drift rose and SCP measurements for summer-winter 2002-03 (June to February). A linear lobe of enhanced deposition, shaded in grey (i), is aligned downwind of the blowout trough. Topographic contour interval is 0.5 m.

The standardized surface change for this period is $+1.5x10^{-2}$ m $month^{-1}$ with an 8% erosional surface (i.e., negative volumetric change/total volumetric change x 100) (Table 6.3). This period of measurement has a calculated drift potential of 243 VU $month^{-1}$, with 45% of the winds from the south-southeast and east-southeast.

For the period of June 2003 to February 2004, net surface change, shown in Figure 6.6, is determined by adding the surface measurement from June to September 2003 and September 2003 to February 2004. Although this period includes the same seasons as above (summer to winter), the pattern of deposition and erosion in the blowout is much different than that of the previous year. Moderate erosion is observed at the seaward edge of the blowout throat, and minor erosion along the base of the north lateral wall. The rest of the north wall, though not measured by pins, is heavily scarped, exposing the rhizomes of stabilizing grasses on the surface (as in Figure 6.4c). There is minor deposition along the central axis of the throat and the south lateral wall, plus major deposition recorded on the same pin from the previous year on the western edge of the north lateral wall. Generally, the depositional lobe shows moderate deposition throughout, with four localized points of major deposition.

With the addition of pins to the north and west of the network, a secondary erosional trough is observed (highlighted in Figure 6.6 i). It extends 15 m landward from the foredune crest, and directly downwind, a linear lobe of enhanced deposition has developed (Figure 6.6 ii). This incipient blowout is aligned closely with an unvegetated depositional ramp at the base of the

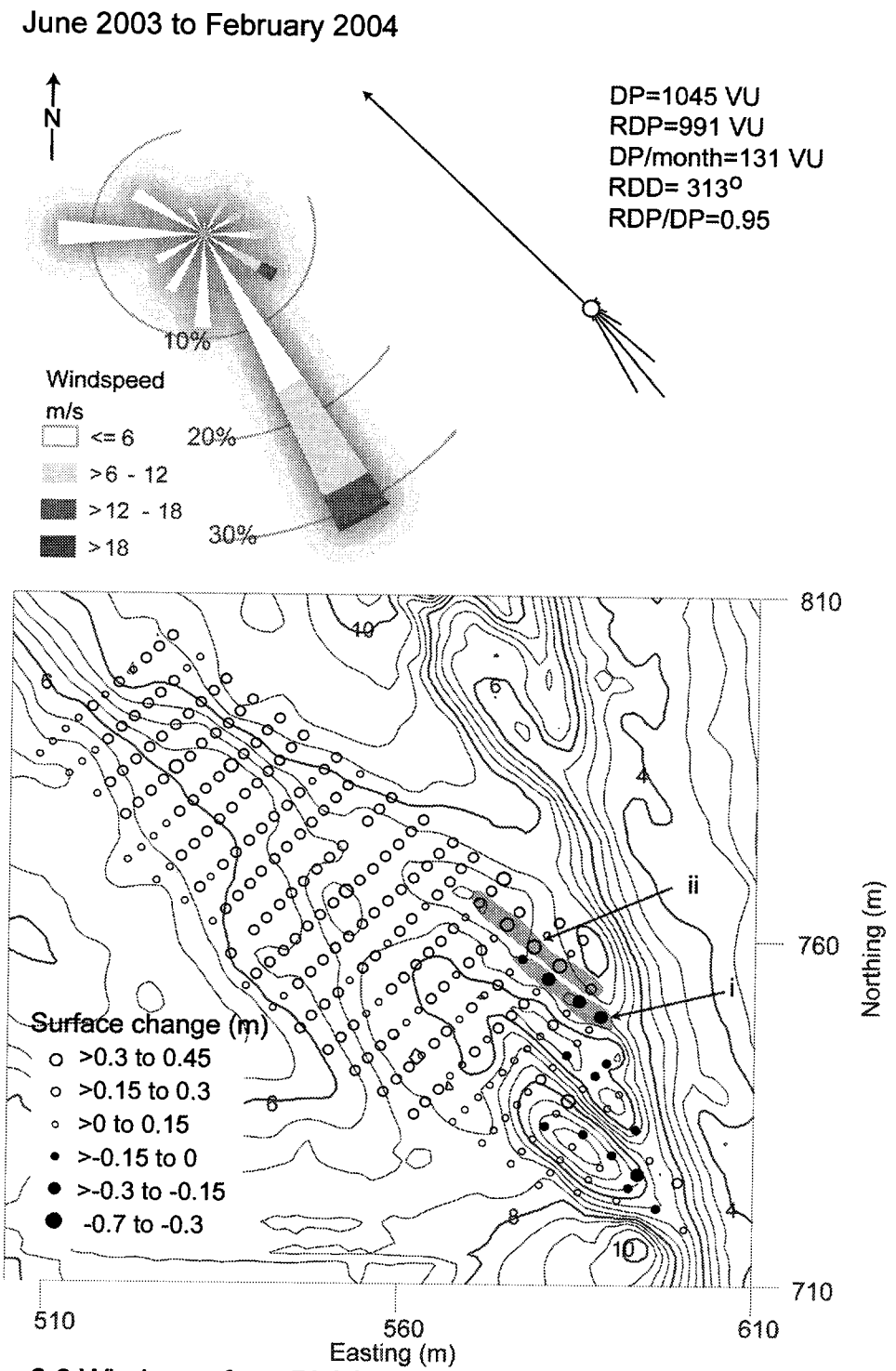

Figure 6.6 Wind rose from BLAST2, Fryberger (1979) drift rose and SCP measurements for summer-winter 2003-04 (June to February). A linear erosional incipient blowout is shaded (i) with an adjacent linear depositional lobe (ii). Topographic contour interval is 0.5 m.

foredune (Figure 6.4a). The trough and depositional lobe align closely with the RDD.

The standardized surface change for this period is higher than the previous year at $+2.0x10^{-2}$ m $month^{-1}$. However, there is a notably lower percentage of erosional surface at only 2% and a lower drift potential at 213 VU $month^{-1}$, compared with the same season the previous year (Table 6.3). Westerly winds constitute 13% of this period, while south-southeast and east-southeast winds show the greatest magnitude and frequency at 32%. This period also has slightly higher directional variability in the wind regime at 0.95, compared with the previous year at 0.97 (Table 6.3).

6.2.2 Winter - summer

Figure 6.7 shows the pattern of surface change, maximum deflation depths and redeposition within the trough-blowout complex for a four-month period from February to June 2003. Along the north lateral wall of the trough, minor (< 0.15 m) erosion is observed (Figure 6.7), and at the time of measurement, no loose sediments were present on the surface, while the rhizomes from the grasses above were exposed (as in Figure 6.4c). The eastern portion of the south lateral wall shows minor erosion, but when measured, it was covered in loose sediments with two avalanche slumps like those seen in Figure 6.4b. Along the central axis of the trough and the western part of the south lateral wall, there is minor accretion (< 0.15 m). The depositional lobe shows predominantly minor accretion throughout, except for a linear lobe aligned with

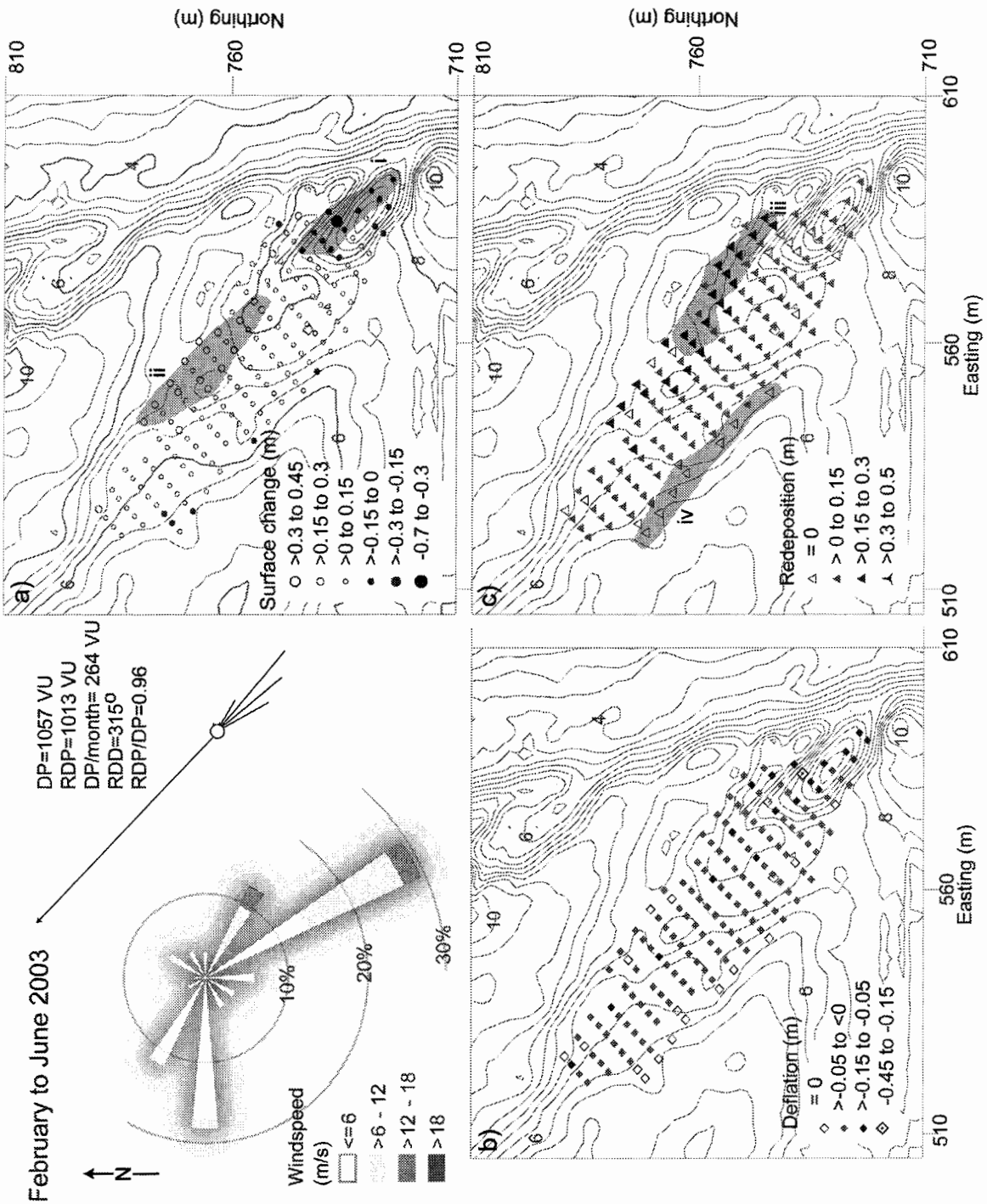

Figure 6.7 Wind rose from BLAST2, Fryberger (1979) drift rose and measurements of surface change (a), deflation (b) and redeposition (c) for winter-summer 2003 (February to June). Shaded polygons, labelled with roman numerals, highlight areas discussed in the text. Topographic contour interval is 0.5 m.

the RDD downwind from the blowout trough that shows moderate accretion (Figure 6.7a ii).

Without washers, analysis of the change to this feature is limited to the observations made above. With washers, another dimension is added to the analysis that presents areas within this trough blowout that experience greater surface activity of both deflation and redeposition. Along the central axis of the trough, minor accretion is observed at two pins. With washers, these pins also show minor to moderate deflation followed by redeposition up to 0.15 m (Figure 6.7). Redeposition values also highlight pins in the throat of the trough and along the northern lateral wall where reworking has occurred as the surface deflated and sediments were redeposited.

The depositional lobe shows predominantly accretion during this period, but with the washers, it is also apparent that just after pin reset, the depositional lobe experienced minor surface deflation followed by minor to moderate (> 0 to < 0.3 m) redeposition (Figure 6.7). With the washers, the depositional lobe is shown to experience surface reworking and not be a solely accretional feature.

During this period, this is a distinct pattern of redeposition ranging from no redeposition along the southern edge of the SCP network, to minor redeposition along the central axis of the deposition lobe and portions of the trough to moderate (> 0.15 m) redeposition along the northern portion of the SCP network (Figure 6.7c). In general, during this period, reworking is minimal to moderate as surface deflation is predominantly less than 0.05 m, with a few localized pins of moderate deflation.

Standardized surface change over the SCP network for this period is $+1.2x10^{-2}$ m $month^{-1}$, with a high percent of erosional surface at 13%. High potential for sediment drift occurred during this period at 264 VU $month^{-1}$ (Table 6.3), with 30% of winds from the west having lower magnitude than the winds from the south-southeast and east-southeast with 42%.

Figure 6.8 shows SCP measurements for a four-month period from February to June 2004. Although this is the same winter-summer period, the magnitude and distribution of surface change is quite different from that of the previous year. In addition, the SCP network has greater spatial coverage with the additional pins along the northern portion of the network.

Minor accretion (< 0.15 m) is observed along the central axis of the trough, while the lateral walls show localized areas of both erosion and accretion. At the base of the north lateral wall, the first two pins show minor erosion, while the third shows moderate deposition (Figure 6.8a). Erosion is observed along a vertical line on the south lateral wall, while 5 m to the inland, minor deposition is observed, likely a result of slumping and avalanching of sediments. This occurs as the base of the lateral walls erodes and the upper slope destabilizes and slumps, thereby resulting in localized enhanced deposition at the base of the walls.

From the washer measurements, the throat of the trough has experienced greater activity than can be observed with net surface change measurements alone. During this period, the central axis has undergone reworking as the surface has been moderately deflated followed by minor to moderate

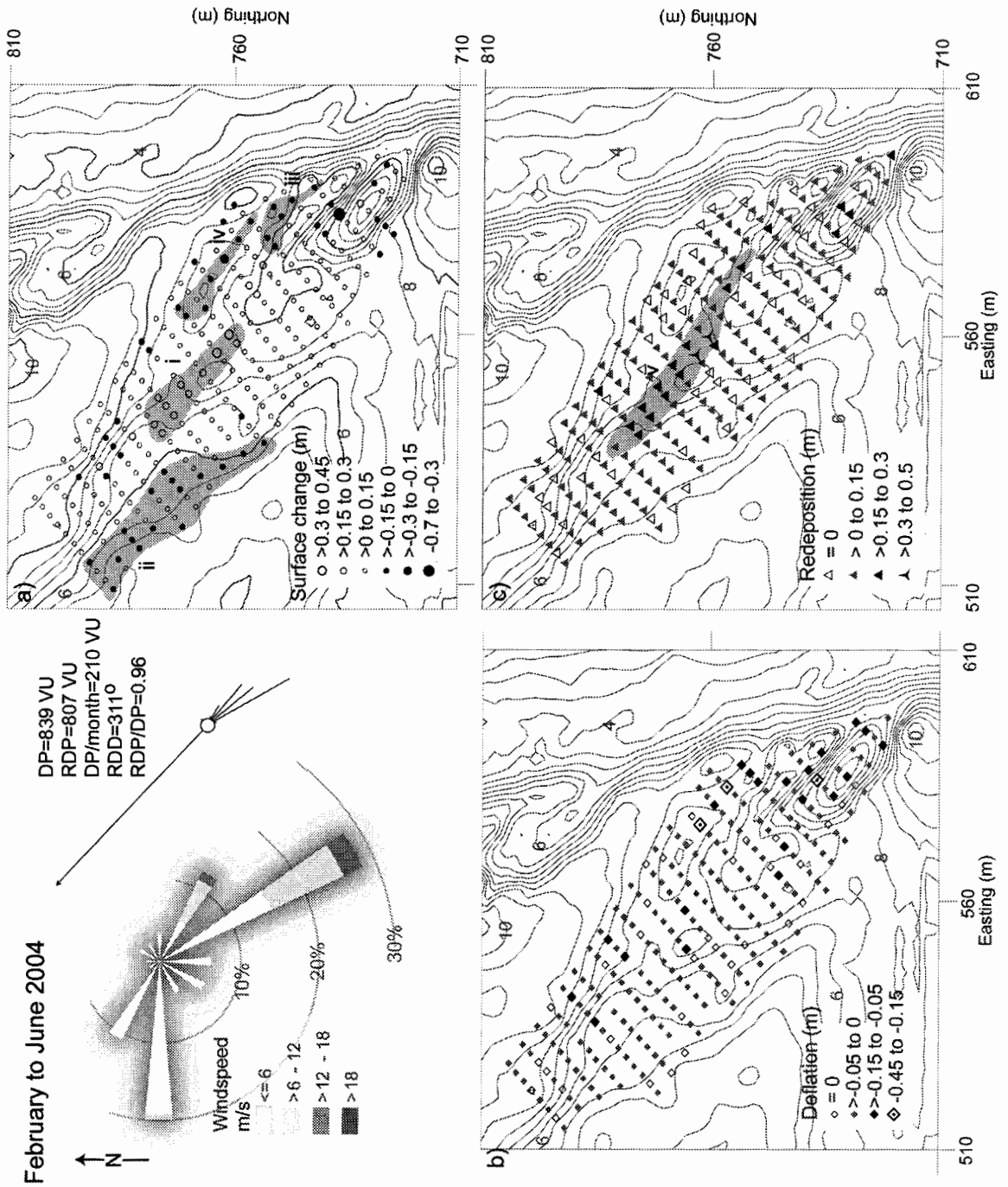

Figure 6.8 Wind rose from BLAST2, Fryberger (1979) drift rose and measurements of surface change (a), deflation (b) and redeposition (c) for winter-summer 2004 (February to June). Shaded polygons, labelled with roman numerals, highlight areas discussed in the text. Topographic contour interval is 0.5 m.

redeposition (> 0.15 to < 0.3 m) (Figure 6.8b and c). Along the base of the south lateral wall, two pins show minor accretion with neither surface deflation nor redeposition. On the north lateral wall there are four pins that show solely erosion with no redeposition. These conditions may suggest that no reworking has occurred at this location or that the reworking has occurred during the measurement period but was not initiated by surface deflation after pin reset (i.e., the surface may have deflated and sediment redeposited, but these processes did not coincide with the timing of the measurements).

The western edge of the SCP network shows minor erosion similar to that observed in spring 2003 (Figure 6.8 ii). This region experienced minimal reworking as both surface deflation and redeposition show values of 0 to < 0.15 m. As this measurement period includes the spring and early summer months, some westerly winds are recorded in the wind rose suggesting the western edge of the SCP network is influenced by these winds.

The depositional lobe landward of the blowout trough shows a uniform pattern of minor accretion, while a linear region of heightened deposition is observed 20 m inland from the blowout, roughly aligned with the RDD (Figure 6.8 i). Predominantly, the depositional lobe and plain experienced minor deflation and minor redeposition, but the linear lobe experienced moderate reworking, as shown from the washer measurements with minor deflation (Figure 6.8b) followed by moderate to major redeposition (Figure 6.8c v).

The standardized surface change for this period is 0.8×10^{-2} m month^{-1}, with 12% erosional surface throughout the study area. The sediment transport

potential for this period is 210 VU month^{-1} with 40% of the winds from the south-southeast and east-southeast, while 31% are from the west.

6.2.3 Summer

Figure 6.9 shows the surface change and pattern of deflation and redeposition for a three-month period from June to September 2003. Along the central axis and the base of the north lateral wall, minor erosion is observed, while minor deposition is observed along the entire south lateral wall (Figure 6.9i). Over the majority of the depositional lobe, minor accretion is observed. However, unlike other measurement periods, the western edge of the SCP network shows numerous pins with minor erosion (Figure 6.9 ii).

During this period, surface deflation is predominantly between 0 and 0.05 m, although no distinct pattern is evident. There are two pins with recorded deflation greater than 0.15 m, one at the base of the north lateral wall and the other in the incipient blowout to the north of the main trough (Figure 6.9b). Along the north lateral wall of the trough, minor redeposition combined with minor deflation have occurred, resulting in reworking, while the southern wall shows no reworking (i.e., no surface deflation and no redeposition). Throughout the depositional lobe and plain there are relative equal proportions of minor and no redeposition, with no evident pattern. There is one localized pin with major (> 0.3 m) redeposition on the northern edge of the SCP network, which also experienced minor deflation resulting in surface reworking (Figure 6.9b and c).

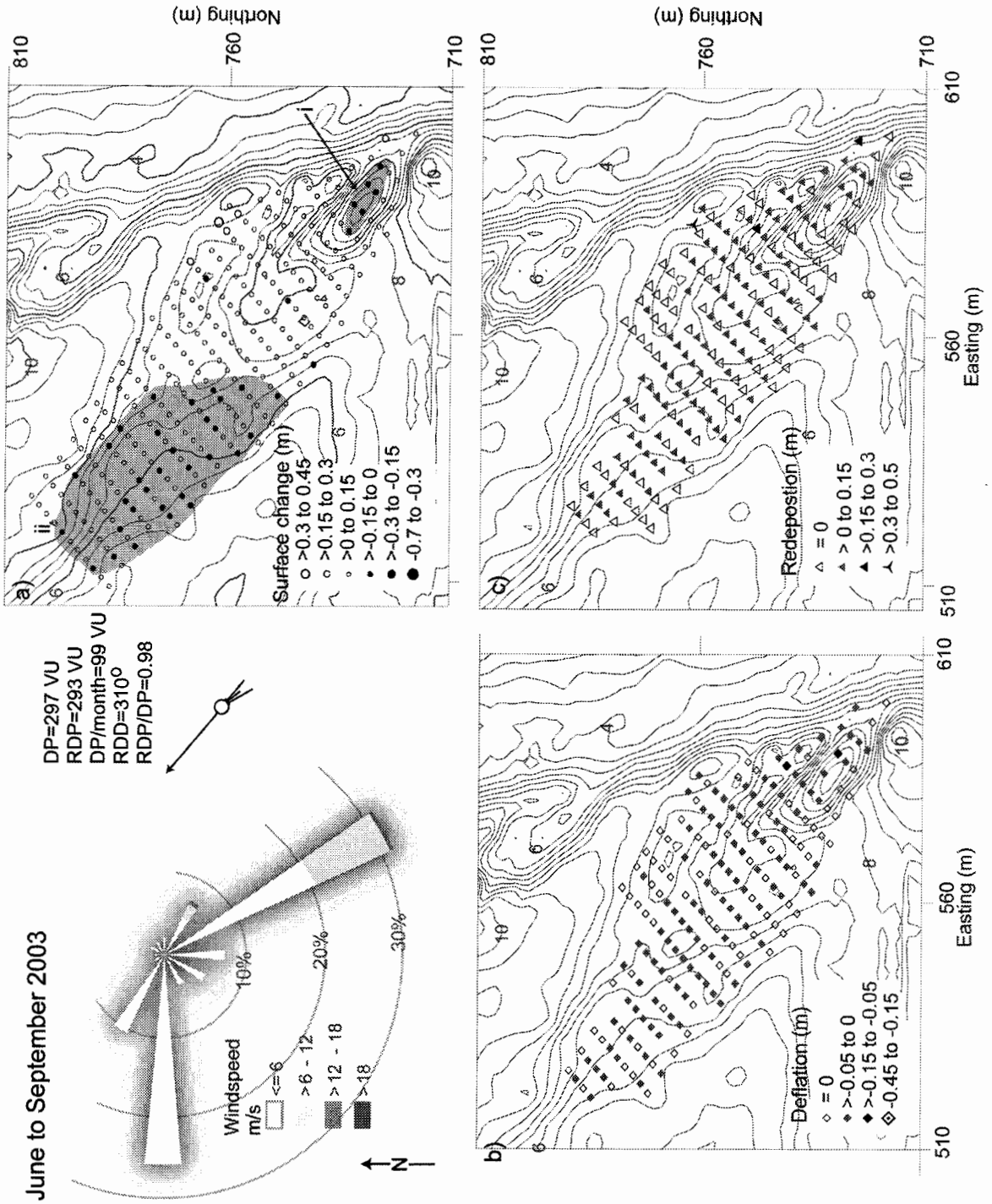

Figure 6.9 Wind rose from BLAST2, Fryberger (1979) drift rose and measurements of surface change (a), deflation (b) and redeposition (c) for summer (June to September 2003). Shaded polygons, labelled with roman numerals, highlight areas discussed in the text. Topographic contour interval is 0.5 m.

Along the northern portion of the SCP network, very little reworking is observed, as most pins show no deflation and no redeposition. Although the surface change measurements show a distinct pattern with erosion in the trough and deposition throughout the depositional lobe, the washers provide an additional dimension of morphological change that is observed within this feature.

This is the shortest measurement period, with only three months, resulting in the least surface change and only five pins recording measurement values of moderate or greater. The standardized surface change for this period is 0.7 $x10^{-2}$ m $month^{-1}$, with a low percent of erosional surface of 4% (Table 6.3). This period has the lowest drift potential at 99 VU $month^{-1}$, with 36% south-southeast and east-southeast winds and 35% west winds. Unlike the monthly wind assessments, no westerly winds above the threshold of sediment transport are shown in the wind rose (Figure 6.9). This is unexpected, as westerly offshore winds were observed transporting sediments within the SCP network during the field season in June and July 2003. This under-sampling of the westerly winds by the BLAST2 station is likely a result of the location and height of the station, which is sheltered by trees to the north and west, thereby decreasing the magnitude and frequency of winds recorded at the station.

6.2.4 Fall - Winter

During a five-month period from September 2003 to February 2004, there is predominantly minor to moderate accretion in the depositional lobe and plain, while the trough and the incipient blowout show localized regions of erosion

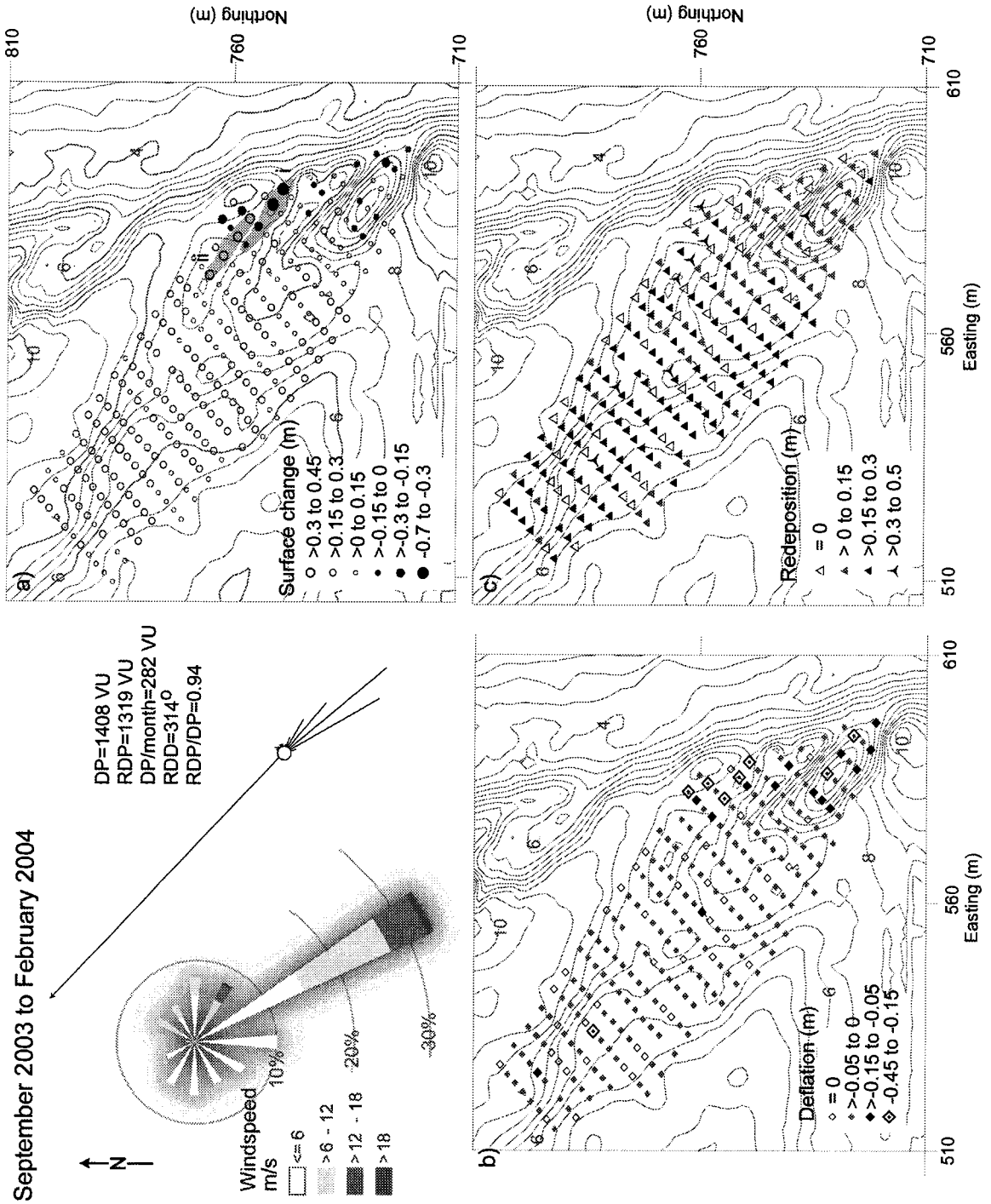

Figure 6.10 Wind rose from BLAST2, Fryberger (1979) drift rose and measurements of surface change (a), deflation (b) and redeposition (c) for fall-winter (September 2003 to February 2004). Shaded polygons, labeled with roman numerals, highlight areas discussed in the text. Topographic contour interval is 0.5 m.

(Figure 6.10a). The pattern of net surface change in the blowout trough is more complex than during other periods. There is localized erosion at the throat of the trough, minor deposition along the central axis and localized minor erosion at the base of both lateral walls (Figure 6.10a). All pins within the trough show minor redeposition, suggesting that this location is not solely erosional, as reworking is occurring within the trough (Figure 6.10c).

Throughout most of the depositional lobe, moderate accretion is observed, except within 15 m directly downwind of the throat of the blowout (Figure 6.10 i), where deposition is predominantly less than 0.15 m. Deflation in the depositional lobe is predominantly minor, with several localized pins recording moderate deflation and one with major deflation (Figure 6.10b). As most of the depositional lobe experienced only minor deflation but moderate to major redeposition, reworking is occurring during the fall-winter period, but only minimally, as redeposition predominates.

Major erosion is observed along the central axis of a small incipient blowout to the north of the main trough that aligns closely with an unvegetated sediment ramp that runs along the driftwood jam and up the foredune (Figure 6.10 i). This region also shows major deflation but only minor redeposition, therefore minimal reworking is occurring (Figure 6.10b and c). Directly downwind, there are four pins with enhanced deposition (> 0.3 m) (Figure 6.10 ii). These pins also show minor deflation (< 0.05 m) and major redeposition (> 0.3 m), therefore this region also shows minimal reworking. This incipient blowout

appears to be a new conduit transporting sediment from the backshore driftwood jam through the foredune to the foredune plain.

The standardized surface change for the fall-winter is the highest of all periods at 2.8 $x10^{-2}$ m $month^{-1}$ but has a lower percent erosional surface at 4%, the same as the summer (Table 6.3). The potential sediment drift for this period is also the highest at 282 VU $month^{-1}$, with 50% of all winds from the south through east-southeast, and minimal westerly winds. Despite the minimal westerly winds, reworking is observed in the trough during the fall-winter months.

6.3 Discussion

6.3.1 Morphodynamics of the foredune-backshore driftwood matrix

During the two-year period of study at this site, the following morphological changes are observed from the cross-shore profiles and topographical survey of the foredune and foredune plain. First, major retreat of the backshore driftwood jam is observed, with a slight increase in elevation at the foredune toe. Second, localized erosion is seen along the seaward face of the foredune in blowouts of varying size. Third, minimal change is observed to the established foredune ridge, both horizontal and vertical. Finally, accretion, generally less than 1 m, is observed on most of the foredune plain landward of the crest.

As discussed in Section 5.1, this region is exposed to a high annual frequency of competent winds (62.3%), predominantly from the southeast. These winds blow obliquely onshore to East Beach, thus encountering a longer effective fetch than shore-perpendicular winds that may provide a greater supply of sand

delivery, dependent on surface moisture and tidal stage (Svasek and Terwindt 1974; Sherman and Bauer 1993; Davidson-Arnott and Law 1996; Bauer and Davidson-Arnott 2002). As HG experiences a macro-tidal range, the fetch length can range from 0 m at a spring high tide to greater than 500 m at a spring low tide, as daily tidal fluctuations control the supply of sediments for aeolian transport to this foredune complex (Ruz and Meur-Ferec 2003).

Recent research shows that secondary airflow effects, including topographic forcing and steering, alter the beach-dune sediment transport process, thereby influencing the morphology of a foredune system (Svasek and Terwindt 1974; Rasmussen 1989; Arens et al. 1995; Hesp 2002; Hesp et al. 2004; Walker et al. in review). At this site, there is evidence of secondary airflow effects including: i) airflow stagnation at the foredune toe, combined with surface roughness effects, resulting in enhanced deposition; ii) steering of airflow toward dune normal; and iii) compression, acceleration and separation of flow up the stoss slope of the foredune.

Oblique onshore winds transport sediment from the beach to the backshore, where surface roughness elements (e.g., vegetation and driftwood) interrupt the airflow, causing rapid reduction in wind speed through flow stagnation and subsequent deposition of entrained sediment (Davidson-Arnott and Law 1990; Arens 1996a; Hesp 2002). Though vegetation on the backshore is thought to be a major control on sediment deposition and dune development in coastal environments (Arens 1996a; Hesp 2002; Walker et al. 2003; Hesp et al. 2004), this may not be the case in HG. Driftwood and flotsam that litter the

backshore on this coast provide an extensive roughness matrix for sediment deposition and accumulation (Walker and Barrie 2004). From the cross-shore profiles and physical observation, the backshore continues to accrete with aeolian sediments until scarped by wave attack of sufficient height and magnitude to remove the logs. After a scarping event, like that observed during the measurement period of June 2003 to February 2004, high onshore sediment delivery to East Beach promotes a beach-dune system with a relatively rapid recovery rate (Figures 6.2 and 6.3).

As sediment accumulates in the driftwood jams, incipient foredunes may develop. This process, contrary to Hesp (2002), does not require vegetation. This is evident by the presence of a well-developed incipient foredune in June 2004 with no vegetation present (Figures 6.2c and 6.3c). At this site, the morphology of these incipient dunes is not dependent on the characteristics of the vegetation (Hesp 1989; Hesp 2002), but rather on the nature of the driftwood matrix (i.e., the shape, size, density, and arrangement of logs).

During this study, the wide driftwood jam (> 50 m) has provided a broad region over which the airflow can be interrupted to induce sediment deposition. When the driftwood jam retreated 15 m between June 2003 and February 2004, the surface area of the sediment sink was reduced. When the driftwood jam is filled with sediment, the surface is smoother, inducing less perturbation of the airflow, thus enhancing aeolian transport and providing a ready source of sediment to the foredunes. During the recovery of the backshore since February 2004, most incoming sediments from the beach were likely trapped in the

driftwood jam, allowing relatively less sediment to be transported into the foredune complex.

Over the two-year study, the driftwood jam receded between 27 (Profile B) and 38 m (Profile A). If the driftwood jam had been smaller or not present, it is likely that the established foredune would have been scarped, as the tens of metres of retreat observed in the backshore might have eroded the foredune. As such, the driftwood jam acts as a buffer for the established foredune, protecting it against major erosion.

Depositional ramps on this coast develop on the driftwood jam and are sparsely vegetated, linear features aligned with southeast winds (Figure 6.11). They are sediment delivery features that form on the backshore, providing enhanced sediment transport up the foredune stoss slope. The photograph in Figure 6.11a was taken during a high onshore wind event in June 2002 at Site 3, in which sediment transport is occurring, as evident from the light coloured, rippled surface along the ramp and at the base of the foredune. In Figure 6.11b, the surface sediments are dark, as the finer quartz sands have been winnowed away, leaving larger, heavy sediments with traces of magnetite.

Evidence of deflection of oblique onshore airflow toward crest normal can be seen from the depositional ramps on the backshore as they curve up the stoss slope (Figures 6.1a and c and 6.11a). Oblique onshore winds are steered toward crest normal as they approach the foredune and the shore normal component is accelerated, thereby shifting the pattern of sediment transport (Svasek and Terwindt 1974; Arens et al. 1995; Hesp et al. 2004). This process is

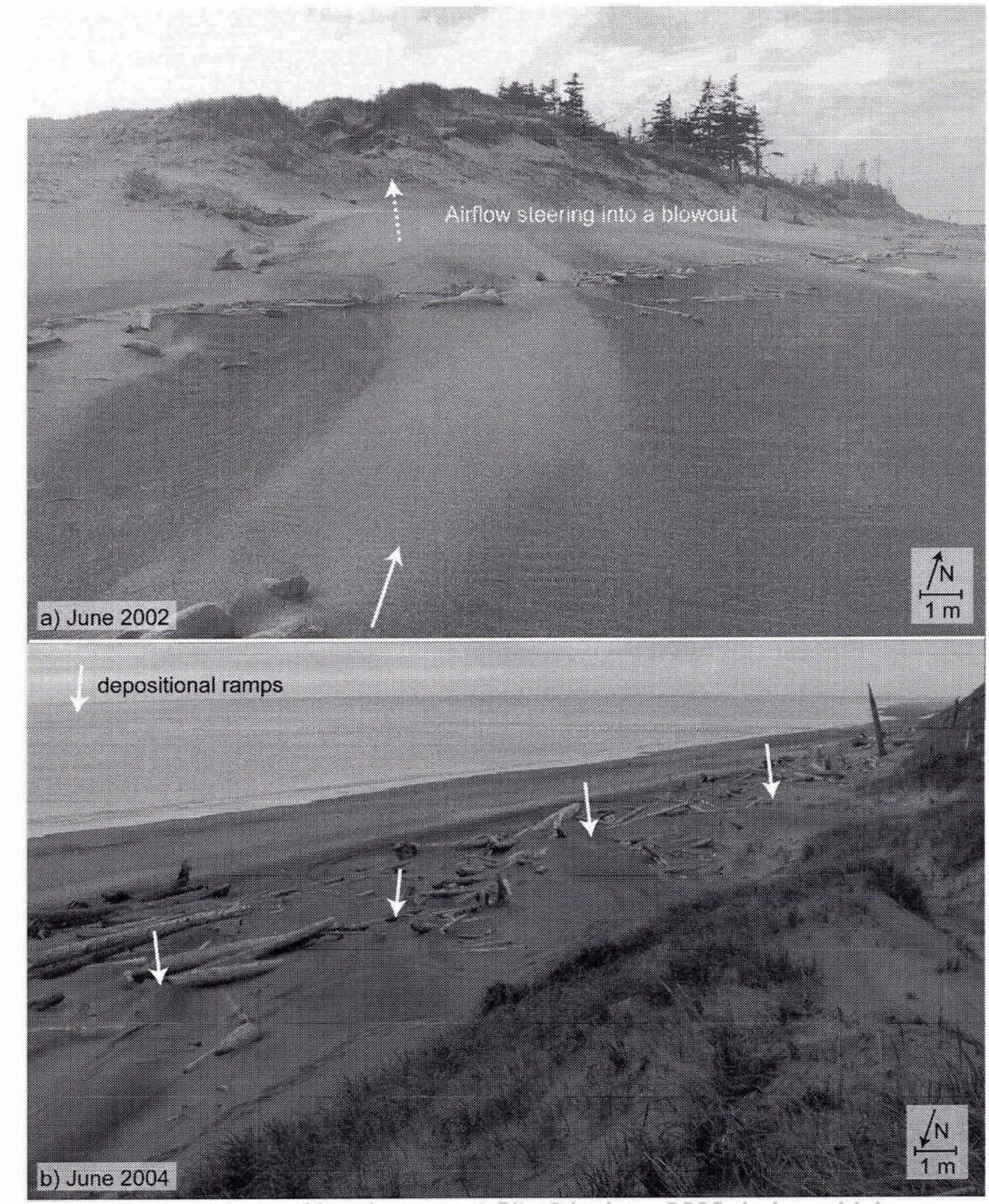

Figure 6.11 a) Depositional ramps at Site 3 in June 2002 during a high onshore wind event with aeolian transport occurring. b) Four distinct depositional ramps highlighted by white arrows on the backshore driftwood jam at Site 2 in June 2004.

highlighted by the white dashed arrow in Figure 6.11a where airflow is steered toward the throat of a blowout. Airflow is steered toward the blowout due to pressure differences between the blowout and the beach as well as topographic steering.

The accretion on the foredune plain is generally less than 1 m during the two-year study period, with several linear lobes of enhanced deposition. These linear features show enhanced accretion 10 to 40 m landward of the foredune crest over a moderately to highly vegetated surface (Figure 6.1c). It is unlikely that all of this sediment was delivered by saltation. A recent study of airflow and sediment transport over a foredune-parabolic dune plain (Anderson and Walker in review) at Site 3 (Section 4.3) identifies grainfall delivery, where sediments are transported in suspension over large distances (i.e., > 250 m) landward of the foredune. They suggest that during onshore wind events, separation of near-surface airflow at the foredune crest may result in sediment entrainment and transport in suspension over significant distances (hundreds of metres).

Over their eight-month period of study, Anderson and Walker (in review) documented grainfall measurements ranging from 11 kg m^{-2} to 110 kg m^{-2} from downwind of the foredune up to 200 m landward of the crest. This mode of transport was also observed by Arens (1996a) where, during strong winds, dense clouds of sand bypassed the foredune crest at a study site on the Dutch coast. Due to the jet-like flow, Arens termed this special mode of suspension 'jettation' (Arens 1996a). Generally, surfaces where saltation and surface creep occur have loose to compact sediments and often have ripples. In contrast, grainfall creates

a loose surface with no ripples and matted vegetation similar to surfaces subject to snowfall. Along the foredune plain, there is evidence of both saltation and grainfall, suggesting that sediments on this plain are transported in both modes.

During this two-year study, the foredune crest remained stable. McKenna Neuman et al. (2000) found on a stoss slope of a transverse dune in Silver Peaks, Nevada, that erosion at the crest occurred during wind speeds just above the threshold of entrainment, while higher magnitude winds resulted in deposition of sand just upwind of the crest. It appears that over the two-year study period, this foredune was in quasi-equilibrium. Onshore airflow was likely accelerated and topographically steered up the stoss slope but instead of enhanced erosion, a balance existed between the removal and the deposition of sediments at the crest. As suggested by McKenna Neuman et al. (2000), the relations between sediment transport and wind speed over the stoss slope are well understood, but the longer term morphological response of these relations is not clear. In this foredune complex over the two-year study, the backshore driftwood jam retreated and the foredune plain accreted, while the foredune crest remained stable.

Aeolian sediment transport in beach-dune systems is a complex process that is not characterized well by current mathematical models of sediment flux. Arens et al. (1995) indicate that estimates of potential sediment transport can underestimate actual rates by up to 70%. For this assessment, the estimated sediment transport rate calculated using the Fryberger (1979) model underestimates the actual volumetric change by approximately 60%.

This major underestimation of sediment flux by applying the Fryberger (1979) model results from the wind data used, as the BLAST2 station is located inland in the deflation plain of a parabolic dune, sheltered by trees and topographic highs to the north and west. As well, the anemometer is at 5 m height instead of the 10 m required for the Fryberger (1979) model, which reduces the magnitude of winds recorded. Although the wind speed was adjusted to 10 m height using Equation 1, a single value for roughness length, was used for all conversions. As wind speed conversions are highly sensitive to variations in the roughness length it is likely that the wind speed at BLAST2 underestimates the wind speed at 10 m. Furthermore, the BLAST2 station is a remote measurement location in terms of the airflow dynamics operating at the foredune. Topographic forcing and steering at the foredune enhance sediment transport from the beach to the foredune complex (Arens 1995). Thus, use of the Fryberger model to estimate rates of sediment transport is not recommended for this foredune complex as it does not incorporate transport-limiting factors (e.g., roughness, localized airflow compression, stagnation and acceleration), nor does it characterize well the supply-limiting factors (e.g., vegetation, moisture and grain characteristics) that control sediment flux in this high-energy coastal environment.

Over the two-year study period, major shoreline retreat was observed at this site, but the established foredune complex did not experience major erosion. The foredune plain accreted, the foredune stoss slope experienced little change, and the backshore retreated and then infilled with aeolian sediments, although in

a much narrower backshore. The sediment-laden driftwood jam has therefore buffered the established foredune from wave scarp and erosion. This morphological response of the established foredune during this study period suggests that it may be responding to coastal retreat and sea-level rise with net accretion as the RDA model predicts (Davidson-Arnott 2003). However, if the backshore is included as part of the dune system, which on this coast is a major part of the sediment budget, then this site experienced net sediment loss during a period of coastal retreat, as suggested by the Bruun (1965) model.

6.3.2 Seasonal morphodynamics of a trough blowout-depositional lobe complex

During this two-year study, seasonal patterns of morphological response in this trough-blowout emerged. The summer months experience the lowest drift potential (99 VU month^{-1}) and lowest surface change (0.7x10^{-2} m month^{-1}), while the fall-winter months experience the highest drift potential (282 VU month^{-1}) and the highest surface change (2.8 x10^{-2} m month^{-1}). However, both periods have the same percentage of erosional surface (4%), with varied spatial distribution and magnitude of erosion. During both periods, minor erosion is observed in the trough blowout, but in the fall-winter, localized major erosion is observed in the incipient blowout to the north of the main trough (Figure 6.10a), while in the summer, no erosion is observed around the foredune crest but is seen along the west of the SCP network (Figure 6.9a).

This pattern of net surface change is directly related to the seasonal bimodal wind regime, with minimal west winds observed in the fall-winter, while west winds predominate in the summer (Section 5.1). There is also greater bare surface observed in the winter months when precipitation is high (Figure 4.1) and vegetation cover lower (Figure 4.5) than in the summer months, when the opposite conditions occur. Although competent westerly winds do not represent a significant portion of the wind roses from BLAST2 (i.e., < 4% for both years), aeolian transport from westerly winds is observed along the western edge of the SCP network during field visits in June 2002, 2003 and 2004.

During the winter-summer period, which includes the spring months when the wind regime shifts from predominantly southeast winds to westerly winds of lower magnitude (Figure 5.2), the highest erosional surface is observed (12-13%). With this high erosional surface, the winter-summer period also receives the second lowest positive surface change at 1.2 $x10^{-2}$ m $month^{-1}$ in the first year and 0.8 $x10^{-2}$ m $month^{-1}$ in the second. When averaged from the two measurement periods, the potential sediment drift for this period is the second highest at 237 VU $month^{-1}$. The variation in surface change between these two years may result from the removal of the driftwood jam in the winter of 2003, which decreases the sediment supply to this system, combined with a lower potential drift.

The measurement period of summer-winter, including the fall months, varies significantly between the two periods of measurement with percent erosional surface at 8% in 2002/03 to 2% in 2003/04. This is likely related to the

addition of 101 pins along the north and west of the SCP network, as this region shows minor to moderate deposition during all measurement periods since installation, except for the pins in the incipient blowout to the north of the main trough. When averaged for the two periods, the potential sediment drift for this period is the second lowest at 187 VU $month^{-1}$, and it would likely have been even lower if the wind data from June 26 to August 15, 2002, had not been lost.

The dominant southeast winds on this coast blow parallel to slightly oblique to the trough of this blowout (Figures 6.5 to 6.10). Though no airflow measurements have yet been conducted at this site, the flow patterns observed by Hesp and Hyde (1996) for a trough blowout of similar type during onshore winds are generally consistent with the pattern of deposition and erosion at this site (Figure 6.12).

Onshore winds approaching a trough blowout are topographically accelerated and steered due to lower pressure in the trough. The trough acts as a conduit, accelerating flow and thereby sediment transport. Winds approaching normal (90°) to the blowout trough are accelerated up the central axis, eroding the trough base and transporting sediment downwind to the depositional lobe (Hesp and Hyde 1996). When winds blow obliquely to the trough, they are steered considerably, creating localized jetting and differential erosion as the airflow shifts from the central axis to the lateral walls (Figure 6.12).

Airflow steering in the trough is evident at this site through the pattern of surface change observed. During the first three measurement periods up to

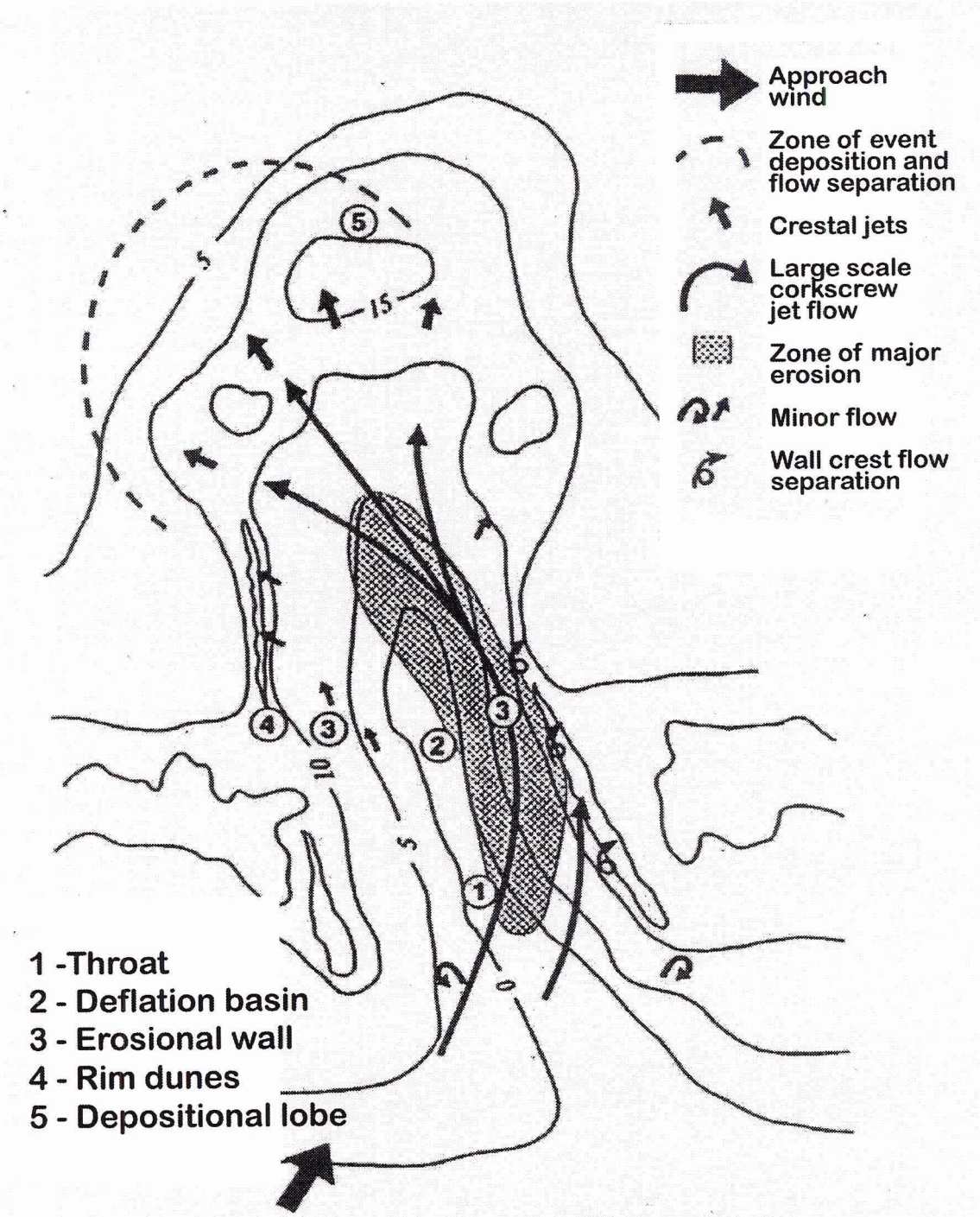

Figure 6.12 Hesp and Hyde's (1996: p.521) schematic illustrating topographic steering within a trough blowout when approach wind angles are oblique to the alignment of the blowout trough. Contour intervals in metres. (Reprinted with permission of the author)

September 2003 (Figures 6.5, 6.7 and 6.9), enhanced erosion is observed along the central axis of the trough and toward the northern wall, leaving exposed sediment strata and rhizomes from the grasses on the surface (Figure 6.4c). This pattern follows the observations made by Hesp and Hyde (1996) and Fraser et al. (1998). In the fall and winter 2003/04 and spring 2004 (Figures 6.10 and 6.8), the pattern of surface change in the trough becomes more complex, lacking distinct zones of erosion and deposition as observed during the previous measurement periods. Instead, there is localized erosion at the throat, minor deposition along the central axis and erosion along the western edge of the south lateral wall.

With the addition of washers to the SCPs, the patterns of maximum surface deflation and redeposition are monitored in combination with the net surface change. When assessed together, these pin measurements highlight regions within the landform that experience surface reworking. During the winter-summer period, reworking occurs on the linear deposition lobe directly downwind from the main trough (Figure 6.13). From the surface change pins alone, this lobe appears to be a region of enhanced deposition compared with the rest of the depositional lobe. From the washers, this area experiences both surface deflation and subsequent redeposition (Figures 6.7 and 6.8). This region does not show reworking during the other measurement periods.

Reworking also occurs in the trough during most measurement periods. The trough is highly erosional and is the conduit for sediment transport as airflow and sediment transport are topographically accelerated. From the SCPs,

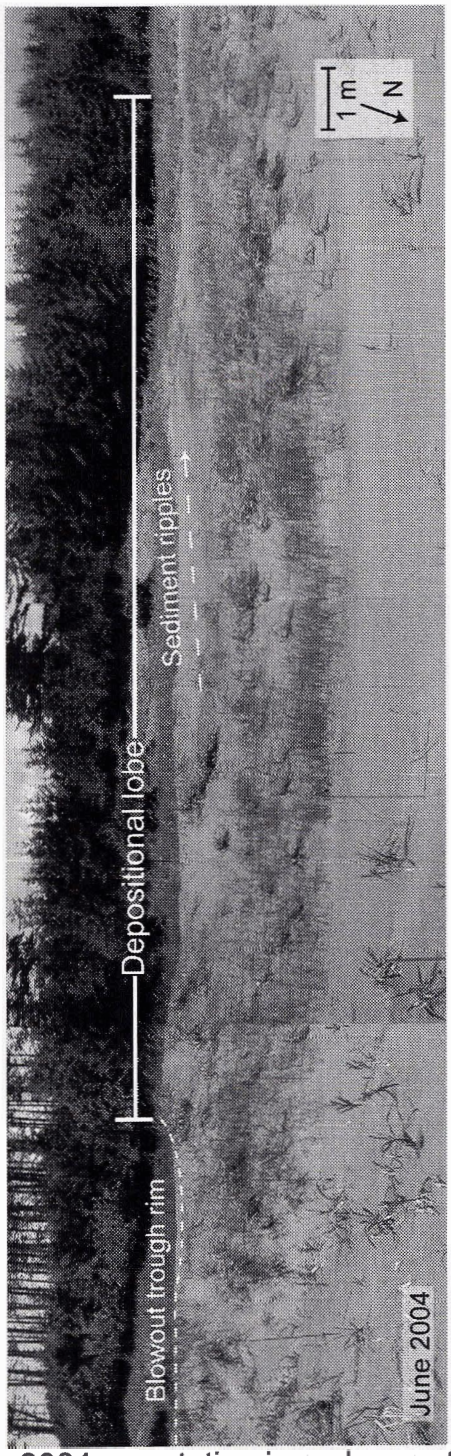

Figure 6.13 From June 2004, vegetation in early growth stage is observed on the depositional lobe. Both ripples and the surface characteristics of grainfall are observed.

predominantly minor erosion is observed during each of the measurement periods. Before September 2003, a pattern of erosion is distinct, mostly localized to the north lateral wall, with less on the south lateral wall. After September 2003, the pattern of net surface change is less distinct, with both accretion and erosion observed. Without the washers this complex pattern can not be easily explained, but with the measurements of deflation and redeposition, the trough appears to be a region of not only enhanced erosion but of enhanced activity through surface reworking.

The blowouts at this site act as conduits of aeolian sediment transport by topographically accelerating flow and increasing localized transport of sediments to the foredune plain. The depositional lobe extends approximately 25 m landward of the rim of the blowout trough. However, during the period of study, the greatest sediment accretion is observed further inland from the blowout trough at distances of 25 to 75 m. This may result from sediment transported through the blowout trough, deposited within 20 m of the trough and then re-entrained and transported further inland. This is supported by the presence of ripples along the surface of the depositional lobe (Figure 6.13).

There is also evidence that the heightened accretion at distances greater than 25 m from the blowout trough may also be from grainfall. As airflow is accelerated up the back slope of the trough, sediments may be entrained and transported in suspension over long distances, as observed by Anderson and Walker (in review). The surface characteristics of grainfall were observed along the northwest portion of the SCP network. Thus, this trough blowout acts as a

conduit for sediment transport where airflow is steered in, accelerated, and then separated, resulting in sand delivery in saltation (to approximately 25 m) and beyond (to at least 75 m) via grainfall.

From studies of blowout dynamics during onshore winds, sediments are eroded from the throat and deposited on the depositional lobe (Jungerius and van der Meulen 1989; Gares 1992; Hesp and Hyde 1996; Byrne 1997). What is less understood is the influence of a secondary mode of competent winds on surface reworking. With the addition of washers, a new dimension of morphological change is highlighted. Plots of the deflation and redeposition highlight regions and seasons in which greater surface activity of the surface is experienced.

Although not evident from the wind roses presented due to the under-sampling of the BLAST2 station, the role of offshore winds does influence the morphology and evolution of erosional features at this site, as observed during field visits in the summers of 2002 and 2003. During strong offshore winds, easterly transport of sediment occurs, moving sediment from the depositional lobe into the trough and into the incipient blowout to the north. In addition, minor surface deflation occurs, but the temporal scale of measurement of the SCP network precludes the measurement of these events.

6.4 Summary and Conclusions

From this two-year study of morphological response of a foredune-trough blowout complex, the following general conclusions can be made. The foredune

plain experienced net accretion (+55 m^3 m^{-1} width a^{-1}) during the period of study, while the foredune stoss slope and crest experienced minimal change. Major reworking is observed in the backshore driftwood jam, with landward retreat up to 37 m while accreting up to 2.2 m. Secondary airflow effects influence the morphological form, including flow stagnation causing sediment deposition at the foredune toe, topographic steering and flow acceleration into blowouts and up the stoss slope, and evidence of flow bypassing at the foredune crest, resulting in grainfall on the foredune plain and minimal change to the foredune crest.

The driftwood jam plays a key role in the evolution of this dune complex, acting both as a buffer against major wave attack and providing a ready source of sediment for aeolian transport. Depositional ramps, which develop as shadow dunes in the driftwood jam, provide enhanced sediment transport to the foredune and beyond. At present, the formation, evolution and extent of influence of both the driftwood jams and depositional rams are not fully understood, but due to their geomorphic importance on this coast, they warrant further study.

In both the foredune plain and the trough blowout-depositional lobe complex, saltation and grainfall appear to be the main mechanisms of sediment delivery. Bagnold's (1941) studies show that saltation accounts for 75% of the bulk transport of sediment. In this high-energy coastal foredune complex, the contribution of grainfall to the overall delivery of sediment is likely high, as evident from the distribution of grainfall surface characteristics (i.e., loose powder-like effect) at this site.

The blowouts at this site act as conduits of aeolian sediment transport by topographically accelerating flow and increasing localized transport of sediments to the foredune plain. From the SCP network, the general trend of surface change observed is net accretion through the network, with localized erosion in the blowout trough and incipient blowout. These data reveal a seasonal trend of erosion and deposition within this trough blowout-depositional lobe complex, resulting in the lowest surface change observed in the summer and the greatest observed in the fall-winter. However, these two periods experience the same percentage of erosional surface at 4%, while the winter-summer months, including the spring, experience the highest erosional surface at 13%.

The spatial distribution of erosion is also seasonally dependent. During all measurement periods, erosion occurs in the blowout trough, but in the summer, localized erosion is also observed along the western portion of the SCP network, while in the fall, winter and early spring, erosion occurs predominantly in the trough of the incipient blowout. This seasonal variation can be partially explained by the seasonal shift in the wind regime from predominant oblique onshore winds in the fall, winter and early spring, and westerly offshore winds of lower magnitude in the summer.

The enhanced erosion observed along the central axis of the trough and along the north lateral wall illustrates that oblique onshore winds are topographically steered in the trough and up the windward slope as presented by Hesp and Hyde (1996) (Figure 6.12). There is evidence of a shift in the pattern of surface change in the trough blowout during the last two measurement

periods. A distinct zone of enhanced erosion along the north lateral wall, as seen in previous measurement periods, is not evident from September 2003 onward. The cause of this shift is not fully understood, although it may result from topographically induced airflow alterations as this trough widens over time.

Surface change pins have been used in many studies to monitor the spatial and temporal morphological change of blowouts and parabolic dunes (Jungerius and van der Meulen 1989; Gares 1992; Byrne 1997; Wolfe et al. 2003). None of these studies have employed washers to monitor maximum deflation depths. This study illustrates that adding washers to SCPs is a useful technique for monitoring morphological change as it provides insight into a new dimension of change within an aeolian sedimentary feature. Monitoring surface deflation and redeposition highlights areas of greater activity though surface reworking, which is not apparent from the SCPs alone. Generally, the washers show that throughout the trough and depositional lobe, surface reworking is occurring during all seasons. This study has shown that monitoring surface reworking is possible. Further research is required to understand the processes operating with the aeolian system that promote greater surface reworking. At present it is not understood whether surface reworking occurs as a result of uni-directional winds of varying frequency and magnitude or from winds from varying directions that promote enhanced surface reworking.

One of the limitations of monitoring reworking using washers is that only surface deflation that occurs after the pins are reset is recorded. If the surface accretes and then is deflated, the change is not recorded by this technique. As a

result, the conclusions regarding the aeolian dynamics during each of the periods are limited, since this technique can not differentiate between no reworking occurring at a certain location and no reworking recorded. If deflation occurs at any time other than directly after pin reset, that deflation is not recorded. Measuring and examining maximum deflation depth and redeposition with SCP and washers shows that this trough blowout-depositional lobe complex, and by extension, most aeolian sedimentary features, experience much more activity and change than can be recorded accurately from surface change measurements alone.

7.0 Summary and Conclusions

The goals of this study were to: i) document and describe dune geomorphology on East Beach, HG, ii) assess regional aeolian activity and relate to dune morphology, and iii) measure and examine the morphodynamics of a foredune-trough blowout complex on East Beach. The geomorphology was qualitatively described at four sites to demonstrate the morphological diversity of dune forms on East Beach. To assess regional aeolian activity, the annual and monthly wind regimes were presented, and three models of aeolian activity and dune mobility were applied and critiqued, using regional meteorological data and comparing with the geomorphic assessment. Finally, the assessment of morphological response and volumetric change of a foredune-trough blowout successfully demonstrates the seasonal morphodynamics of a representative aeolian landform on this coast.

East Beach, HG, is host to a diverse aeolian landscape that is a product of late Quaternary and modern sea-level variations, the biogeographical setting, the littoral processes and onshore delivery of sands. Unlike many Canadian dune fields, the coastal dunes of BC, but specifically those on East Beach, HG, experience little or no snow cover throughout the year that would restrict sediment availability for transport. Therefore, the major climatic limitations on aeolian transport and dune development are the frequency and magnitude of transporting wind events and their timing relative to tide stage and precipitation events, as well as vegetation growth stage and cover. East Beach is subject to high annual wind energy with distinct seasonal modes in the regime. Wind

magnitude is greatest in the fall, winter and early spring, when precipitation is greatest. In the summer months, when vegetation cover on the dunes increases significantly, wind magnitude is much lower, with greater directional variability.

The morphological diversity of aeolian landforms is described for four distinct sites. Site 1 (Parabolic and blowout dunes - Rose Point East) has a discontinuous established foredune backed by a wide, vegetated dune plain with coppice and shadow dunes. Landward of Dune Road, a suite of blowouts and parabolic dunes are in varying stages of development. Site 2 (Foredune-parabolic dune complex) hosts the longest parabolic dune complex (1.2 km) on East Beach, with a single ridge established foredune. The foredune is breached in several places by blowouts of both saucer and trough shape. There is a wide, dynamic backshore driftwood jam at this site presently acting as a buffer for the established foredune against scarping from storm surge. Site 3 (Locally prograding foredunes south of Lummi Creek) has four large parabolic dunes with a coalesced deflation plain. There are two distinct established foredune morphologies at this site. The northern portion has a single ridge that is highly erosional with multiple blowouts, while the southern portion has five distinct generational foredunes due to scarp by a driftwood-dammed lake and localized progradation. Site 4 (Eroding relict parabolic dunes) has a relatively narrow backshore, with minimal driftwood. An incipient foredune is developing in the backshore, but this site lacks an established foredune. Instead, this site is host to large erosional blowouts that are the truncated arms of relict, stabilized parabolic dunes.

Hesp's (1999) model, when applied to East Beach, shows morphological stages ranging from a Stage 1 at Site 1 to a Stage 4 and 4b at Site 3. The application of Hesp's model of foredune evolution allows a greater understanding of the evolutionary stage of an established foredune, thereby providing a broader landform interpretation than just description. This model also allows comparison between sites on the same coastline and between other global sites.

At all four sites, driftwood plays a key role in beach-dune morphodynamics as a backshore roughness element that traps and accretes sediment and, once filled, provides a ready supply of sand to the dune system. It also provides a buffer against storm wave attack as seen at Site 2 where the backshore driftwood jam retreated up to 37 m over two years, although the established foredune was not scarped. Enhanced transport of sediment from the backshore to the foredune complex is facilitated by the presence of depositional ramps, linear aeolian features that form on the backshore over and through the driftwood jam.

The application and critique of three regional models in HG has shown that each describes relevant aspects of the sediment transport process and morphological regime, but none were able to describe the whole system well. The Fryberger (1979) model characterizes well the maximum potential sediment drift and directional variability in this region. But when potential sediment drift is converted to sediment flux, the results grossly underestimate the actual transport rates in this foredune complex. This underestimation results from a combination of the location and height of the BLAST2 meteorological station and the

limitations of the sediment transport model, which can not characterize the enhanced transport rate resulting from topographic airflow effects. Although the Fryberger (1979) model underestimates actual flux, it does provide a good relative measure of wind energy that can be used to compare between other sites globally. As well, it was successfully used to compare wind energies between measurement periods of the SCP network in the trough blowout.

As Fryberger's (1979) original morphological classification described only one environment in which parabolic dunes might be found, his original classification can not be applied in HG. To extend the Fryberger (1979) morphological classification, this study presents the wind regimes from four coastal sites where parabolic dunes are found: Haida Gwaii, BC, Canada; the Oregon coast, USA; Greenwich, PEI, Canada; and Aberffraw, North Wales, UK. These sites illustrate that parabolic dunes can be found in wind regimes ranging from intermediate to high wind energy (226 to 3,176 VU), with directional variability ranging from obtuse bimodal to narrow unimodal (0.43 to 0.8). Further studies are required to extend the characterization of wind regimes in which coastal parabolic dunes can be found.

The application of the Lancaster (1988) dune mobility index in HG is limited to the inland regions removed from the external sediment supply from the nearshore. As this mobility index was developed in a continental setting, where the sediment supply is fixed and dune mobility is controlled solely by wind capacity and vegetation cover, it does not characterize well the mobility of dune systems that are controlled by additional factors. The Lancaster (1988) dune

mobility index should not be applied to a coastal setting or other settings in which an external sediment supply is influencing the mobility of the dunes. However, further investigation is warranted with regards to the ability of this model to characterize the propensity for dune stabilization once the dunes migrate inland, away from the external sediment source.

The Tsoar and Illenberger (1998) model incorrectly classifies the dune system in HG as unvegetated and highly mobile. This model was developed on the premise that vegetation growth is partially controlled by wind strength and directional variability, as represented by the Fryberger (1979) model. However, in this high energy environment, the mobility of these dunes is variable from fully vegetated and inactive inland to fully active, with moderate vegetation cover along the foredune. This model does not differentiate between inland and coastal dune systems and can not characterize the complexity of the coastal dune system in HG.

The two-year study of the foredune-trough blowout complex has provided a detailed morphodynamic assessment that is representative of the foredune systems on this rapidly retreating coast. During this period, major sediment accretion has occurred in the foredune plain (55 m^3 m-$width^{-1}$ a^{-1}), and the backshore driftwood jam has receded up to 37 m, while the foredune stoss slope the has experienced minimal change. Predominantly the accretion in the foredune plain was less than 1 m with localized linear lobes of enhanced deposition (> 1 m).

The trough blowout-depositional lobe complex shows net accretion during all measurement periods, with a distinct seasonal morphologic and volumetric response. During the fall, winter, and early summer, when sediment drift potential was greatest, the largest surface change was observed. During the summer, when the drift potential was least, the net surface change was also the least of all periods, but the pattern of erosion shifted from the foredune crest to the western edge of the SCP network. This results from the seasonal bimodal shift in the wind regime and suggests this landform, although aligned with the dominant southeast wind direction, is morphologically altered by secondary modes in the wind regime.

This study has successfully presented an adaptation of a monitoring technique used in the nearshore and applied it in an aeolian sedimentary environment. Using surface change pins with washers allows for the monitoring of maximum surface deflation and redeposition, and when combined, they highlight areas of surface reworking as well as areas that experience no reworking. Further investigation is required to assess the processes and wind regime characteristics that promote enhanced surface reworking by monitoring the SCP network at greater frequency.

7.1 Future research considerations

This study has highlighted several areas in which further research is warranted including:

- Work to extend Fryberger's (1979) morphological classification by assessing the wind regimes and landform interpretations at other sites globally.
- A quantitative assessment of dune migration, coastal retreat and dune stabilization in Haida Gwaii through the ortho-rectification of historical air photos and use of georeferenced LIDAR images. This would allow a quantitative assessment of the Lancaster (1988) mobility index to determine if dune activity in the inland regions is accurately modelled by this index. Further research would be required to determine the extent of influence of the nearshore sediment supply to the inland dune system.
- Investigation of the process and influence of grainfall as a sediment delivery mechanism to the dunes to better model and understand the total aeolian sediment delivery process in coastal dune systems. In turn, this would have relevance for improved modelling of coastal sediment budgets that include onshore and backshore components of mass transfer.
- Continued monitoring of the topographic survey, cross-shore profiles and SCP network to assess, over a longer term, the response of this system to sea-level rise and coastal retreat. To enhance this morphological analysis, a reduced temporal scale is recommended that would allow true seasonal, or even monthly, assessment of morphological response.
- Further assessment of SCPs with washers to quantify total volumetric change, including the surface deflation and redeposition, as well the wind regime characteristics that promote enhanced surface reworking.

- More analysis and discussion of the Tsoar and Illenberger (1998) dune mobility index in both coastal and continental dune systems to assess if there is benefit to applying this model instead of the Lancaster (1988) and Fryberger (1979) models.

References

Abeysirigunawardena, D. and Walker, I.J., Sea level response to climatic variability in northern British Columbia. Unpublished data, research manuscript in preparation.

Allan, J.C. and Komar, P.D., 2002. Extreme storms on the Pacific Northwest Coast during the 1997-98 El Nino and 1998-99 La Nina. Journal of Coastal Research, 18(1): 175-193.

Amos, C.L., Barrie, J.V. and Judge, J.T., 1995. Storm-enhanced sand transport in a macrotidal setting, Queen Charlotte Islands, British Columbia, Canada. In: B.W. Flemming and A. Bartoloma (Editors), Tidal Signatures in Modern and Ancient Sediments. Special Publication of the International Association of Sedimentologists. International Association of Sedimentologists, 53-68.

Anderson, J.L. and Walker, I.J., in review. Airflow and sediment transport variations within a backshore-parabolic dune plain complex: Northeast Graham Island, British Columbia, Canada. Geomorphology, accepted March 2005.

Anderson, R.S. and Willetts, B.B., 1991. A review of recent progress in our understanding of aeolian sediment transport. Acta Mechanica, 1: 1-19.

Anthonsen, K.L., Chlemmensen, L.B. and Jensen, J.H., 1996. Evolution of a dune from crescentic to parabolic form in response to short-term climatic changes: Rabjerg Mile, Skagen Odde, Denmark. Geomorphology, 17: 63-77.

Arens, S.M., 1996a. Patterns of sand transport on vegetated foredunes. Geomorphology, 17(4): 339-350.

Arens, S.M., 1996b. Rates of aeolian transport on a beach in a temperate humid climate. Geomorphology, 17(1-3): 3-18.

Arens, S.M., van Kaam-Peters, H.M.E. and van Boxel, J.H., 1995. Airflow over foredunes and implications for sand transport. Earth Surface Processes and Landforms, 20(4): 315-332.

Ash, J.E. and Wasson, R.J., 1983. Vegetation and sand mobility in the Australian desert dunefield. Zeitschrift fur Geomorphologie NF, Supplementbande 45: 7-25.

Bagnold, R.A., 1941. The physics of blown sand and desert dunes. Methuen, London.

Bailey, S.D. and Bristow, C.S., 2004. Migration of parabolic dunes at Aberffraw, Anglesey, north Wales. Geomorphology, 59(1-4): 165-174.

Barrie, J.V. and Conway, K., 2002. Rapid sea level changes and coastal evolution on the Pacific margin of Canada. Journal of Sedimentary Geology, 150: 171-183.

Barrie, J.V. and Conway, K.W., 1996. Sedimentary processes and surficial geology of the Pacific margins of the Queen Charlotte Islands, British Columbia. *In* Current Research, 1996E; Geological Survey of Canada, 1-6.

Bauer, B.O. and Davidson-Arnott, R.G., 2002. A General Framework for Modelling Sediment Supply to Coastal Dunes Including Wind Angle, Beach Geometry, and Fetch Effects. Geomorphology, 49: 89-108.

Belly, P.Y., 1964. Sand movement by wind. United States Army Corps of Engineers, Coastal Engineering Research Center.

Bird, E., 2003. Coastal Dunes, Coastal Geomorphology: An Introduction. John Wiley & Sons Ltd., West Sussex, England.

Blaise, B., Clague, J.J. and Mathewes, R.W., 1990. Time of maximum Late Wisconsin glaciation, west coast Canada. Quaternary Research, 34: 282-295.

Blumberg, D.G. and Greeley, R., 1993. Field studies of aerodynamic roughness length. Journal of Arid Environments, 25: 39-48.

Boggs, S., 2000. Principles of Sedimentology and Stratigraphy. Prentice Hall, Portland, Oregon.

Bruun, P., 1962. Sea Level Rise as a Cause of Shore Erosion. Journal of Waterways and Harbors Division (ASCE), 88: 116-130.

Bullard, J.E., 1997. A note on the use of the "Fryberger Method" for evaluating potential sand transport by wind. Journal of Sedimentary Research, 67(3A): 499-501.

Bullard, J.E., Wiggs, G.F.S. and Nash, D.J., 2000. Experimental study of wind directional variability in the vicinity of a model valley. Geomorphology, 35(2): 127-143.

Byrne, M.L., 1997. Seasonal sand transport through a trough blowout at Pinery Provincial Park, Ontario. Canadian Journal of Earth Sciences, 34(11): 1460-1466.

Byrne, M.L. and McCann, S.B., 1993. The internal structure of vegetated coastal sand dunes, Sable Island, Nova Scotia. Sedimentary Geology, 84: 199-218.

Carson, M.A. and Maclean, P.A., 1986. Development of hybrid aeolian dunes: The William River dune field, Northwest Saskatchewan, Canada. Canadian Journal of Earth Sciences, 23(12): 1974-1990.

Carter, R.W.G., 1988. Coastal Environments: An Introduction to the Physical, Ecological and Cultural Systems of Coastlines. Academic Press, New York.

Carter, R.W.G., Hesp, P.A. and Nordstrom, K.F., 1990. Erosional landforms in coastal dunes. In: K.F. Nordstrom, N.P. Psuty and R.W.G. Carter (Editors), Coastal Dunes: Form and Process. John Wiley and Sons, London, 217-249.

Catto, N., MacQuarrie, K. and Hermann, M., 2002. Geomorphic response to Late Holocene climate variation and anthropogenic pressure, northeastern Prince Edward Island, Canada. Quaternary International, 87: 101-117.

Clague, J.J., Harper, J.R., Hebda, R.J., Howes, D.E., 1982. Late Quaternary sea levels and crustal movements, coastal British Columbia. Canadian Journal of Earth Sciences, 19: 597-618.

Conway, K.W. and Barrie, J.V., 1994. Coastal erosion on the east coast of Graham Island, Queen Charlotte Islands, British Columbia; *In* Current Research 1994-E; Geological Survey of Canada: 53-58.

Cooper, W.S., 1958. Coastal Sand Dunes of Oregon and Washington. Geological Society of America Memoir, 72. Waverly Press Inc., Baltimore, M.D.

Dalzell, K., 1989. The Queen Charlotte Islands Vol.1: 1774-1966. Harbour Publishing, Maderia Park, BC.

Davidson-Arnott, R.G., 2003. Modelling the response of sandy coasts to sea-level rise. In: W. Kamphuis (Editor), Canadian Coastal Conference 2003. Proceedings of the Canadian Coastal Conference 2003, Queen's University, Kingston, ON Canada.

Davidson-Arnott, R.G. and Law, M.N., 1996. Measurement and prediction of long-term sediment supply to coastal foredunes. Journal of Coastal Research, 13(3): 654-663.

Davidson-Arnott, R.G.D., 1996. Measurement and prediction of long-term sediment supply to coastal foredunes. Journal of Coastal Research, 13(3): 654-663.

Davidson-Arnott, R.G.D., Johnston, P., Ollerhead, J. and Walker, I.J., 2003. Seasonal Variations in the Beach and Foredune System, Greenwich Dunes, Prince Edward Island National Park. Parks Canada Project No. PEI-2002-01R Final Report, Parks Canada, Greenwich, Prince Edward Island.

Davidson-Arnott, R.G.D. and Law, M.N., 1990. Seasonal patterns and controls on sediment supply to coastal foredunes. Long Point, Lake Erie. In: K.F. Nordstrom, N.P. Psuty and R.W.G. Carter (Editors), Coastal Dunes: Form and Process. John Wiley & Sons, Baltimore, 177-200.

Dong, Z., Wang, H., Liu, X. and Wang, X., 2003. The blown sand flux over a sandy surface: a wind tunnel investigation on the fetch effect. Geomorphology, 1363: 1-11.

EC-AES, 1977. MANOBS - Manual of Surface Weather Observations, Atmospheric Environment Service, Environment Canada, Downsview.

EC-CMC, 2002a. Canadian Climate Normals. Environment Canada. http://www.climate.weatheroffice.ec.gc.ca/climate_normals/results_e.htm.

EC-CMC, 2002b. Techical Documentation for Hourly Weather (HLY01) Data, Canadian Meteorological Centre, Environment Canada. http://www.climate.weatheroffice.ec.gc.ca/prods_servs/documentation_index_e.html.

Eid, B., Calnan, C., Henschel, M. and McGrath, B., 1993. Wind and Wave Climate Atlas Volume IV: The West Coast of Canada. Transport Canada (Report no. TP 10820E), Halifax.

Erpul, G., Gabriels, D. and Norton, L.D., 2004. Wind effects on sediment transport by raindrop-impacted shallow flow: a wind tunnel study. Earth Surface Processes and Landforms, 29: 955-967.

Fedge, D. and Josenhans, H., 2000. Drowned forests and archaeology on the continental shelf of British Columbia, Canada. Geology, 28: 99-102.

Folk, R.L., 1966. A review of grain size parameters. Sedimentology, 6: 73-93.

Fraser, G.S., Bennett, S.W., Olyphant, G.A. and Bauch, N.J., 1998. Windflow circulation patterns in a coastal dune blowout, south coast of Lake Michigan. Journal of Coastal Research, 14(2): 451-460.

Fryberger, S.G., 1979. Dune forms and wind regime. In: E.D. McKee (Editor), A Study of Global Sand Seas, USGS Professional Paper 1052, Washington, 137-169.

Fryberger, S.G., 1980. Dune forms and wind regime, Mauritania, West Africa: implications for past climate. Paleocology of Africa, 12: 79-96.

Fryberger, S.G., 1991. Unusual sedimentary structures in the Oregon coastal dunes. Journal of Arid Research, 21(2): 131-150.

Gares, P.A., 1992. Topographic changes associated with coastal dune blowouts at Island Beach State Park, New Jersey. Earth Surface Processes and Landforms, 17: 589-604.

Gedalof, Z. and Smith, D.J., 2001. Interdecadal climate variability and regime-scale shifts in Pacific North America. Geophysical Research Letters, 28: 1515-1518.

Greenwood, B. and Hale, P.B., 1980. Depth of activity, sediment flux and morphological change in a barred nearshore environment. In: S.B. McCann (Editor), The Coastline of Canada: Littoral Processes and Shore Morphology. Geological Survey of Canada Paper, 80-10: 89-109.

Greenwood, B. and Sherman, D.J., 1984. Waves, currents, sediment flux and morphological response in a barred nearshore system. In: B. Greenwood and R.A. Davis, Jr. (Editors), Hydrodynamics and Sedimentation in Wave-Dominated Coastal Environments. Marine Geology, 60: 31-61.

Harper, J.R., 1980. Coastal Processes on Graham Island, Queen Charlotte Islands, British Columbia, Current Research, Part A, Geological Survey of Canada, Paper 80-1A: 13-18.

Hesp, P., Davidson, D.A., Walker, I.J. and Ollerhead, J., 2004. Flow dynamics over a foredune at Prince Edward Island, Canada. Geomorphology, in press.

Hesp, P.A., 1982. Dynamics and morphology of foredunes in South East Australia. Ph.D. Thesis, University of Sydney, Sydney.

Hesp, P.A., 1988. Surfzone, beach, and foredune interactions on the Australian south east coast. Journal of Coastal Research (Special Issue No. 3): 15-25.

Hesp, P.A., 1989. A review of biological and geomorphological processes involved in the initiation and development of incipient foredunes. Proceedings of the Royal Society of Edinburgh, 96B: 181-201.

Hesp, P.A., 1996. Flow dynamics in a trough blowout. Boundary-Layer Meteorology, 77: 305-330.

Hesp, P.A., 1999. The beach backshore and beyond. In: A.D. Short (Editor), Handbook of Beach Shoreface Morphodynamics. John Wiley & Sons Ltd., Chichester, New York, Weinheim, Brisbane, Singapore, Toronto, 145-270.

Hesp, P.A., 2000. Coastal Sand Dunes: Form and Function, CDVN Technical Bulletin No. 4. Forest Research, Rotorua.

Hesp, P.A., 2002. Foredunes and blowouts: initiation, geomorphology and dynamics. Geomorphology, 48: 245-268.

Hesp, P.A. and Hyde, R., 1996. Flow dynamics and geomorphology of a trough blowout. Sedimentology, 43: 505-525.

Hesp, P.A., Illenberger, W., Rust, I., McLachlan, A. and Hyde, R., 1989. Some aspects of transgressive dunefield and transverse dune geomorphology, south coast, South Africa. Zeitschrift für Geomorphologie, Supplementbaende. 73: 111-123.

Hesp, P.A. and Thom, B.G., 1990. Geomorphology and evolution of active transgressive dunefields. In: K.F. Nordstrom, N.P. Psuty and R.W.G. Carter (Editors), Coastal Dunes: Form and Process. John Wiley & Sons Ltd., pp. 253-288.

Hetherington, R. and Barrie, J.V., 2004. Interaction between local tectonics and glacial unloading on the Pacific margin of Canada. Quaternary International, 120: 65-77.

Hsu, S., 1971. Wind stress criteria in eolian sand transport. Journal of Geophysical Research, 76: 8684-8686.

Hunter, R.E., Richmond, B.M. and Alpha, T.R., 1983. Storm-controlled oblique dunes of the Oregon Coast. Geological Society of America Bulletin, 94: 1450-1465.

Jackson, D.W.T. and McCloskey, J., 1997. Preliminary results from a field investigation of aeolian sand transport using high resolution wind and transport measurements. Geophysical Research Letters, 24(2): 163-166.

Jackson, N.L. and Nordstrom, K.F., 1998. Aeolian transport of sediment on a beach during and after rainfall, Wildwood, NJ, USA. Geomorphology, 22(2): 151-157.

Jungerius, P.D. and van der Meulen, F., 1989. The development of dune blowouts, as measured with erosion pins and sequential air photos. Catena, 16: 369-376.

Kawamura, R., 1951. Study of sand movement by wind, Institute of Science and Technology, Tokyo.

Klee, G.A., 1999. The Coastal Environment: Toward Integrated Coastal and Marine Santuary Management. Prentice-Hall Inc., New Jersey.

Knight, M., Thomas, D.S.G. and Wiggs, G.F.S., 2003. Challenges of calculating dunefield mobility over the 21st century. Geomorphology, 59(1-4): 197-213.

Kocurek, G. and Lancaster, N., 1999. Aeolian system sediment state: theory and Mojave Desert Kelso dune field example. Sedimentology, 46(3): 505-515.

Kocurek, G., Robinson, N.I. and Sharp, J.M., 2001. The response of the water table in coastal aeolian systems to changes in sea level. Sedimentary Geology, 139(1): 1-13.

Komar, P.D. 1976. Beach Processes and Sedimentation. Englewood Cliffs, New Jersey, Prentice Hall Inc.

Lancaster, N., 1988. Development of linear dunes in the southwestern Kalahari, southern Africa. Journal of Arid Environments, 14: 233-244.

Lancaster, N., 1995. Geomorphology of Desert Dunes. Physical Environment Series. Routledge, New York.

Lancaster, N., 1997a. Arid Geomorphology. Progress in Physical Geography, 21(2): 285-290.

Lancaster, N., 1997b. Response of eolian geomorphic systems to minor climatic change: examples from the southern California deserts. Geomorphology, 19: 333-347.

Lancaster, N. and Baas, A., 1998. Influence of vegetation cover on sand transport by wind: field studies at Owens Lake, California. Earth Surface Processes and Landforms, 23(1): 69-82.

Lancaster, N. and Helm, P., 2000. A test of a climatic index of dune mobility using measurements from the southwestern United States. Earth Surface Processes and Landforms, 25: 197-207.

Larsen, C.F., Echelmeyer, K.A., Freymueller, J.T. and Motyka, R.J., 2003. Tide gauge records of uplift along the Pacific-North American plate boundary, 1937 to 2001. Geophysical Research, 108(B4): 32-34.

Lettau, H.H. and Lettau, K., 1978. Experimental and micro-meteorological field studies on dune migration. In: K. Lettau and H.H. Lettau (Editors), Exploring the World's Driest Climate. University of Wisconsin-Madison, Institute for Environmental Studies, 110-147.

McKee, E.D. 1979. An introduction to the study of global sand seas. *In* A Study of Global Sand Seas, E. McKee, ed., Washington, U. S. Geological Survey Paper 1052, 1- 20.

McKenna Neuman, C., 1993. A review of aeolian transport processes in cold environments. Progress in Physical Geography, 17(2): 99-117.

McKenna Neuman, C., Lancaster, N. and Nickling, W.G., 1997. Relations between dune morphology, air flow, and sediment flux on reversing dunes, Silver Peak, Nevada. Sedimentology, 44: 1103-1113.

McKenna Neuman, C., Lancaster, N. and Nickling, W.G., 2000. The effect of unsteady winds on sediment transport on the stoss slope of a transverse dune, Silver Peak, NV, USA. Sedimentology, 47: 211-226.

McKenna Neuman, C. and Maxwell, C., 1999. A wind tunnel study of the resilience of three fungal crusts to particle abrasion during aeolian sediment transport. Catena, 38: 151-173.

McKenna Neuman, C. and Scott, M.M., 1998. A wind tunnel study of the influence of pore water on aeolian sediment transport. Journal of Arid Environments, 39: 403-419.

Muhs, D.R., Maat, P.B., 1993. The potential response of eolian sands to greenhouse warming and precipitation reduction on the Great Plains of the U.S.A. Journal of Arid Environments, 25: 351-361.

Muhs, D.R. and Wolfe, S.A., 1999. Sand dunes of the northern Great Plains of Canada and the United States. Geological Survey of Canada Bulletin 534: 183-197.

Nickling, W.G., 1988. The initiation of particle movement by wind. Sedimentology, 35: 499-511.

Nickling, W.G. and Davidson-Arnott, R.G.D., 1990. Aeolian sediment transport on beaches and coastal sand dunes, Symposium on Coastal Sand Dunes. Coastal Zone Engineering, Institute for Mechanical Engineering, National Research Council, Guelph, Ontario, 1-35.

Nickling, W.G. and McKenna Neuman, C., 1999. Recent investigations of airflow and sediment transport over desert dunes. In: A.S. Goudie, I. Livingstone and S. Stokes (Editors), Aeolian environments, sediments and landforms. John Wiley & Sons, Chichester, 15-47.

Nickling, W.G. and Wolfe, S.A., 1994. The morphology and origin of Nebkhas, region of Mopti, Mali, West Africa. Journal of Arid Environments, 28: 13-30.

Oke, T.R., 1978. Boundary Layer Climates. Methuen & Co, New York.

Olivier, M.J. and Garland, G.G., 2003. Short-term monitoring of foredune formation on the east coast of South Africa. Earth Surface Processes and Landforms, 28: 1143-1155.

Parsons, D.R., Walker, I.J. and Wiggs, G.F.S., 2004. Numerical modelling of flow structures over idealised transverse aeolian dunes of varying geometry. Geomorphology, 59: 149-164.

Pojar, J. and MacKinnon, A. (Editors), 1994. Plants of Coastal British Columbia including Washington, Oregon and Alaska. Lone Pine Publishing, Vancouver, B.C.

Pye, K. and Tsoar, H., 1990. Aeolian sand and sand dunes. Unwin Hyman, Boston.

Pye, K., 1985. Controls on fluid threshold velocity, rates of aeolian sand transport and dune grain size parameters along the Queensland coast. In: O.E. Barndorff-Nielsen, J.T. Møller, K.R. Rasmussen and B.B. Willetts (Editors), Proceedings of International Workshop on the Physics of Blown Sand. University of Aarhus, Aarhus, 483-510.

Rasmussen, K.R., 1989. Some aspects of flow over coastal dunes. Proceedings of the Royal Society of Edinburgh, 96B: 129-147.

Robertson-Rintoul, M.J., 1990. A quantitative analysis of the near-surface wind flow pattern over coastal parabolic dunes. In: K.F. Nordstorm and N.P. Psuty (Editors), Coastal Dunes: Form and Process. John Wiley & Sons Ltd., West Sussex, England, 392.

Ruz, M.-H. and Meur-Ferec, C., 2003. Influence of high water levels on aeolian sand transport: upper beach/dune evolution on a macro-tidal coast, Wissant Bay, northern France. Geomorphology, 60(1-2): 73-87.

Sarre, R.D., 1987. Aeolian sand transport. Progress in Physical Geography, 11: 157-82.

Sarre, R.D., 1989. Aeolian sand drift from the intertidal zone on a temperate beach: potential and actual rates. Earth Surface Processes and Landforms, 14: 247-258.

Schlichting, H., 1955. Boundary Layer Theory. Pergamon Press, New York.

Shabbar, A., Bonsal, B. and Khandekar, M., 1997. Canadian Precipitation patterns associated with the Southern Oscillation. Journal of Climate, 10: 3016-3027.

Shaw, J., Taylor, R.B., Forbes, D.L., Ruz, M.H. and Solomon, S., 1998. Sensitivity of the coasts of Canada to sea-level rise. Bulletin 505, Geological Survey of Canada, Ottawa.

Sherman, D.J., 1990. Evaluation of aeolian sand transport equations using intertidal-zone measurements, Saunton Sands, England. Discussion. Sedimentology, 37(2): 385-388.

Sherman, D.J. and Bauer, B.O., 1993. Dynamics of beach-dune systems. Progress in Physical Geography, 17(4): 413-447.

Sherman, D.J. and Hotta, S., 1990. Aeolian sediment transport: theory and measurement. In: K.F. Nordstrom, N.P. Psuty and R.W.G. Carter (Editors), Coastal Dunes: Form and Process. John Wiley and Sons, London, 15-38.

Sherman, D.J., Jackson, D.W.T., Namikas, S.L. and Wang, J., 1998. Wind-blown sand on beaches: an evaluation of models. Geomorphology, 22: 113-133.

Storlazzi, C.D., Willis, C.M. and Griggs, G.B., 2000. Comparative impacts of the 1982-3 and 1997-1998 El Nino winters on the central California coast. Journal of Coastal Research, 16: 1022-1036.

Svasek, J.N. and Terwindt, J.H.J., 1974. Measurements of sand transport by wind on a natural beach. Sedimentology, 21: 311-322.

Taylor, P.A. and Lee, R.J., 1984. Simple guidelines for estimating wind speed variations due to small scale topographic features. Climatological Bulletin, 18: 3-32.

Thomson, D., 1995. The seasons, global temperature, and precession. Science, 268: 59-68.

Thornthwaite, C.W. and Mather, J.R., 1957. Instructions and tables for computing potential evapotranspiration and the water balance. Publications in Climatology, 10(3): 1-311.

Touma, J., 1977. Dependence of the Wind Profile Power Law on Stability for Various Locations. Journal of the Air Pollution Control Association, 27(9): 863-866.

Tsoar, H., 1989. Linear dunes-forms and formation. Progress in Physical Geography, 13: 507-528.

Tsoar, H., 2002. Climatic Factors Affecting Mobility and Stability of Sand Dunes. In: J.A. Lee and T. Zobeck, M. (Editors), Proceedings of ICAR5/GCTE-SEN Joint Conference, International. Center for Arid and Semiarid Lands Studies, Texas Tech University, Lubbock, Texas, USA Publication 02-2.

Tsoar, H. and Arens, S.M., 2003. Mobilization e estabilização de dunas de areia em climas húmidos e arid (Mobilization and stabilization of sand dunes in humid and arid climates). Mercator, 2(3): 131-145.

Tsoar, H. and Illenberger, W., 1998. Re-evaluation of sand dune mobility indices. Journal of Arid Lands Studies, 7S: 265-268.

UKMetOffice, 2004. 1971-2000 climate averages, Wales. UK Met Office, http://www.metoffice.com/climate/uk/averages/19712000/areal/wales.html.

van den Anker, J.M., Jungerius, P.D. and Mur, L.R., 1985. The role of algae in the stabilization of coastal dune blowouts. Earth Surface Processes and Landforms, 10: 189-192.

van der Wal, D., 1998. Effects of fetch and surface texture on aeolian sand transport on two nourished beaches. Journal of Arid Environments, 29(3): 533-547.

van Dijk, P.M., Stroosnijder, K. and de Lima, J.L., 1996. The influence of rainfall on transport of beach sand by wind. Earth Surface Processes and Landforms, 21: 341-352.

Viles, H.A. and Goudie, A.S., 2003. Interannual, decadal and multidecadal scale climatic variability and geomorphology. Earth-Science Reviews, 61: 105-131.

Walker, I.J. and Barrie, J.V., 2004. Geomorphology and sea-level rise on one of Canada's most 'sensitive' coasts: Northeast Graham Island, British Columbia. Journal of Coastal Research, SI 39.

Walker, I.J., Hesp, P.A., Davidson-Arnott, R.G.D. and Ollerhead, J., 2003. Topographic effects on airflow over a vegetated foredune: Greenwich Dunes, Prince Edward Island, Canada, Coastal Sediments '03. The Proceedings of The Fifth International Symposium on Coastal Engineering and Science of Coastal Sediment Processes 2003. World Scientific Publishing Corp. and East Meets West Productions, Corpus Christi, Texas, USA.

Walker, I.J., Hesp, P.A., Davidson-Arnott, R.G.D. and Ollerhead, J., in press. Topographic steering of offshore airflow over a vegetated foredune: Greenwich Dunes, Prince Edward Island, Canada. Journal of Coastal Research.

Walker, I.J. and Nickling, W.G., 2002. Dynamics of secondary airflow and sediment transport over and in the lee of transverse dunes. Progress in Physical Geography, 26(1): 47-75.

Wasson, R.J. and Nanninga, P.M., 1986. Estimating wind transport of sand on vegetated surfaces. Earth Surface Processes and Landforms, 11: 505-514.

Wiedemann, A.M., Dennis, L.R.J. and Smith, F.H., 1999. Plants of the Oregon Coastal Dunes. Oregon State University Press, Corvallis, Oregon.

Wiggs, G.F.S., Baird, A.J. and Atherton, R.J., 2004. The dynamic effects of moisture on the entrainment and transport of sand by wind. Geomorphology, 59(1-4): 13-30.

Wiggs, G.F.S., Livingstone, I., Thomas, D.S.G. and Bullard, J.A., 1996a. Airflow and roughness characteristics over partially vegetated linear dunes in the Southwest Kalahari desert. Earth Surface Processes and Landforms, 21: 19-34.

Wiggs, G.F.S., Livingstone, I. and Warren, A., 1996b. The role of streamline curvature in sand dune dynamics: evidence from field and wind tunnel measurements. Geomorphology, 17: 29-46.

Wiggs, G.F.S., Thomas, D.S.G. and Livingstone, I., 1995. Dune mobility and vegetation cover in the southwest Kalahari desert. Earth Surface Processes and Landforms, 20(6): 515-529.

Willetts, B.B., 1979. The influence of grain characteristic shape on size determination, with particular reference to elutriation. *In* Eurotech 120 - Collection techniques of sizing and tracking particles in fluids. Technical University of Denmark, Fluid Mechanics Department, Copenhagen, Austria.

Willetts, B.B., 1983. Transport by wind of granular materials of different grain shapes and densities. Sedimentology, 30: 669-679.

Wilson, I.G., 1971. Desert sandflow basins and a model for the development of ergs. Geographical Journal, 137(2): 180-199.

Wolfe, S.A., 1997. Impact of increased aridity on sand dune activity in the Canadian Prairies. Journal of Arid Environments, 36: 421-432.

Wolfe, S.A. and David, P.P., 1997. Parabolic dunes: Examples from the Great Sand Hills, southwestern Saskatchewan. Canadian Geographer - Geographe Canadien, 41(2): 207-213.

Wolfe, S.A., Hugenholtz, C., Ollerhead, J. and Walker, I.J., 2003. Morphology and development of blowouts, Great Sand Hills, southern Saskatchewan, Canadian Association of Geographers, Victoria, BC, May 27-31, 2002.

Wolfe, S.A., Huntley, D.J. and Ollerhead, J., 1995. Recent and late Holocene sand dune activity in southwestern Saskatchewan. Geological Survey of Canada, Current Research 1995-B: 131-140.

Wolfe, S.A. and Lemmen, D.S., 1999. Monitoring dune activity in the Great Sand Hills region, Saskatchewan. Geological Survey of Canada Bulletin 534: 199-210.

Wolfe, S.A., Muhs, D.R., David, P.P. and McGeehin, J.P., 2000. Chronology and geochemistry of late Holocene eolian deposits in the Brandon Sand Hills, Manitoba, Canada. Quaternary International, 67: 61-74.

Wolfe, S.A. and Nickling, W.G., 1993. The protective role of sparse vegetation in wind erosion. Progress in Physical Geography, 17: 50-68.

Wolfe, S.A. and Walker, I.J., unpublished data. Unpublished optical dates from Haida Gwaii (2003-04).

Zhang, Y., Wallace, J.M. and Battisti, D.S., 1997. ENSO-like inter-decadal variability: 1900-93. Journal of Climate: 1004-1020.

VITA

Surname: Pearce (na. Brouwer) Given Names: Kim Irene

Place of Birth: Surrey, British Columbia, Canada

Educational Institutions Attended:

University of Victoria 1996 to 2005

Degrees Awarded:

B.Sc. University of Victoria 2002

Honours and Awards:

2004	Graduate student presentation competition - Western Division Canadian Association of Geographers, Medicine Hat – Honourable mention
2002-2004	Graduate Teaching and Research Fellowship
2003	Derrick Sewell Graduate Scholarship
2003	Northern Scientific Training Program
2003	The Geological Survey of America
2002	Excellence Recruitment Award

Publications and Presentations:

Pearce, K.I; and Walker, I.J. (in press). Frequency and magnitude biases in the 'Fryberger' model with implications for characterizing geomorphically effective winds. In: Walker, I.J. & Roy, A.G (eds), *Fluid flow & sediment transport processes in geomorphology: innovations, insights & advances in measurement. Geomorphology,* Special Issue.

Pearce, K.I. and Walker, I.J. **2005**. Morphologic and volumetric change of a foredune-trough blowout complex, East Beach, Haida Gwaii (Queen Charlotte Islands), BC. Annual Meeting of the Western Division, Canadian Association of Geographers. March 11-13, 2005. University of Lethbridge, Lethbridge, Alberta.

Pearce, K.I.; and Walker, I.J. **2004**. Aeolian sand transport potential and morphodynamics of a trough blowout: East Beach, Haida Gwaii, B.C. Association

of Washington Geographers, Spring Meeting. April 23-24, 2004. University College of the Fraser Valley (UCFV) Abbotsford, B.C.

Pearce, K.I.; and Walker, I.J. **2004**. Sand transport potential and foredune morphodynamics on an 'extreme' coastline: Northeast Graham Island, Haida Gwaii (Queen Charlotte Islands), BC. Annual Meeting of the Western Division, Canadian Association of Geographers. March 18-20, 2004. Medicine Hat College, Medicine Hat, Alberta (Honourable mention).

Pearce, K.I.; and Walker, I.J. **2003**. Systematic biases in wind data and Fryberger-type sand drift calculations with implications for the frequency and magnitude of geomorphically effective winds. On the edge, Annual Meeting of the Canadian Association of Geographers, May 27-31, 2003. University of Victoria, Victoria, British Columbia.

Pearce, K.I.; and Walker, I.J. **2003**. Preliminary assessment of aeolian sediment transport and dune activity in a moist coastal environment: Graham Island, Haida Gwaii (Queen Charlotte Islands), B.C. Annual Meeting of the Western Division, Canadian Association of Geographers, March 13-15, 2003. University of Northern British Columbia Prince George, British Columbia.

Kim Pearce
Department of Geography,
University of Victoria,
P.O. Box 3050 STN CSC
Victoria, B.C., V8W 3P5, Canada

April 20, 2005

Patrick. A Hesp
Department of Geography & Anthropology
Louisiana State University
227 Howe-Russell Geoscience Complex
Baton Rouge, LA 70803-4105

Dear Patrick Hesp,

This letter follows our recent email interactions. I am completing a master's thesis at the University of Victoria entitled "Aeolian geomorphology of northeast Graham Island, Haida Gwaii (Queen Charlotte Islands), British Columbia." I would like your permission to reprint in my thesis the following four figures:

Hesp, P. 2002. Foredunes and blowouts: initiation, geomorphology and dynamics. Gemorphology. 48: 245-268.

1) Figure 3 (page 253) A model of established foredune morphology,

Hesp, P. A. (1999). The beach backshore and beyond. Handbook of Beach Shoreface Morphodynamics. A. D. Short. Chichester, New York, Weinheim, Brisbane, Singapore, Toronto, John Wiley & Sons Ltd.: 145-270.

2) Figure 6.12 (page 161) Schematic of saucer and trough blowouts, and
3) Figure 6.14 (page 164) Evolution from a blowout to a parabolic dune.

Hesp, P.A. and R. Hyde. 1996. Flow dynamics and geomorphology of a trough blowout. Sedimentology. 43: 505-525.

4) Figure 14 a (page 521) Oblique approach winds steered within a trough blowout

The requested permission extends to any future revisions and editions of my thesis, including non-exclusive world rights in all languages, and to the prospective publication of my thesis through the National Library of Canada and its agents, including UMI (University Microfilms International). These rights will in no way restrict republication of the material in any form by you or by others authorized by you. Your signing of this letter will also confirm that you own [or your company owns] the copyright to the above-described material.

If these arrangements meet with your approval, please sign this letter where indicated below and return it to me at the address included at the beginning of this letter. Thank you very much.

Sincerely,

Kim Pearce

Kim Pearce

PERMISSION GRANTED FOR THE
USE REQUESTED ABOVE:

NAME: Patrick Hesp

DATE: April 21, 2005

BRITISH COLUMBIA

Ministry of Management Services

Product Sales and Services

Intellectual Property Program Box 9492
~~Box 9459~~ Stn Prov Govt
Victoria BC V8W 9W7

Copyright Permission Request Form

Date of Request 20/04/2005

File Number: 7200001452

Organization Requesting Copyright Permission:

Kim Pearce
Kim Pearce - Student
PO Box 3050 STN CSC
Victoria British Columbia V8W 3P5

Publication Information

Title: Air Photos

ISBNNumber: **ISSNNumber:**

Intended Audience: N/A

Copyright Request

Number of Copies 20 **Excerpt** Various Airphotos

Proposed Use: Thesis

Permission/Instructions ☑ **Approved** ☐ **Denied**

Permission is granted to Kim Pearce, student at University of Victoria, to reproduce BC Airphotos: BC4362_221/227/233, BC40109_116, BC80008_207/220/221/228/230, and BCB97035_4/6/12/14/184/187/189 (the "Material").

It is understood that the reproduced Material will be included in Kim Pearce's thesis entitled "Aeolian geomorphology of northeast Graham Island, Haida Gwaii (Queen Charlotte Islands), British Columbia", and that thesis will be available to learners and scholars through the National Library of Canada and University of Victoria.

It is further understood that no more than 20 copies will be reproduced.

*Permission is not granted for the commercial publication and reproduction of the material except under the National Library of Canada "Non-exclusive license to reproduce theses".

Frank Hudson
Director

Approval Date: 22/04/2005